AD

USAAVLABS TECHNICAL REPORT 68-86

BEHAVIOR OF FIBER-REINFORCED PLASTIC LAMINATES UNDER UNIAXIAL, BIAXIAL, AND SHEAR LOADINGS

By

Charles W. Bert

Byron L. Mayberry

John D. Ray

January 1969

U. S. ARMY AVIATION MATERIEL LABORATORIES
FORT EUSTIS, VIRGINIA

CONTRACT DAAJ02-67-C-0111
UNIVERSITY OF OKLAHOMA RESEARCH INSTITUTE
NORMAN, OKLAHOMA

122

Disclaimers

The findings in this report are not to be construed as an official Department of the Army position unless so designated by other authorized documents.

When Government drawings, specifications, or other data are used for any purpose other than in connection with a definitely related Government procurement operation, the United States Government thereby incurs no responsibility nor any obligation whatsoever; and the fact that the Government may have formulated, furnished, or in any way supplied the said drawings, specifications, or other data is not to be regarded by implication or otherwise as in any manner licensing the holder or any other person or corporation, or conveying any rights or permission, to manufacture, use, or sell any patented invention that may in any way be related thereto.

Trade names cited in this report do not constitute an official endorsement or approval of the use of such commercial hardware or software.

Disposition Instructions

Destroy this report when no longer needed. Do not return it to the originator.

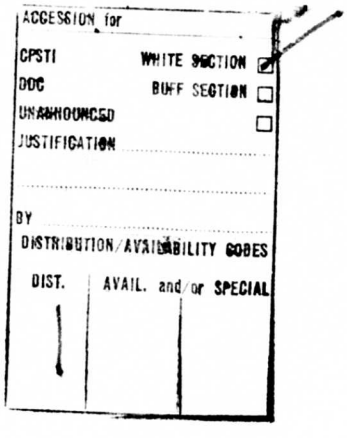

DEPARTMENT OF THE ARMY
HEADQUARTERS US ARMY AVIATION MATERIEL LABORATORIES
FORT EUSTIS, VIRGINIA 23604

This research effort was carried out under Contract DAAJ02-67-C-0111 by the University of Oklahoma Research Institute to evaluate the vibrational characteristics of composite structural components.

This report has been reviewed by the U.S. Army Aviation Materiel Laboratories and is considered to be technically sound.

This report is published for the dissemination of information and the stimulation of further research.

Task 1F162204A17001
Contract DAAJ02-67-C-0111
USAAVLABS Technical Report 68-86
January 1969

BEHAVIOR OF FIBER-REINFORCED PLASTIC LAMINATES UNDER UNIAXIAL, BIAXIAL, AND SHEAR LOADINGS

By
Charles W. Bert
Byron L. Mayberry
John D. Ray

Prepared by
University of Oklahoma Research Institute
Norman, Oklahoma

For
U.S. ARMY AVIATION MATERIEL LABORATORIES
FORT EUSTIS, VIRGINIA

SUMMARY

As a part of a larger research program to bring about acceptability of fiber-reinforced plastics for primary load-bearing members of Army aircraft structures, a series of mechanical tests was conducted on fiber glass-epoxy laminates. The loadings used were uniaxial tension; biaxial tension with principal-stress ratios of 1:2, 1:1, and 2:1; and pure shear. The most unique tests were those involving the biaxial loadings. These tests were carried out on a specially designed test fixture using a cable-pulley system in conjunction with a conventional universal testing machine. Data were obtained on the limit strength and apparent ultimate strength of flat laminates subjected to biaxial loading. Under biaxial loading, the parallel-ply lamination arrangement was found to be slightly superior to the cross-ply and quasi-isotropic lamination arrangements. The shear tests were accomplished on thin-walled tubular specimens subjected to pure torsion.

FOREWORD

This report was prepared by the University of Oklahoma Research Institute (OURI) under Phase II of U.S. Army Aviation Materiel Laboratories (USAAVLABS) Contract DAAJ02-67-C-0111 for research conducted during the period from July 1, 1967 to July 31, 1968. Work under this contract has also included sandwich-shell vibrational investigations (Phase I), reported separately in Technical Report 68-85, titled Vibration Evaluation of Sandwich Conical Shells with Fiber-Reinforced Composite Facings.

The research effort is a continuation of the research accomplished under three previous contracts and reported in the following USAAVLABS reports:

1. Technical Report 67-65, Fabrication and Full Scale Structural Evaluation of Sandwich Shells of Revolution Composed of Fiber Glass Reinforced Plastic Facings and Honeycomb Cores.

2. Technical Report 65-66, The Effect of Resin Content and Voids on the Strength of Fiberglass-Reinforced Plastics for Airframe Use.

3. Technical Report 65-60, Dynamic Elastic, Damping, and Fatigue Characteristics of Fiberglass-Reinforced Sandwich Structure.

4. Technical Report 65-15, Strength Properties and Relationships Associated with Various Types of Fiberglass-Reinforced-Facing Sandwich Structure.

5. Technical Report 64-37, Research in the Field of Fiberglass-Reinforced Sandwich Structure for Airframe Use.

The present report was written by Dr. Charles W. Bert, project director and Professor of Aerospace and Mechanical Engineering; Mr. Byron L. Mayberry, research engineer; and Dr. John D. Ray, project director.

Special acknowledgment is made to Mr. Frederick Lehmann in connection with fabricating the specimens, and to Mr. Jack Holland in fabricating the special test equipment and in performing most of the experiments.

BLANK PAGE

TABLE OF CONTENTS

LIST OF ILLUSTRATIONS

LIST OF TABLES

LIST OF SYMBOLS

a	major semi-axis dimension of elliptical reduced-thickness test section, in.
A	constant of integration in Equation (71)
A_{ij}	in-plane stiffness
$[A^*_{ij}]$	inverse of A_{ij}
b	minor semi-axis dimension of elliptical reduced-thickness test section, in.
B	constant of integration in Equation (71)
B_j	constant in Equation (45)
c	subscript, contour; superscript, compression
C	constant of integration in Equation (71)
C_{ij}	Cauchy stiffness coefficients, psi
cr	subscript, critical
E, $\bar{E}$, E_{ii}, $\bar{E}_{ii}$	Young's elastic modulus, psi
f, i	subscript, direction of normal to plane on which stress acts
g, j	subscript, direction in which stress component acts
G, $\bar{G}$	shear modulus, psi
h	total plate thickness, in.
H_i	strength coefficients appearing in Equation (38), $(psi)^{-2}$
J	polar area moment, $in.^4$
k	typical set of plies
K	set of plies; scale factor in Appendix I
$K_{\alpha\beta}$	empirical constant in Chamis strength theory
L	operating length, in.
$\bar{L}$	defined in Equation (55)

m	$\cos \theta_k$
$\bar{M}$	defined in Equation (55)
n	typical individual ply
$\bar{n}$	$\sin \theta_k$
N	total number of plies
N_{fg}, N'_{fg}	force per unit length, lb/in.
N_p, N_q	principal loads per unit length, lb/in.
P	measured load, lb
P_h	hydrostatic stress, psi
Q_{ij}	reduced stiffness coefficients (aligned with symmetry axis)
Q'_{ij}	reduced elastic constants (at angle θ_k with major symmetry axis)
R	mean radius, in.
R_i	inside radius, in.
R_o	outside radius, in.
r	dimensionless ratio appearing in Equation (39)
S_i	surface area, $in.^2$
S_L	stress at 0.01 percent offset, psi
S_{L6}	shear stress at 0.01 percent offset, psi
S_U	stress at maximum load, psi
S_{U6}	shear stress at maximum torque, psi
t	wall thickness, in.
T	torque, in.-lb; or superscript, tension
U	potential strain energy per unit volume, $in.\text{-}lb/in.^3$
x, y	rectangular position coordinates in the plane of the plate, in.
z	distance from midplane of plate, in.

α, β	T or C
$\varepsilon_{\overline{fg}}$	strain components, in./in.
θ	angle between coordinate axes and material-symmetry axes, deg
λ	quantity defined in Equation (14)
$\overline{\lambda}$	quantity defined in Equation (67)
ν, ν_{ij}	Poisson's ratio
$\sigma_{\overline{fg}}$, σ'_{ij}	stress components, psi
ϕ	Airy stress function defined in Equation (70)

BLANK PAGE

1. INTRODUCTION

Under the sponsorship of the U.S. Army Aviation Materiel Laboratories (USAAVLABS), the University of Oklahoma Research Institute (OURI) has been conducting a major research program for the past five years in the area of fiber glass reinforced plastics (FRP) suitable for primary structures of U.S. Army aircraft. Tasks which have been completed include the evaluation of

(1) Several sandwich fabrication techniques (Reference 1).

(2) Effect of primary fabrication variables on conventional strength properties of laminates (References 1, 2, and 3).

(3) Several honeycomb-core sandwich configurations as small panels sized to fail in face rupture and various buckling modes (References 1, 4, and 5).

(4) Fatigue properties of sandwich material as beams with FRP facings and honeycomb core (References 6 and 7).

(5) Dynamic stiffness and damping of sandwich material in the form of beams (References 6 and 8).

(6) Fabrication and static buckling of full-size sandwich shell structures in the form of cylindrically curved panels, complete cylinders, and truncated cones (References 9, 10, 11, and 12).

(7) Vibrational frequencies, modes, and damping of full-size, sandwich, truncated conical shells (References 13 and 14).

The objectives of the present research were (1) to develop equipment and procedures for determining the mechanical behavior of laminates, (2) to evaluate the mechanical behavior of fiber glass reinforced plastic (FRP) laminates under uniaxial tension, biaxial tension (1:2, 1:1, and 2:1 principal-load ratios), and pure shear, and (3) to relate this behavior to laminate mechanics analysis methods.

For simplicity, most previous evaluations of the mechanical behavior of composite materials were limited to simple loadings, i.e., uniaxial tension and compression, flexure, and pure shear (References 15 and 16). In some of these investigations, the very significant effects of angular orientation of the loading with respect to the major material-symmetry axis of the composite material have been studied (References 17 and 18). However, in many regions of practical aircraft structures, the material is subjected to biaxial loadings, i.e., loads in two directions.

There is a large amount of biaxial-load test data for metallic alloys used in aircraft structures. However, in contrast, only a very limited amount of such data is available for composite materials.

In the present program, an original cable-and-pulley system reacted by a rigid frame was used to load the specimen biaxially. With this simple arrangement, described in Section 5a, the specimen is loaded biaxially, although the external load is applied in one direction only.

The material used was 181-style E-glass cloth impregnated with Epon-828 epoxy and activated by curing agent Z. In Table I are tabulated the lamination arrangements and loading orientations used.

TABLE I. LAMINATION ARRANGEMENTS AND LOADINGS

Lamination Arrangement	Type of Loading	No. of Plies	Angular Orientation of Loading, deg
Parallel ply	Biaxial 1:1	4	0 & 45
	Biaxial 1:2	4	0 & 90*
	Shear	4	0 & 45
	Uniaxial tension	4	0 & 90
Cross ply (balanced)	Biaxial 1:1	4	0
	Biaxial 1:2	4	0**
	Shear	4	0 & 45
	Uniaxial tension	4	0**
Quasi-isotropic (0°-60°-120°)	Biaxial 1:1	6	0 & 45
	Biaxial 1:2	6	0 & 90*
	Shear	6	0 & 45
	Uniaxial tension	6	0 & 90

*A 1:2 biaxial loading at 90 deg is sometimes designated at a 2:1 biaxial loading at 0 deg.

**In a balanced cross-ply laminate, there is no difference between the effect of a loading at 90 deg and that of the same loading at 0 deg. Thus, tests at only 0 deg needed to be conducted.

Five tests were carried out for each combination tabulated above. Thus, there were 50 biaxial tests, 30 shear tests, and 25 uniaxial tension tests, or a total of 105 tests.

2. THEORY OF THE IN-PLANE STIFFNESSES OF COMPOSITE PLATES SYMMETRICALLY LAMINATED OF ORTHOTROPIC LAYERS

The general theory presented here starts in Section 2a with development from first principles of the general three-dimensional theory of anisotropic elasticity. Then the general theory is reduced to the practical case of a thin orthotropic layer, such as one layer in an FRP composite.

In Section 2b the theory is presented for a plate loaded in its plane only and consisting of an arbitrary number of sets of orthotropic plies. Each set consists of an arbitrary number of pairs of plies, and each pair has one ply located a certain distance above the midplane of the laminated plate and the other ply located the same distance below the midplane. All plies in a given set have the same orientation.

a. A Single Orthotropic Layer

The currently popular idea of considering a composite material, consisting of oriented fibers imbedded in a matrix, to behave macroscopically as a homogeneous, anisotropic material is used here. However, this is not new, since it was used as early as 1914 by Huber (Reference 19) in connection with reinforced concrete slabs.

The anisotropic elastic coefficients may be determined either experimentally or analytically. In the past decade, literally dozens of papers have been published on theoretical micro-mechanics analyses for predicting the anisotropic elastic coefficients of single layers reinforced with unidirectional fibers (such as obtained in the filament-winding process). Many of these have been verified experimentally to be sufficiently accurate for engineering design. In contrast, the authors know of no theoretical analysis for predicting the stiffness of a single layer of a woven-fabric reinforced composite. However, it is well known that due to the crimp of the fibers in a woven-cloth reinforced composite, such composites have lower stiffnesses than unidirectionally reinforced composites with the same fiber content. Therefore, in the present work, the anisotropic elastic coefficients are determined purely by means of experiments (see later sections).

Anisotropic materials have material properties which depend upon the directional orientation. The most general stress-strain relation for a linear elastic material is known as generalized Hooke's law. For a general three-dimensional anisotropic body, generalized Hooke's law can be expressed in a Cartesian coordinate system $(\bar{x}, \bar{y})$ as follows (Reference 20):

$$\begin{bmatrix} \sigma_{\bar{x}\bar{x}} \\ \sigma_{\bar{y}\bar{y}} \\ \sigma_{\bar{z}\bar{z}} \\ \sigma_{\bar{y}\bar{z}} \\ \sigma_{\bar{z}\bar{x}} \\ \sigma_{\bar{x}\bar{y}} \end{bmatrix} = \begin{bmatrix} C_{11} & C_{12} & C_{13} & C_{14} & C_{15} & C_{16} \\ C_{21} & C_{22} & C_{23} & C_{24} & C_{25} & C_{26} \\ C_{31} & C_{32} & C_{33} & C_{34} & C_{35} & C_{36} \\ C_{41} & C_{42} & C_{43} & C_{44} & C_{45} & C_{46} \\ C_{51} & C_{52} & C_{53} & C_{54} & C_{55} & C_{56} \\ C_{61} & C_{62} & C_{63} & C_{64} & C_{65} & C_{66} \end{bmatrix} \begin{bmatrix} \epsilon_{\bar{x}\bar{x}} \\ \epsilon_{\bar{y}\bar{y}} \\ \epsilon_{\bar{z}\bar{z}} \\ \epsilon_{\bar{y}\bar{z}} \\ \epsilon_{\bar{z}\bar{x}} \\ \epsilon_{\bar{x}\bar{y}} \end{bmatrix} \quad (1)$$

The $\sigma_{\bar{f}\bar{g}}$ are the stress components, the $\epsilon_{\bar{f}\bar{g}}$ are the strain components, and the C_{ij} are the Cauchy stiffness coefficients. The subscripts on the stresses are determined as follows: the first subscript denotes the direction of the normal to the plane on which the stress acts, and the second subscript denotes the direction in which the stress component acts. For example, $\sigma_{\bar{x}\bar{y}}$ denotes a stress acting on a plane perpendicular to the $\bar{x}$ axis and in the direction of the $\bar{y}$ axis. A similar notation holds for the strain components; i.e., the first subscript denotes the direction of the normal to the plane being strained, and the second subscript denotes the direction in which the strain is taking place.

Of the six stress components, the three having both subscripts the same ($\bar{x}\bar{x}$, $\bar{y}\bar{y}$, $\bar{z}\bar{z}$) are oriented in a direction normal to the surface on which they are acting and thus are called normal stresses. The other three stress components ($\bar{y}\bar{z}$, $\bar{z}\bar{x}$, $\bar{x}\bar{y}$) are oriented in a direction tangential to the surface on which they act and are known as shear stresses.

It is noted that the subscript notation used in Equation (1) for the Cauchy coefficients is dependent only on the position of the coefficient in the array. The particular order in which the elements appear in the stress and strain column matrixes is fairly well standardized, having been used many years ago by A.E.H. Love; Reference 20 is the last edition of his book.

Equation (1) can be rewritten more compactly in matrix notation as follows:

$$[\sigma_i] = [C_{ij}][\epsilon_j] \quad (2)$$

where $[\sigma_i]$ and $[\epsilon_j]$ are the column vectors representing the respective stress and strain components, C_{ij} is the square matrix of Cauchy stiffness coefficients, and the subscripts of the stress and strain components have been redesignated as follows:

$$\bar{x}\bar{x} \rightarrow 1, \quad \bar{y}\bar{y} \rightarrow 2, \quad \bar{z}\bar{z} \rightarrow 3,$$

$$\bar{y}\bar{z} \rightarrow 4, \quad \bar{z}\bar{x} \rightarrow 5, \quad \bar{x}\bar{y} \rightarrow 6$$

An alternate, but more complicated, notation for the stiffness coefficients is Cartesian tensor notation. However, this requires four subscripts on each coefficient*, and thus the simpler double-subscript matrix notation is used here.

Assuming that there are no electromechanical effects and that the deformation takes place isothermally, it can be shown by use of thermodynamics (Reference 22) that Castigliano's theorems must hold for infinitesimal displacements of a linear elastic material.** These theorems can be expressed mathematically as follows:

$$\begin{aligned} \partial U/\partial \varepsilon_{fg} &= \sigma_{fg} \\ \partial U/\partial \sigma_{fg} &= \varepsilon_{fg} \end{aligned} \tag{3}$$

where U is the potential strain energy per unit volume,

$$U = \sum \int \sigma_{fg} \, d\varepsilon_{fg}$$

Equations (3) require that the matrix of Cauchy coefficients be symmetric, i.e.,

$$C_{ji} = C_{ij} \tag{4}$$

A single layer of any known composite material has certain planes of elastic symmetry. In a layer consisting of unidirectionally oriented fibers, the material-symmetry planes are the plane normal to the fibers and any two orthogonal planes parallel to the fibers. In a perpendicularly woven-cloth layer such as used in the experiments reported here, the material-symmetry planes are the two planes normal to the two fiber orientations and the plane of the layer itself. Such a system of three

---

*The general stiffness-coefficient tensor would have $(3)^4 = 81$ elements. However, neglecting microstructural effects (Reference 21) as is customary in classical theory of elasticity, equilibrium requires that the stress tensor be symmetric ($\sigma_{gf} = \sigma_{fg}$) and infinitesimal-displacement kinematics requires that the strain tensor be symmetric ($\varepsilon_{gf} = \varepsilon_{fg}$). Thus, the coefficient tensor would have only 36 independent elements, in agreement with Equation (1).

**In the case of geometrical nonlinearity (large displacements) or material nonlinearity (nonlinear stress-strain relation), the complimentary energy must be used instead of the potential energy (Reference 23).

orthogonal planes of material symmetry is said to be rectangularly orthotropic.* The intersections of the three orthogonal planes of symmetry make three orthogonal axes referred to as the material-symmetry directions. If the Cartesian coordinate axes are selected to coincide with the material-symmetry directions, 24 of the 36 coefficients appearing in the stiffness-coefficient array in Equation (1) disappear. Incorporating this fact, as well as the symmetry relation, Equation (4), the three-dimensional array becomes:

$$\begin{matrix} C_{11} & C_{12} & C_{13} & 0 & 0 & 0 \\ C_{12} & C_{22} & C_{23} & 0 & 0 & 0 \\ C_{13} & C_{23} & C_{33} & 0 & 0 & 0 \\ 0 & 0 & 0 & C_{44} & 0 & 0 \\ 0 & 0 & 0 & 0 & C_{55} & 0 \\ 0 & 0 & 0 & 0 & 0 & C_{66} \end{matrix} \qquad (5)$$

To reduce relation (5) to a two-dimensional case, a state of generalized plane stress is assumed; i.e., the layer is assumed to be sufficiently thin compared to its other dimensions that all three components in the thickness direction are negligible. Thus,

$$\begin{aligned} \sigma_{\bar{z}\bar{z}} &= 0 = C_{31}\,\varepsilon_{\bar{x}\bar{x}} + C_{32}\,\varepsilon_{\bar{y}\bar{y}} + C_{33}\,\varepsilon_{\bar{z}\bar{z}} \\ \sigma_{\bar{y}\bar{z}} &= 0 = C_{44}\,\varepsilon_{\bar{y}\bar{z}} \\ \sigma_{\bar{z}\bar{x}} &= 0 = C_{55}\,\varepsilon_{\bar{z}\bar{x}} \end{aligned} \qquad (6)$$

The last two of Equations (6) imply that the thickness-direction shear strains $\varepsilon_{\bar{y}\bar{z}}$ and $\varepsilon_{\bar{z}\bar{x}}$ are zero.

Although the thickness-direction normal stress $\sigma_{\bar{z}\bar{z}}$ is zero, the thickness-direction normal strain $\varepsilon_{\bar{z}\bar{z}}$ is not zero in general. However, $\varepsilon_{\bar{z}\bar{z}}$ may be expressed in terms of $\varepsilon_{\bar{x}\bar{x}}$ and $\varepsilon_{\bar{y}\bar{y}}$ by means of the first of Equations (6). For a thin orthotropic layer with the coordinate axes $\bar{x}$, $\bar{y}$ coinciding with the material-symmetry directions, the stress-strain relations are

* More complicated classes of elastic symmetry than orthotropic are found in single crystals of crystalline materials (Reference 24), and tree trunks are examples of cylindrically orthotropic material (Reference 25). Also, in micromechanics analyses of fiber-reinforced composites, hexagonal symmetry is sometimes assumed (Reference 26). However, the macroscopic behavior of a thin layer of fiber-reinforced composite material is represented adequately as a rectangularly orthotropic material.

as follows:

$$\begin{bmatrix} \sigma_{\bar{x}\bar{x}} \\ \sigma_{\bar{y}\bar{y}} \\ \sigma_{\bar{x}\bar{y}} \end{bmatrix} = \begin{bmatrix} Q_{11} & Q_{12} & 0 \\ Q_{12} & Q_{22} & 0 \\ 0 & 0 & Q_{66} \end{bmatrix} \begin{bmatrix} \varepsilon_{\bar{x}\bar{x}} \\ \varepsilon_{\bar{y}\bar{y}} \\ \varepsilon_{\bar{x}\bar{y}} \end{bmatrix} \tag{7}$$

where the reduced stiffness coefficients are related to the three-dimensional Cauchy coefficients as follows:

$$\begin{aligned} Q_{11} &= C_{11} - (C_{13}^2/C_{33}) \\ Q_{12} &= C_{12} - (C_{13}C_{23}/C_{33}) \\ Q_{66} &= C_{66} \end{aligned} \tag{8}$$

It is noted that in the array of five non-zero reduced-stiffness coefficients appearing in Equation (7), only four are independent.*

Rather than using the stiffness coefficients, most design and structural engineers use the so-called engineering moduli: Young's elastic moduli E_{11} and E_{22}, Poisson's ratios ν_{12} and ν_{21}, and shear modulus G. They are most easily defined by writing the strains in terms of the stresses as follows:

$$\begin{bmatrix} \varepsilon_{\bar{x}\bar{x}} \\ \varepsilon_{\bar{y}\bar{y}} \\ \varepsilon_{\bar{x}\bar{y}} \end{bmatrix} = \begin{bmatrix} 1/E_{11} & -\nu_{12}/E_{11} & 0 \\ -\nu_{21}/E_{22} & 1/E_{22} & 0 \\ 0 & 0 & 1/G \end{bmatrix} \begin{bmatrix} \sigma_{\bar{x}\bar{x}} \\ \sigma_{\bar{y}\bar{y}} \\ \sigma_{\bar{x}\bar{y}} \end{bmatrix} \tag{9}$$

In view of the symmetry resulting from the general reciprocal relation, Equation (4),

$$\nu_{21}/E_{22} = \nu_{12}/E_{11} \tag{10}$$

Then one of the Poisson's ratios can be expressed in terms of the other and the two Young's moduli. Thus, the four independent engineering elastic moduli for a thin orthotropic layer are E_{11}, E_{22}, ν_{12}, and G.

*It is often assumed that fiber-reinforced composites (especially filament-wound ones) behave isotropically in the plane normal to the fibers. Thus, they are said to be "transversally isotropic", although a better term would be "monotropic" (Reference 27). However, since no thickness-direction quantities enter into the stress-strain relations for a thin member, there is no difference between the elastic coefficients of such a material and an orthotropic one.

Ordinary isotropic materials are a special case of orthotropic materials. However, it is emphasized that there are two necessary and sufficient conditions for a material to be isotropic:

$$E_{22} = E_{11} = E \tag{11}$$

(This implies that $\nu_{21} = \nu_{12} = \nu$)

$$E/G = 2(1 + \nu) \tag{12}$$

Unidirectionally reinforced composites usually have $E_{22} << E_{11}$. In contrast, a bidirectionally reinforced layer, such as a single layer of woven-cloth-reinforced composite, usually has $E_{22} \approx E_{11}$. However, this does not necessarily mean that Equation (12) is satisfied. In fact, for most cloth-reinforced composites, $E/G > 2(1 + \nu)$.

In experimental stress analyses, in which strains rather than stresses are measured experimentally, it is necessary to invert Equations (9), with the following result:

$$\begin{bmatrix} \sigma_{xx} \\ \sigma_{yy} \\ \sigma_{xy} \end{bmatrix} = \begin{bmatrix} E_{11}/\lambda & \nu_{21}E_{11}/\lambda & 0 \\ \nu_{12}E_{22}/\lambda & E_{22}/\lambda & 0 \\ 0 & 0 & G \end{bmatrix} \begin{bmatrix} \epsilon_{xx} \\ \epsilon_{yy} \\ \epsilon_{xy} \end{bmatrix} \tag{13}$$

where

$$\lambda = 1 - \nu_{12}\nu_{21} \tag{14}$$

Direct comparison of the coefficients appearing in Equations (7) and (14) yields the following relations among the reduced-stiffness coefficients and the engineering moduli:

$$Q_{11} = E_{11}/\lambda \quad , \quad Q_{12} = \nu_{21}E_{11}/\lambda = \nu_{12}E_{22}/\lambda \quad , \quad Q_{22} = E_{22}/\lambda \quad , \quad Q_{66} = G \tag{15}$$

Sometimes it is necessary, even in a single-orthotropic layer structure, to refer the elastic coefficients to axes which do not coincide with the material-symmetry axes. An example of this is a rectangular plate consisting of a single orthotropic layer having its major material-symmetry axis oriented at an acute angle with the longest side of the plate. Then the

stress tensor and the strain tensor* transform as a second-rank tensor, and the Mohr stress and strain circles may be used in the two-dimensional case. The transformed stress-strain relations, related to new orthogonal axes x, y which do not coincide with the material-symmetry axes, are written as follows:

$$\begin{bmatrix} \sigma_{xx} \\ \sigma_{yy} \\ \sigma_{xy} \end{bmatrix} = \begin{bmatrix} Q'_{11} & Q'_{12} & Q'_{16} \\ Q'_{12} & Q'_{22} & Q'_{26} \\ Q'_{16} & Q'_{26} & Q'_{66} \end{bmatrix} \begin{bmatrix} \varepsilon_{xx} \\ \varepsilon_{yy} \\ \varepsilon_{xy} \end{bmatrix} \tag{16}$$

where the transformed Q' are related to the aligned Q by the following relations:

$$\begin{bmatrix} Q'_{11} \\ Q'_{12} \\ Q'_{16} \\ Q'_{22} \\ Q'_{26} \\ Q'_{66} \end{bmatrix} = \begin{bmatrix} m^4 & 2m^2\bar{n}^2 & \bar{n}^4 & 4m^2\bar{n}^2 \\ m^2\bar{n}^2 & m^4 + \bar{n}^4 & m^2\bar{n}^2 & -4m^2\bar{n}^2 \\ m^3\bar{n} & m^3\bar{n} - m\bar{n}^3 & m\bar{n}^3 & 2(m^3\bar{n} - m\bar{n}^3) \\ \bar{n}^4 & 2m^2\bar{n}^2 & m^4 & 4m^2\bar{n}^2 \\ -m\bar{n}^3 & -m^3\bar{n} + m\bar{n}^3 & m^3\bar{n} & 2(-m^3\bar{n} + m\bar{n}^3) \\ m^2\bar{n}^2 & -2m^2\bar{n}^2 & m^2\bar{n}^2 & (m^2 - \bar{n}^2)^2 \end{bmatrix} \begin{bmatrix} Q_{11} \\ Q_{12} \\ Q_{22} \\ Q_{66} \end{bmatrix} \tag{17}$$

where $m \equiv \cos \theta_k$, $\bar{n} \equiv \sin \theta_k$. It is noted that since the layer is orthotropic, Q_{16} and Q_{26} do not exist. However, in general, this does not imply that Q'_{16} and Q'_{26} are zero also.

One of the most distinct differences between the elastic behavior of an orthotropic material and that of one which is isotropic is in connection with the directions of principal stresses and of principal strains. In isotropic materials, it is well known that the directions of principal stresses and of principal strains coincide. However, as pointed out very clearly by Greszczuk (Reference 28), this is generally not the case in orthotropic materials. In practical numerical examples he cited, the two principal directions differed by as much as 15 to 30 degrees.

*The ordinary stress components form the stress tensor. However, in order for the strain components to make up a tensor, the ordinary shear strains (such as used here) must be multiplied by a factor of one half. This accounts for the necessity of introducing a factor of one half to shear strains on the Mohr's strain circle.

b. General Symmetrically Laminated Plates

The theory of stiffness of laminated plates presented in this section generally follows the work of Tsai (References 17 and 29), except that in Section 2b, provision is made for symmetrically laminated sets of plies. All plies of a given set are assumed to have the same properties and orientation. By a symmetrically laminated set, we mean one which has corresponding pairs of plies located above and below the midplane of the plate. Then there can be no coupling between bending/twisting effects and in-plane (stretching/plane shear) effects.* Thus, when a symmetrically laminated plate is subject to in-plane loading, no bending effects are induced.

Generally a laminated plate has different stresses in different sets of plies. Thus, one cannot speak of a single stress at a given plate cross section; it is necessary to speak of N, the load resultant expressed in force per "length of run" (width), which is the combined effect of the stresses in the various sets of plies. In general,

$$N'_{fg} = \int_{-h/2}^{h/2} \sigma_{fg}\, dz \tag{18}$$

where h is the total plate thickness, and z is the distance from the midplane of the plate.

The in-plane stiffnesses A_{ij} of a laminated plate are defined as follows:

$$\begin{bmatrix} N'_{xx} \\ N'_{yy} \\ N'_{xy} \end{bmatrix} = \begin{bmatrix} A_{11} & A_{12} & A_{16} \\ A_{12} & A_{22} & A_{26} \\ A_{16} & A_{26} & A_{66} \end{bmatrix} \begin{bmatrix} \epsilon_{xx} \\ \epsilon_{yy} \\ \epsilon_{xy} \end{bmatrix} \tag{19}$$

where, strictly speaking, the ϵ refers to the strain components in the midplane. However, since the only loading considered here is in-plane loading and since there are no bending or twisting effects induced by coupling, within the framework of thin-plate theory, there can be no strain gradients through the thickness. In other words, within the assumptions of the present theory, the in-plane strain components cannot vary through the thickness.

In view of the Equations (18) and (19) and the subsequent discussion, it is clear that the general equation for calculating the composite stiffness coefficients is as follows:

*For treatment of such coupling effects, the reader is referred to the works of Stavsky (Reference 30) and Tsai (Reference 17).

$$A_{ij} \equiv \sum_{n=1}^{N} \int_{-h/2}^{h/2} Q'^{(n)}_{ij} dz \tag{20}$$

where n refers to a typical individual ply, N is the total number of plies, and $Q'_{ij}(n)$ is the reduced elastic coefficient of the nth ply.

Assuming that the elastic coefficients of each individual ply are uniform through the thickness of the ply and that there are K sets of plies (k being a typical set), with all plies in a given set having the same properties oriented in the same direction, Equation (20) becomes

$$A_{ij} = \sum_{k=1}^{K} \sum_{i=1}^{N/K} (z_{i+1} - z_i)\, Q'^{(k)}_{ij} \tag{21}$$

If it is further assumed that all plies have the same thickness and that all K sets have the same number of plies, Equation (21) can be simplified still further as follows:

$$A_{ij} = (h/K) \sum_{k=1}^{K} Q'^{(k)}_{ij} \tag{22}$$

Sometimes it is convenient to express the composite coefficients in the form of engineering properties defined as follows:

$$\begin{aligned} \bar{E}_{11} &= (1 - \bar{\nu}_{12}\bar{\nu}_{21})(A_{11}/h) \\ \bar{E}_{22} &= (1 - \bar{\nu}_{12}\bar{\nu}_{21})(A_{22}/h) \\ \bar{G} &= A_{66}/h \\ \bar{\nu}_{12} &= A_{12}/A_{22} \end{aligned} \tag{23}$$

In all of the theory presented here, the interply shear strain energy has been neglected. This strain energy is due to relative rotation between two adjacent plies, and it has been treated by Clark and Chamis (References 16 and 31). However, for the lamination arrangements used in the present research, this effect would be relatively small.

Tsai (Reference 18) has shown the importance of the residual stresses, caused by thermoelastic effects produced by the difference between the laminating temperature and the operating temperature, in determining failure of laminates. However, since all of the laminates used in the present program were made under closely controlled conditions and tested at temperatures which varied very little, this effect would be the same (i.e., a constant factor) in all of the tests covered. Thus, in the theory presented here, thermoelastic effects are omitted for

brevity. More detailed information on this topic is given in References 16 and 32.

c. Parallel-Ply Laminates

Any parallel-ply laminate consisting of identical layers is obviously symmetrically laminated. Then K = 1 and Equation (22) becomes

$$A_{ij} = h\, Q'_{ij} \tag{24}$$

It is convenient to select the composite reference axes to coincide with the material-symmetry axes. Then $\theta = 0$ and Equation (24) can be rewritten as follows:

$$A_{ij} = h\, Q_{ij} \tag{25}$$

Specifically,

$$\begin{aligned} A_{11} &= h\, Q_{11} = h\, E_{11}/\lambda \\ A_{12} &= h\, Q_{12} = h\, \nu_{12}\, E_{22}/\lambda \\ A_{22} &= h\, Q_{22} = h\, E_{22}/\lambda \\ A_{66} &= h\, Q_{66} = h\, G; \quad A_{16} = A_{26} = 0 \end{aligned} \tag{26}$$

Obviously,

$$\bar{E}_{11} = E_{11}, \quad \bar{E}_{22} = E_{22}, \quad \bar{G} = G, \quad \bar{\nu}_{12} = \nu_{12} \tag{27}$$

It is noted that a parallel-ply laminate consisting of identical orthotropic layers behaves orthotropically also.

d. Cross-Ply Laminates

The smallest number of plies with which it is possible to have a symmetrically laminated cross-ply laminate is four, as shown schematically in Figure 1.

The cross-ply laminate consists of two sets of layers, i.e., K = 2. The layers aligned in the same direction as the outer layers (in the case of a four-ply laminate, these are the outer layers only) are designated as set 1, and the other layers (i.e., the perpendicular layers) are designated as set 2. Then Equation (22) becomes

$$A_{ij} = (h/2)\ [Q'^{(1)}_{ij} + Q'^{(2)}_{ij}] \tag{28}$$

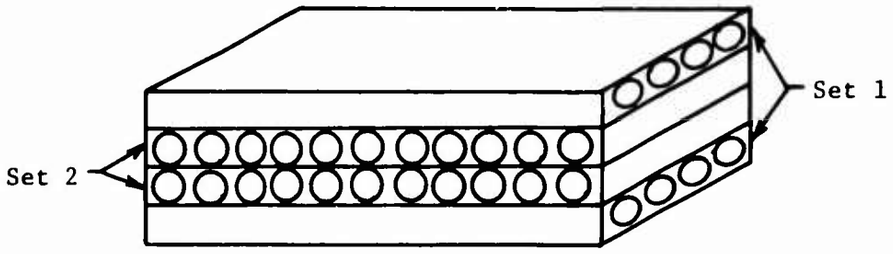

Figure 1. Schematic Diagram of Symmetrically Laminated Cross-Ply Composite.

For convenience, the direction of major material symmetry of set 1 is designated as direction 1 of the composite. Then

$$Q'^{(1)}_{ij} = Q_{ij}$$
$$Q'^{(2)}_{ij} = Q_{ij} \tag{29}$$

Specifically,

$$A_{11} = (h/2)(Q_{11} + Q_{22}) = (h/2)(E_{11} + E_{22})/(1 - \nu_{12}\,\nu_{21})$$
$$A_{12} = (h/2)(Q_{12} + Q_{21}) = h\,Q_{12} = h\,\nu_{12}E_{22}/(1 - \nu_{12}\,\nu_{21})$$
$$A_{22} = (h/2)(Q_{22} + Q_{11}) = (h/2)(E_{22} + E_{11})/(1 - \nu_{12}\,\nu_{21}) = A_{11} \tag{30}$$
$$A_{66} = (h/2)(Q_{66} + Q_{66}) = h\,Q_{66} = hG$$
$$A_{16} = A_{26} = 0$$

Then

$$\bar{E}_{11} = (1/2)(E_{11} + E_{22}) = E_{22}, \quad G = G$$
$$\bar{\nu}_{12} = \nu_{12}\,(2E_{22})/(E_{11} + E_{22}) \tag{31}$$

It is noted that a symmetrically laminated cross-ply laminate has identical Young's moduli ($\bar{E}_{11} = \bar{E}_{22}$), but it nevertheless behaves orthotropically (rather than isotropically) because $\bar{G} \neq \bar{E}/[2(1 + \bar{\nu})]$.

Care must be exercised in interpreting strain-gage data obtained on cross-ply laminates. This is shown by the following analysis. For set 1,

$$\begin{bmatrix} \sigma_{11}^{(1)} \\ \sigma_{22}^{(1)} \\ \sigma_{66}^{(1)} \end{bmatrix} = \begin{bmatrix} Q_{11}^{(1)} & Q_{12}^{(1)} & 0 \\ Q_{12}^{(1)} & Q_{22}^{(1)} & 0 \\ 0 & 0 & Q_{66}^{(1)} \end{bmatrix} \begin{bmatrix} \varepsilon_{11} \\ \varepsilon_{22} \\ \varepsilon_{66} \end{bmatrix} \tag{32}$$

A similar group of relationships holds for set 2.

To determine the actual biaxial-load ratio attained in the test section, another set of relations is necessary. For gages aligned with the material-symmetry axes,

$$N_{11} = A_{11}\ \varepsilon_{11} + A_{12}\ \varepsilon_{22}$$

$$N_{22} = A_{12}\ \varepsilon_{11} + A_{22}\ \varepsilon_{22}$$

Thus

$$N_{22}/N_{11} = (A_{12}\ \varepsilon_{11} + A_{22}\ \varepsilon_{22})/(A_{11}\ \varepsilon_{11} + A_{12}\ \varepsilon_{22})$$

or

$$N_{22}/N_{11} = [A_{12} + A_{22}\ (\varepsilon_{22}/\varepsilon_{11})]/[A_{11} + A_{12}\ (\varepsilon_{22}/\varepsilon_{11})]$$

or

$$N_{22}/N_{11} = [\bar{\nu}_{12} + (\varepsilon_{22}/\varepsilon_{11})]/[1 + \bar{\nu}_{12}\ (\varepsilon_{22}/\varepsilon_{11})] \tag{33}$$

e. Quasi-Isotropic Laminates

Werren and Norris (Reference 33) have shown mathematically that it is possible to orient the individual layers (or sets of layers) in multiple-layer laminates in such a way that the resulting in-plane elastic behavior is isotropic, i.e., has elastic coefficients which are independent of orientation in the plane. The conditions which must be met by the laminating arrangement to achieve this isotropic behavior are as follows: (1) there must be three or more sets of layers, (2) the individual layers must have identical thicknesses and identical orthotropic elastic coefficients with respect to their material-symmetry axes, and (3) a typical set of layers k (ranging from one to K) must be oriented at the following angle with respect to a reference direction:

$$\theta_k = \pi\ (k - 1)/K \tag{34}$$

In the light of the coupled theory (References 17 and 30), the Werren-Norris design would be isotropic with respect to in-plane stiffness,

but not with respect to bending stiffness and bending/in-plane coupling. Thus, the Werren-Norris design is called quasi-isotropic here.

To apply Equation (22) with the $Q_{ij}^{(k)}$ given by Equation (17) and the θ_k given by Equation (34), certain sums presented by Werren and Norris (Reference 33) are needed:

$$\sum_{k=1}^{K} \cos^4 [\pi(k - 1)/K] = \sum_{k=1}^{K} \sin^4 [\pi(k - 1)/K] = 3K/8$$

$$\sum_{k=1}^{K} \sin^2 [\pi(k - 1)/K] \cos^2 [\pi(k - 1)/K] = K/8 \tag{35}$$

$$\sum_{k=1}^{K} \cos^3 [\pi(k - 1)/K] \cos [\pi(k - 1)/K]$$

$$= \sum_{k=1}^{K} \cos [\pi(k - 1)/K] \sin^3 [\pi(k - 1)/K] = 0$$

The elements of the in-plane stiffness matrix are given by the following expressions:

$$\begin{aligned} A_{11}/h &= A_{22}/h = (1/8)[3(Q_{11} + Q_{22}) + 2(Q_{12} + Q_{66})] \\ A_{12}/h &= (1/8)(6\, Q_{12} + Q_{11} + Q_{22} - 4\, Q_{66}) \\ A_{66}/h &= (1/8)(4\, Q_{66} + Q_{11} + Q_{22} - 2\, Q_{12}) \\ A_{16}/h &= A_{26}/h = 0 \end{aligned} \tag{36}$$

It is noted that since $A_{16} = A_{26} = 0$, the in-plane stiffness exhibits at least orthotropic symmetry. Furthermore, since $A_{11} = A_{22}$ and $A_{66} = (1/2)(A_{11} - A_{12})$, the in-plane stiffness has complete symmetry, i.e., it is isotropic. It is important to notice that the A_{ij} are unaffected by the order of lamination; i.e., the (n + 1) layer does not have to be next to the n layer, etc. Also, the A_{ij} are independent of the number of layers N.

Converting the above expressions, Equations (36), to engineering moduli yields the following results:

$$\begin{aligned} \bar{\nu} &= (E_{11} + E_{22} + 6\nu_{21}E_{11} - 4\lambda G)/(3E_{11} + 3E_{22} + 2\nu_{21}E_{11} + 4\lambda G) \\ \bar{E} &= (1/8)(1 - \nu^{-2})\lambda^{-1}(3E_{11} + 3E_{22} + 2\nu_{21}E_{11} + 4\lambda G) \\ \bar{G} &= \bar{E}/[2(1 + \bar{\nu})] \end{aligned} \tag{37}$$

3. THEORY OF THE STRENGTH OF COMPOSITE PLATES SYMMETRICALLY LAMINATED OF ORTHOTROPIC LAYERS AND SUBJECT TO IN-PLANE BIAXIAL LOADING

Unlike the theory of stiffness presented in Section 2, there is no universal agreement as to the appropriate macroscopic theory to describe the strength of anisotropic composites under multiaxial loading. As in the case of monolithic metallic alloys, certain theories fit certain materials; while some materials exhibit different modes of failure depending upon the temperature, rate of loading, and other environmental conditions, and thus require different theories for different conditions.

In composite materials, there are at least three distinct methods of predicting multiaxial strength:

(1) Empirical and semiempirical macroscopic theories

(2) Fracture mechanics (for brittle materials)

(3) Plastic tensile instability (for ductile materials)

Of these three approaches, only the first one is adequately developed at present for direct comparison with experimental results. Approaches of this type are reviewed in Section 3a and compared with the limited test data previously available in Section 3b. The theories reviewed in Section 3a are applied to symmetrically laminated composite plates in Section 3c.

The application of fracture mechanics to anisotropic materials is in such an embryonic stage that this approach has not yet been extended to the case of multiaxial loading. However, for those readers desiring information on the subject of fracture mechanics of anisotropic and composite materials, this topic is included in the Selected Bibliography presented at the end of this report. Although Hill's theory of orthotropic plasticity has been applied to prediction of plastic tensile instability (ductile fracture) of orthotropic sheets subject to in-plane biaxial loading, the Hill theory itself has not been adequately verified for fibrous composites. However, theories of anisotropic plasticity and plastic tensile instability in anisotropic materials are included in the Selected Bibliography.

a. Strength Theories for Single-Layer Orthotropic Composite Materials

Perhaps the most widely used yield-strength criterion for orthotropic materials is the following one proposed in 1948 by Hill (Reference 34) as follows (for the general three-dimensional case):

$$H_1 (\sigma_2 - \sigma_1)^2 + H_2 (\sigma_3 - \sigma_1)^2 + H_3 (\sigma_1 - \sigma_2)^2 + 2H_4 \sigma_4^2 + 2 H_5 \sigma_5^2 + 2H_6 \sigma_6^2 = 1 \qquad (38)$$

Equation (38) has been found to predict with sufficient accuracy the initial yielding of many metallic alloys. Since Equation (38) coincides with the von Mises yield criterion for the case of a material which is isotropic, it can be considered to be a generalization of that criterion. The major limitations of Equation (38) are that it assumes that hydrostatic stress ($P_h = \sigma_1 + \sigma_2 + \sigma_3$) does not affect yielding and that the yield strengths in simple compression are identical to the yield strengths in simple tension along the same axes.

For the case of a thin layer, $\sigma_3 = \sigma_4 = \sigma_5 = 0$; i.e., a state of generalized plane stress (GPS) exists. Then Equation (38) reduces to the following relation:

$$(\sigma_1/S_1)^2 + (\sigma_2/S_2)^2 - r^{-1}\,(\sigma_1/S_1)(\sigma_2/S_2) + (\sigma_6/S_6)^2 = 1 \qquad (39)$$

It is noted that Equation (39) can be visualized as a surface in three-dimensional stress space (σ_1, σ_2, σ_6) as shown in Figure 2. Despite the fact that the failure surface is three-dimensional, the type of failure being depicted is due to a planar stress system. This is definitely more complicated than in the case of a simple isotropic material, for which GPS failure can be represented by a curve in two-dimensional stress space (σ_1, σ_2), as discussed in References 35 and 36. The reason for the additional complexity in the case of materials which behave anisotropically is that failure is definitely affected by the amount of shear stress acting on the planes normal to the material-symmetry axes. In contrast, in a simple isotropic material, one can select directions (principal-stress directions) such that no shear stress acts and these coincide with material-symmetry directions, since any direction is one of the latter. The three-dimensional failure surface representation of failure of anisotropic materials under GPS conditions has been used by Norris (Reference 37), Ashkenazi (References 38 and 39), and Chamis (Reference 16). Finally, it should be mentioned that failure as discussed in connection with plots such as Figure 3 can be defined in any manner desired for the particular application: initial yielding, 0.2-percent offset yield, 100,00 cycles of fatigue loading, 10,000 hours of elevated-temperature life, ultimate, etc. Here, failure is construed to mean initial yielding only.

Tsai (Reference 18) showed that if the material is assumed to be a unidirectional fiber-reinforced composite having the same properties in the thickness direction as it has in the plane normal to the fibers, $r = S_1/S_2$ and Equation (39) becomes

$$(\sigma_1/S_1)^2 + (\sigma_2/S_2)^2 - (\sigma_1\sigma_2/S_1^2) + (\sigma_6/S_6)^2 = 1 \qquad (40)$$

Norris and McKinnon (Reference 40) suggested the following strictly empirical strength relationship:

$$(\sigma_1/S_1)^2 + (\sigma_2/S_2)^2 + (\sigma_6/S_6)^2 = 1 \qquad (41)$$

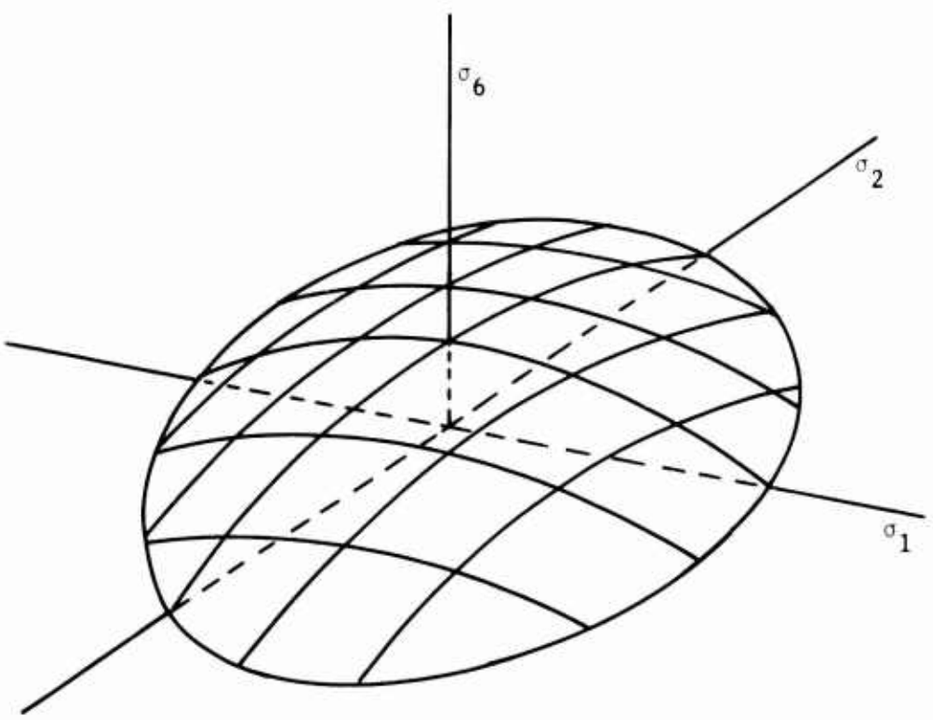

Figure 2. Possible GPS Failure Surface Predicted by Hill and Tsai.

Later Norris (Reference 37) derived the following relationships by assuming that the distortional energy at failure was a constant:

$$(\sigma_1/S_1)^2 + (\sigma_2/S_2)^2 - (\sigma_1/S_1)(\sigma_2/S_2) + (\sigma_6/S_6)^2 = 1 \qquad (42)$$

$$(\sigma_2/S_2)^2 = 1 \qquad (43)$$

$$(\sigma_1/S_1)^2 = 1 \qquad (44)$$

It is noted that Equation (42) is a special case (r = 1) of Equation (39). Apparently Equation (42) was also derived independently by Ashkenazi (Reference 41). The GPS failure surface predicted by Equations (42) through (44) is shown in Figure 3.

In several theories, provision was made for hydrostatic-stress effects; namely, in the work of Marin (Reference 42), Hu and Pae (Reference 43), and Bert et al (Reference 36). The latter investigators proposed the following form of relationship for the generalized-plane-stress case:

$$B_1 \sigma_1^2 + B_2 \sigma_2^2 + B_3 \sigma_1 \sigma_2 + B_4 \sigma_1 + B_5 \sigma_2 = 1 \qquad (45)$$

It is interesting to note that Equation (45) is the equation of a generalized conic curve and that it has five constants which can be determined experimentally by five tests in the tension-tension quadrant: uniaxial tension at 0 and 90 deg, and 1:1, 1:2, and 2:1 biaxial tension at 0 deg. However, it should be noted that Equation (45) is applicable only to cases when the principal-stress directions coincide with the material-symmetry directions, since it does not contain σ_6.

The maximum-strain failure criterion has been proposed by some recent investigators (Reference 44); however, no experimental verification of this criterion has been published. Also, recently McGill (Reference 45) showed that the classical representation of this criterion for GPS conditions was incorrect.

Several attempts have been made to account for the known difference between tensile and compressive strengths in actual fibrous composites. The first of these was Norris, who suggested that in applying Equations (42) through (44), if σ_i (i = 1, 2) is tensile, then the tensile S_i should be used. Another approach was used by Stassi-D'Alia (Reference 46); his proposed relation is as follows for the case of biaxial principal stresses aligned with the material-symmetry axes:

$$\sigma_1^2 + \sigma_2^2 - \sigma_1 \sigma_2 + S_1^T (K - 1)(\sigma_1 + \sigma_2) = KS_1^T \qquad (46)$$

where $K = S_1^C/S_1^T$ and S_1^C and S_1^T are the compressive and tensile strengths in direction 1. In this theory, it is assumed that yielding occurs when the octahedral shear stress reaches a value which is proportional to the hydrostatic stress. However, as pointed out by Chamis

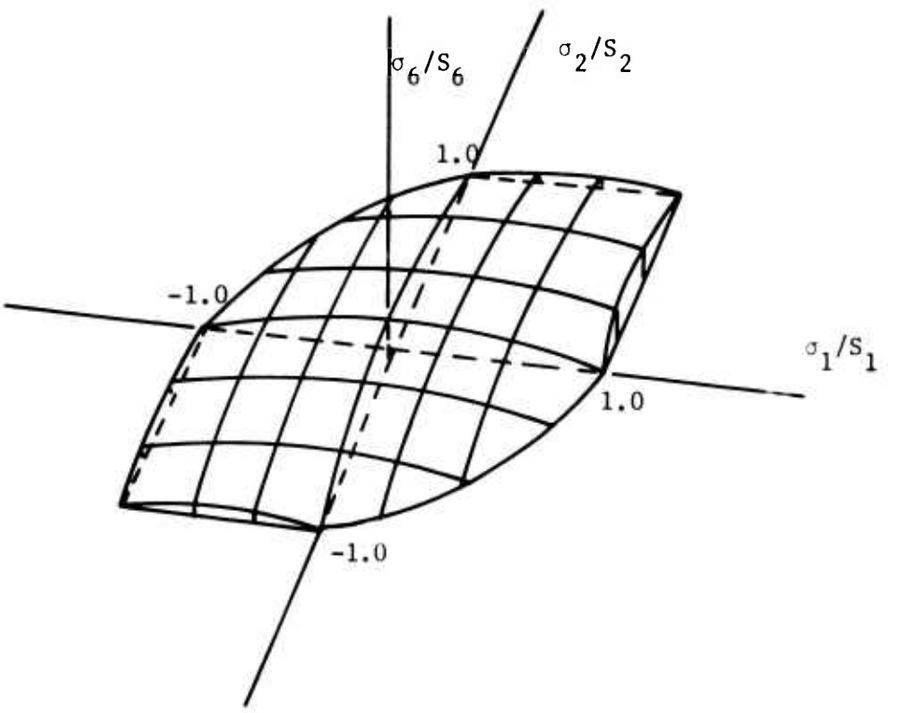

Figure 3. Possible GPS Failure Surface Predicted by Norris.

(Reference 16), in the Stassi-D'Alia theory, it is implied that the following relationship holds:

$$S_2^C/S_2^T = S_1^C/S_1^T \tag{47}$$

Unfortunately, actual filamentary composites do not generally satisfy Equation (47).

Hoffman (Reference 47) has extended the work of Hill to account for different strengths in tension and compression. For the general three-dimensional case, his result can be expressed as follows:

$$H_1 (\sigma_2 - \sigma_1)^2 + H_2 (\sigma_3 - \sigma_1)^2 + H_3 (\sigma_1 - \sigma_2)^2 + 2H_4 \sigma_4^2$$

$$+ 2H_5 \sigma_5^2 + 2H_6 \sigma_6^2 + H_7 \sigma_1 + H_8 \sigma_2 + H_9 \sigma_3 = 1 \tag{48}$$

The nine coefficient H_1 through H_9 are uniquely determined by nine simple tests: three uniaxial tensile strengths, three uniaxial compressive strengths, and three pure shear strengths. When the compressive strength along each material-symmetry axis is equal to the corresponding tensile strength, H_7 through H_9 vanish and Equation (48) reduces to Hill's relation, Equation (38).

Further assuming that the material is a unidirectional one having the same properties in the thickness and transverse planar directions, Hoffman reduced Equation (48) to the following for the generalized-plane-stress case:

$$(\sigma_1^2/S_1^C S_1^T) + (\sigma_2^2/S_1^C S_1^T) - (\sigma_1 \sigma_2/S_1^C S_1^T) + [(S_1^T)^{-1}$$

$$- (S_1^C)^{-1}] \sigma_1 + [(S_2^T)^{-1} - (S_2^C)^{-1}] \sigma_2 + (\sigma_6/S_6)^2 = 1 \tag{49}$$

It is noted that when $S_1^C = S_1^T$ and $S_2^C = S_2^T$, Equation (49) reduces to Tsai's result, Equation (40). The GPS failure surface corresponding to Equation (48) is shown in Figure 4.

Gol'denblat and Kopnov (Reference 48) have used tensor consic rations to arrive at a failure theory even more general than Hoffman's, because they took into consideration the dependence of shear strength on direction (i.e., sign).

Recently, Capurso (Reference 49) presented a yield condition which is a generalization of the Tresca maximum-shear-stress yield condition to the case of an orthotropic material with different tensile and compressive strength. However, unlike all of the other theories which take into consideration $\sigma_i^T \neq \sigma_i^C$, this theory is unaffected by hydrostatic stress.

All of the failure criteria discussed so far have been phenomenological in nature and have not taken into account any specific mechanism of failure or any mechanical properties of the individual constituent materials. One of the earliest attempts to take these latter aspects into consideration was made by Stowell and Liu (Reference 50), who proposed a simple mechanistic model having three failure modes: fiber failure, matrix shear failure, and matrix transverse failure. However, they have applied their criterion to only the case of uniaxial loading applied at any arbitrary angle to the major material-symmetry axis of the composite.

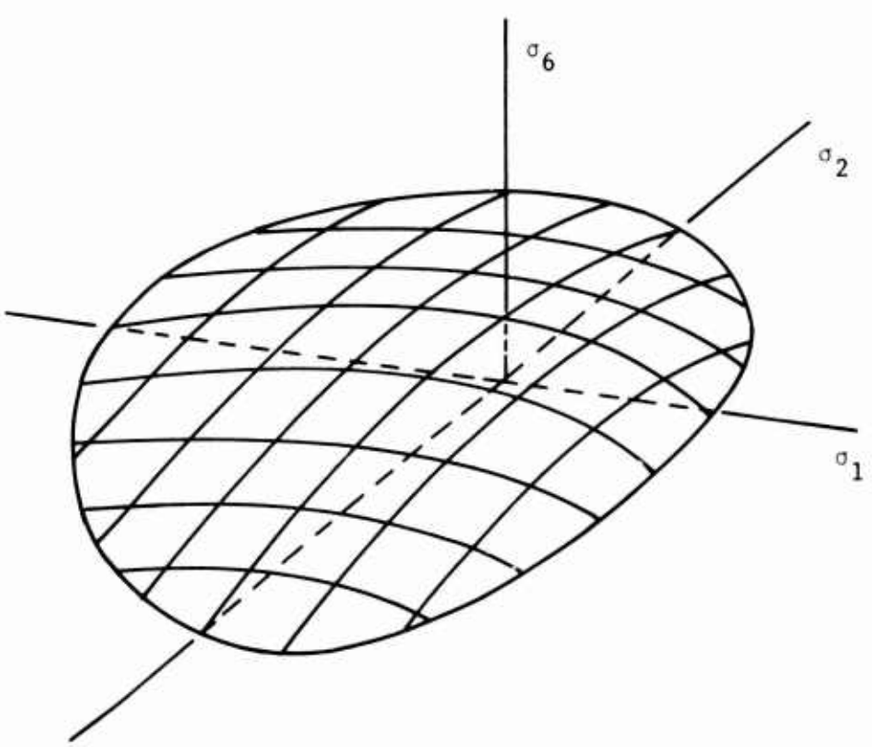

Figure 4. Possible GPS Failure Surface Predicted by Hoffman's Criterion for S_1^C/S_1^T and S_2^C/S_2^T,

Additional research on the distortion-energy criterion was carried out by Griffith and Baldwin (Reference 51), and Chamis (Reference 16) extended their work to incorporate different tensile and compressive strengths. For the generalized-plane-stress case, Chamis' equation can be written as follows:

$$(\sigma_1^\alpha/S_1^\alpha)^2 + (\sigma_2^\beta/S_2^\beta)^2 - K_{\alpha\beta}\,(\sigma_1^\alpha/|S_1^\alpha|)$$

$$(\sigma_2^\beta/|S_2^\beta|) + (\sigma_6/S_6)^2 = 1 \qquad (50)$$

where α, β = T or C, i.e., tension or compression, and $K_{\alpha\beta}$ is an empirical constant determined from biaxial tests. The way in which Chamis has taken into consideration different tensile and compressive strengths is to empirically determine a different $K_{\alpha\beta}$ for different quadrants, i.e., $K_{CC} \neq K_{TT} \neq K_{CT}$. Also, as he pointed out, the surface may have discontinuous derivatives at the quadrant junctures, as shown in Figure 5.

b. Comparison of Strength Predictions with Existing Test Data for Single-Layer Orthotropic Materials

The sparse amount of experimental strength data on composite materials available for comparison with various strength theories has been limited to three kinds of loading: (1) uniaxial loading (tension and compression) at various off-axis orientations, (2) pure shear loading at various orientations, and (3) biaxial loading.

For the case of uniaxial loading at an angle θ with the major material-symmetry axis, the applied uniaxial stress σ_1' must be resolved into components along the material-symmetry axes as follows:

$$\sigma_1 = \sigma_1' m^2, \quad \sigma_2 = \sigma_1' \bar{n}^2, \quad \sigma_6 = -\sigma_1' m\bar{n} \qquad (51)$$

where as before $m = \cos \theta_k$ and $\bar{n} = \sin \theta_k$.

These stress components can now be substituted in any desired strength theory to obtain a theoretical prediction of off-axis strength.

The Forest Products Laboratory has obtained fair to good agreement between the Norris distortion-energy strength theory, Equation (42), and experimental uniaxial data for plywood (Reference 37) and various glass fabrics impregnated with various resins (References 52, 53, and 54).

Recently Tsai et al (Reference 55) have compared off-axis uniaxial tension and compression data for a unidirectional glass fiber/epoxy laminate with the predictions of the maximum-normal-stress, maximum-shear-stress, and distortion-energy theories. They found the best agreement with the Tsai version of the distortion-energy theory, Equation (40), where tensile properties (S_1^T, S_2^T) were used for tension loading and (S_1^C, S_2^C) were used for compressive loading. In Reference 47, Hoffman showed good agreement between his generalized strength theory predictions and both tensile and compressive off-axis uniaxial data for GRP.

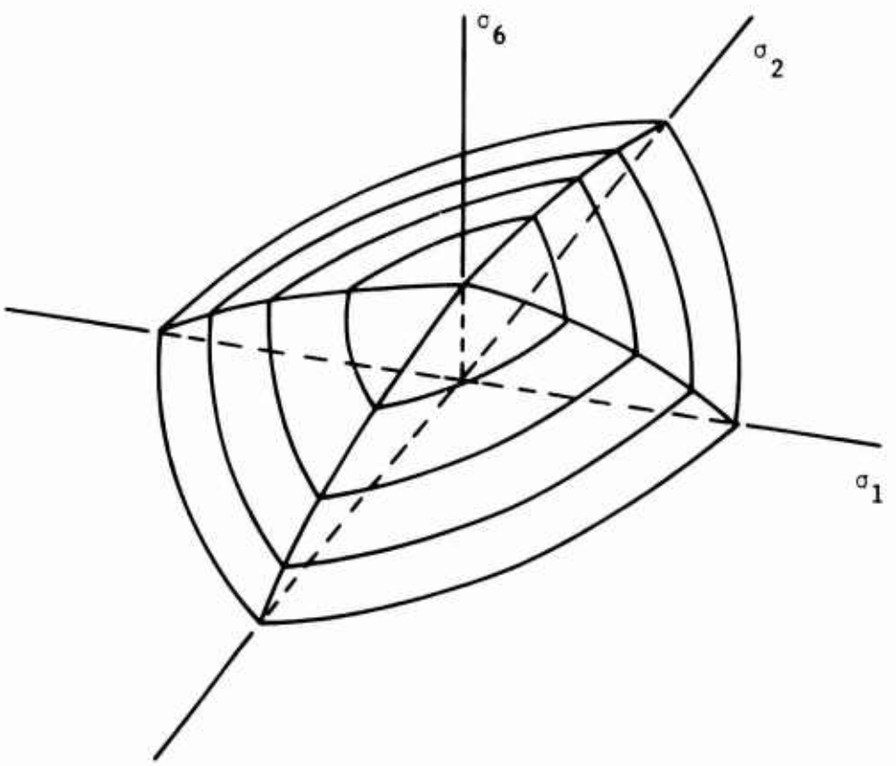

Figure 5. Possible GPS Failure Surface Predicted by Chamis.

For pure shear loading at an off-axis angle, the applied shear stress σ_6' must be resolved into the following material-symmetry stress components:

$$\sigma_1 = 2\sigma_6' \, mn, \quad \sigma_2 = -2\sigma_6' \, mn, \quad \sigma_6 = \sigma_6' \, (m^2 - n^2) \tag{52}$$

Data from off-axis pure-shear tests have been quite limited. In tests on plywood (Reference 37) and various glass-fabric/resin combinations (References 52, 53, and 54), the agreement with the Norris distortion-energy criterion was rather poor. Only very limited data are available on strength of composites under biaxial loading, apparently all for the aligned case (i.e., $\theta = 0$). Ely (Reference 56) tested glass-fabric/epoxy circular tubes subject to combinations of hoop tension and axial compression. He used the Stassi-D'Alia theory to test his results, with good agreement. However, Chamis (Reference 16) showed later that Ely's test results could also be represented by the Chamis empirical criterion.

Weng (Reference 57) tested two grades of graphite composite, in the form of circular tubes, under biaxial loading in all four quadrants (tension T/compression C, T/T, C/T, C/C). The results were fitted well by the Chamis empirical criterion with a different value of $K_{\alpha\beta}$ for each quadrant (see Table II.)

TABLE II. VALUES OF $K_{\alpha\beta}$ IN THE CHAMIS EMPIRICAL CRITERION FOR VARIOUS COMPOSITE AND BIAXIAL-LOADING QUADRANTS

Material	Quadrant	$K_{\alpha\beta}$
Glass-fabric/epoxy	C/T	- 0.36
Grade JT graphite	T/T	0.50 to 0.90
	T/C	0.40
	C/C	1.00 to 1.45
	C/T	0.40
Grade ATJ graphite	T/T	- 0.6 to - 1.60
	T/C	0 to 1.20
	C/C	0 to - 1.20
	C/T	0.6 to 1.20

Gol'denblat and Kopnov (Reference 48) showed good agreement with their theory for two kinds of FRP in all four quadrants.

In the present work, some of the biaxial-load tests were conducted with the biaxial principal stresses σ_1' and σ_2' aligned at an angle ($\theta = 45$ deg) to the material-symmetry axes. In this case, the stress components associated with the material-symmetry axes can be calculated from the following equations:

$$\begin{aligned} \sigma_1 &= \sigma_1' m^2 + \sigma_2' \bar{n}^2 \\ \sigma_2 &= \sigma_1' \bar{n}^2 + \sigma_2' m^2 \\ \sigma_6 &= -(\sigma_1' - \sigma_2') m\bar{n} \end{aligned} \tag{53}$$

c. Strength of Symmetrically Laminated Composite Plates

The strength of laminated composite plates can be quite different than that of a single layer, even in the case of symmetrical lamination. This is due to three factors: (1) the heterogeneity of the composite in the thickness direction, (2) the thermally induced residual stresses, and (3) interply strain energy.

Perhaps the first investigator to consider the heterogeneity of the composite in the thickness direction was Tsai (Reference 18), who applied a failure criterion to each ply to determine which one failed (yielded) first and then used degraded properties for each failed ply to determine a new stress distribution until complete failure (i.e., failure of all of the plies) occurred. This concept was extended further by Tsai et al (Reference 55).

Tsai (Reference 18) also included the effect of the residual stresses which are induced thermally due to the difference between the laminate curing temperature and the operating temperature. Since this factor is very nearly constant in the experimental program reported here, as mentioned in Section 2b, this effect is omitted in the present analytical work.

The effect of interply shear strain energy on strength was discussed in detail by Chamis (Reference 16). However, as mentioned in Section 2h, this effect is relatively small and thus is neglected in the present analysis.

Although, so far as is known by the present investigators, the effect of filament crossovers has not been considered theoretically in any published analysis, it was discussed qualitatively by Tsai et at (Reference 55).

For the present case, the use of symmetric lamination arrangements eliminates coupling between in-plane and out-of-plane effects.

Furthermore, since the loading is applied in the plane, no bending moments are induced. Under these simplified conditions, Tsai's general analysis is reduced considerably. The strains can be found by inverting Equation (19) as follows:

$$\begin{bmatrix} \varepsilon_{xx} \\ \varepsilon_{yy} \\ \varepsilon_{xy} \end{bmatrix} = \begin{bmatrix} A^*_{11} & A^*_{12} & A^*_{16} \\ A^*_{12} & A^*_{22} & A^*_{26} \\ A^*_{16} & A^*_{26} & A^*_{66} \end{bmatrix} \begin{bmatrix} N_{xx} \\ N_{yy} \\ N_{xy} \end{bmatrix} \tag{54}$$

where the $[A^*_{ij}]$ matrix represents the inverse of the $[A_{ij}]$ matrix. An alternative but equivalent approach is to use Equations (23) to compute E_{11}, E_{22}, G, and ν_{12} and to use the following relationships:

$$\begin{bmatrix} \varepsilon_{xx} \\ \varepsilon_{yy} \\ \varepsilon_{xy} \end{bmatrix} = (1/h) \begin{bmatrix} (\bar{E}'_{11})^{-1} & -\bar{\nu}'_{12}/\bar{E}'_{11} & (\bar{\beta}'_{12})^{-1} \\ -\bar{\nu}_{12}/\bar{E}'_{11} & (\bar{E}'_{22})^{-1} & (\bar{\beta}'_{21})^{-1} \\ (\bar{\beta}'_{12})^{-1} & (\bar{\beta}'_{21})^{-1} & (\bar{G}')^{-1} \end{bmatrix} \begin{bmatrix} N_{xx} \\ N_{yy} \\ N_{xy} \end{bmatrix} \tag{55}$$

where

$$(\bar{E}'_{11})^{-1} = (\bar{E}_{11})^{-1} m^4 + \bar{L}\, m^2 \bar{n}^2 + (\bar{E}_{22})^{-1} \bar{n}^4$$

$$(\bar{E}'_{22})^{-1} = (\bar{E}_{11})^{-1} \bar{n}^4 + \bar{L}\, m^2 \bar{n}^2 + (\bar{E}_{22})^{-1} m^4$$

$$\bar{\nu}'_{12}/\bar{E}'_{11} = (\bar{\nu}_{12}/\bar{E}_{11}) - \bar{M}\, m\bar{n}$$

$$(\bar{G}')^{-1} = (\bar{G})^{-1} + 4\bar{M}\, m\bar{n}$$

$$(\bar{\beta}'_{12})^{-1} = [(\bar{E}_{22})^{-1} \bar{n}^2 - (\bar{E}_{11})^{-1} m^2 + (\bar{L}/2)(m^2 - \bar{n}^2)]\, 2\, m\bar{n}$$

$$(\bar{\beta}'_{21})^{-1} = [(\bar{E}_{22})^{-1} m^2 - (\bar{E}_{11})^{-1} \bar{n}^2 + (\bar{L}/2)(m^2 - \bar{n}^2)]\, 2\, m\bar{n}$$

$$\bar{L} = (\bar{G})^{-1} - (\bar{\nu}_{12}/\bar{E}_{11}) - (\bar{\nu}_{21}/\bar{E}_{22})$$

$$\bar{M} = (\bar{E}_{11})^{-1} + (\bar{E}_{22})^{-1} - \bar{L}$$

Once the strains are determined from either Equation (54) or Equation (55), the stresses in the respective layer can be calculated by use of Equation (16). Then the stress components can be expressed in terms of the desired strength theory as presented in Section 3a.

4. SPECIMEN DESIGN, DEVELOPMENT, AND PRELIMINARY EVALUATION

As mentioned in Section 1, the primary objective of this research is the mechanical characterization of laminated composite materials, with particular emphasis on biaxial loading. The separate determination of the uniaxial tensile and shear properties was necessary to complete the characterization of the material and to permit correlation with theoretical predictions of stiffness and strength.

This section discusses the basic philosophy, experimental development, and final design of the test specimens in the data gathering portion of the research program.

a. Biaxial-Loading Specimens

Reference 36 contains a critique of the various kinds of specimens used to obtain biaxial-load test data for metallic alloys. Some of the same kinds of specimens have been used to obtain limited biaxial-load test data for composites. Closed-end, thin-walled, internally pressurized cylinders of glass-filament-wound construction have been used to simulate solid-propellant rocket-motor casings (Reference 58). However, only one biaxial-load condition (tension 1:2) was covered, and the results of such tests are affected by stress nonuniformities near the ends. To obtain data for deep-diving submersible applications, some tests have been conducted on cylindrical shells subject to external pressure, giving a 1:1 compression biaxial-load condition (Reference 59).

Recently cruciform sandwich-beam specimens have been used to determine biaxial yield strengths of boron-fiber-reinforced plastic (Reference 60). The disadvantages of this type of specimen are the stress concentrations produced at the corner fillets, the possible effect of the core-to-facing bond on the laminate strength, and the fact that the facings experience some bending action in addition to the primary membrane action.

In biaxial-load tests on metals, Terry and McClaren (Reference 61) used flat specimens with a reduced-thickness test section and four loading pins. In crack propagation tests under biaxial loading, Douglas Aircraft Division (Reference 62) used a machined slit to simulate a crack (instead of a reduced thickness test section) and eight loading pins. In some very recent FRP laminates tests reported after the present program began, there was no reduced-thickness section and four loading pins were used (Reference 63).

The basic philosophy underlying the development of the biaxial-loading specimens was to evolve flat laminate specimens which were simple to fabricate and yet capable of developing high-stress levels and a uniform tension stress field of prescribed biaxial-load ratio in the test section.

To eliminate bending and twisting effects induced by in-plane loading,

it was decided to use symmetrical laminating arrangements. This eliminated coupling between in-plane and out-of-plane effects, as discussed in Section 2.

Preliminary tests indicated that the thicker section of the specimens should be approximately three times as thick as the reduced-thickness test section. This choice is predicated on the following considerations: If there is not sufficient difference in thickness between the test section and the remainder of the specimen, failure would usually occur in the vicinity of the grips. (This occurred in all of the nonreduced-thickness-section specimens reported in Reference 63.) On the other hand, if there is too much difference in thickness, three-dimensional geometric stress concentration would artificially raise the stress level at the edge of the test section. Fortunately, the natural filleting which occurs in the fabrication of the specimens (see Section 6a) helps to reduce this stress concentration. Another limitation is the maximum thickness of laminate from which excess resin can be successfully bled.

A series of preliminary uniaxial tension tests brought out what turned out to be the most critical problem in the development of the specimens: the problem of achieving adequate load-carrying capacity in the metal tabs used to transfer the load from the loading device to the specimen. (The loading device is described in Section 5a.) Interspersing layers of metallic shim stock between the FRP layers, clamping the tabs externally, and adding a ceramic thickener to the bonding adhesive did not help. Even with the use of tapered-thickness tabs, a shear load-carrying capacity of only 1500 psi was achieved. For simplicity, a minimum number of loading pins (four) was used in the biaxial-loading specimens.

In-plane biaxial-load tests have previously been carried out on metals by Terry and McClaren (Reference 61). They stated that after trying various designs for the contour of the reduced-thickness test section, they selected their final design, which was a square contour with rounded corners. Although it was stated that uniformity of strain distribution was the criterion used for selection of the final contour design, no strain distribution data were reported.

The test-section contours used in the present program were based on two-dimensional elasticity theory, as described in Appendix I. The resulting contours were a circular contour for the specimens subject to a biaxial-load ratio of 1:1 and a $1:\sqrt{2}$ elliptical contour for the biaxial-load ratio of 1:2. It should be noted that the reduced-thickness contour synthesized in Appendix I results theoretically in a uniform biaxial-stress state in the test section only. To achieve a uniform stress state in the surrounding thicker section would require a local ring-type reinforcement of varying cross-sectional area. However, it is more desirable to have a nonuniform stress field in the thicker section: higher stresses adjacent to the test section, gradually decreasing as the distance from test section is increased (to compensate for the increased localized stresses in the vicinity of the loading tabs).

The scale (i.e., the actual size) of the test-section contour was based on the following considerations: The test section must be large enough to allow an ample sample of material and in particular to be sufficiently larger than the strain gages used. On the other hand, space limitations on the maximum size of the loading fixture and provision for adequate distance between the edges of the specimen and the edge of the test section placed a maximum limit on the test-section size.

Preliminary tests on 1:1 biaxial specimens indicated that a minimum test-section thickness of four plies was necessary to minimize specimen warpage. Also, in these preliminary tests, brittle lacquer was applied to the specimen to obtain a qualitative indication of the stress field throughout the specimen.* Over the whole reduced-thickness test section, the brittle-lacquer crack pattern was bidirectional, like that shown in Reference 64; this indicated that a biaxial stress field was developed throughout the test section. In the thicker section adjacent to the test section, the cracks were radially oriented, thus indicating that the maximum stresses were circumferential. These brittle-lacquer tests indicated a very highly stressed region at the edge of the specimen between two adjacent loading tabs. To alleviate this undesirable condition, the sides of loading tabs were rounded, and considerably more care was taken in achieving smooth, generously curved outer edges of the specimens.

Additional preliminary strain evaluations were carried out on a 1:1 biaxial specimen using metallic-foil-type electric-resistance strain gages (Budd C6-141B single gages and Budd C6-141-R3V strain rosettes). The gage locations are shown in Figure 6, and the load-strain data are presented in Figure 7. The good uniformity of the strain-gage readings associated with the same orientation in the test section substantiates the validity of the specimen design. The slight difference due to orientation is attributed to the slight difference between E_{11} (in the warp direction) and E_{22} (in the weave direction) for this material. As a result of the strain uniformity with respect to orientation within the test section, it was decided to use only two strain gages in the main data-gathering tests rather than a more expensive three-element rosette which would be necessary if neither the principal-stress direction nor the principal-strain direction were known.

Since the highest strains were recorded in the region between two adjacent loading tabs, the loading-tab external-corner radii were increased to the final value of 1.5 inches. The final proof of the

*Although photoelastic coatings used in conjunction with a reflective polariscope are generally more accurate than brittle lacquers, it was not possible to find a photoelastic coating having a satisfactory combination of high stress-optical sensitivity and low in-plane stiffness (product of Young's mudulus and coating thickness).

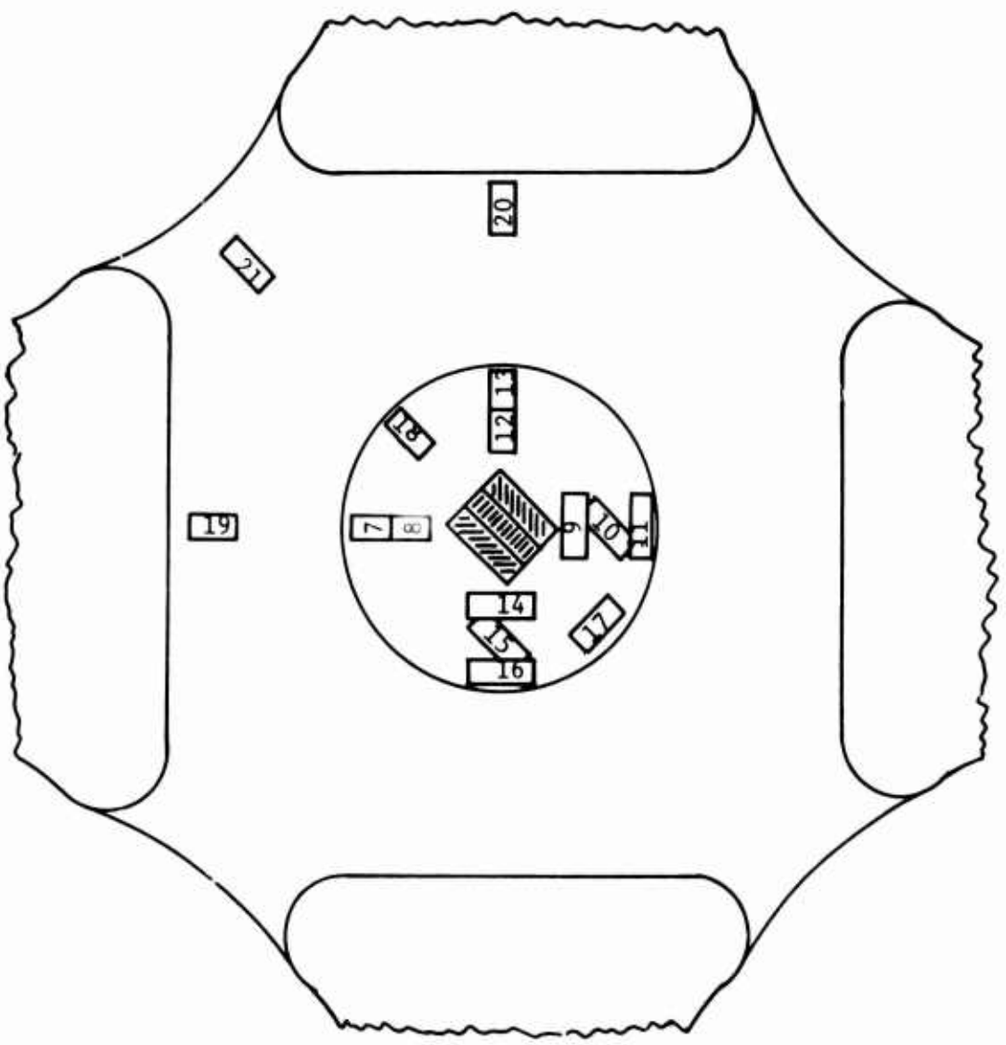

Gage Numbers 1, 2, 3 Front Rosette
Gage Numbers 4, 5, 6 Back Rosette

Figure 6. Gage Locations on Preliminary 1:1 Biaxial-Loading Specimen.

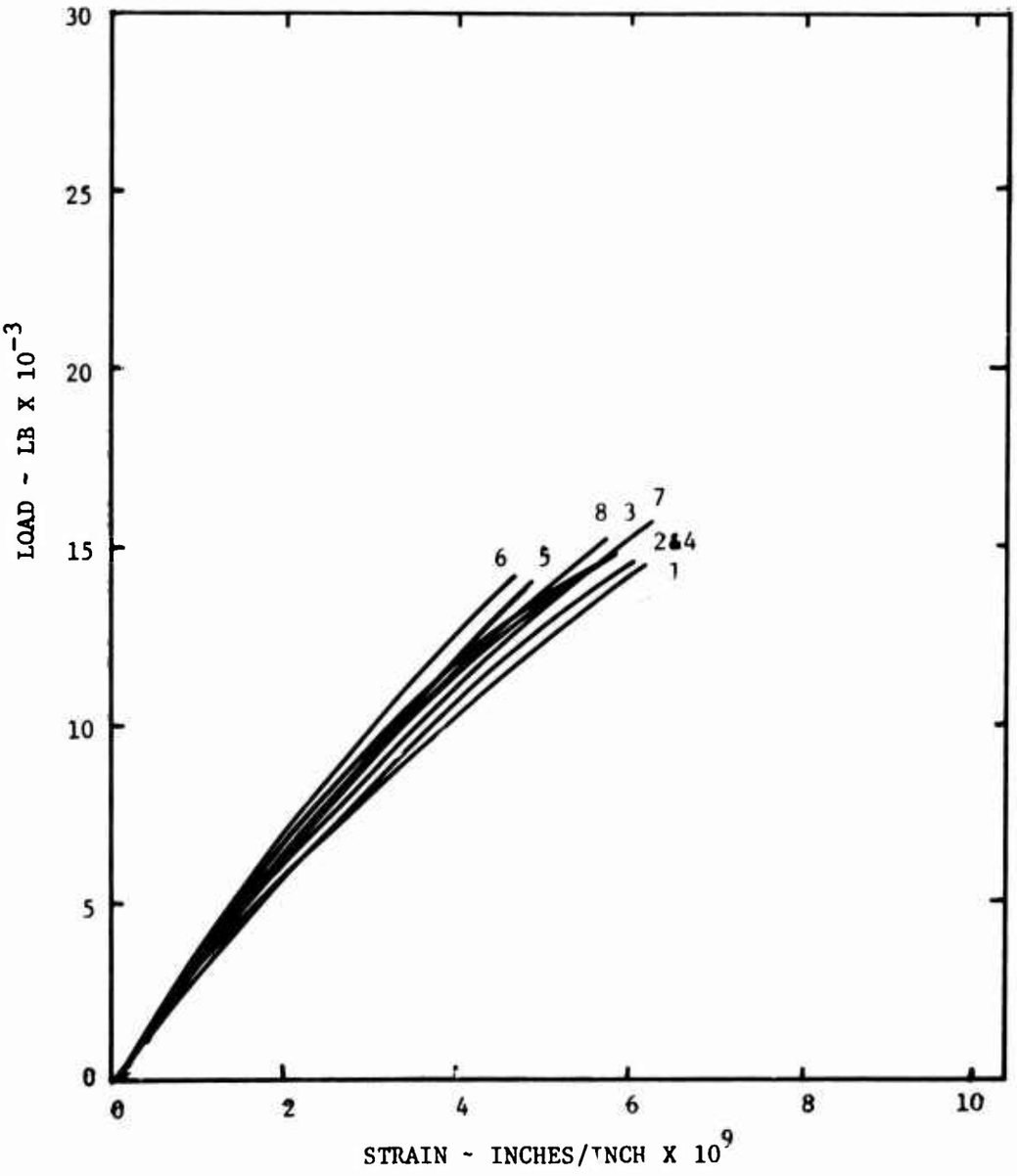

a. Gages 1 Through 9

Figure 7. Load-Strain Data on Preliminary Strain Field Evaluation of 1:1 Biaxial-Loading Specimen.

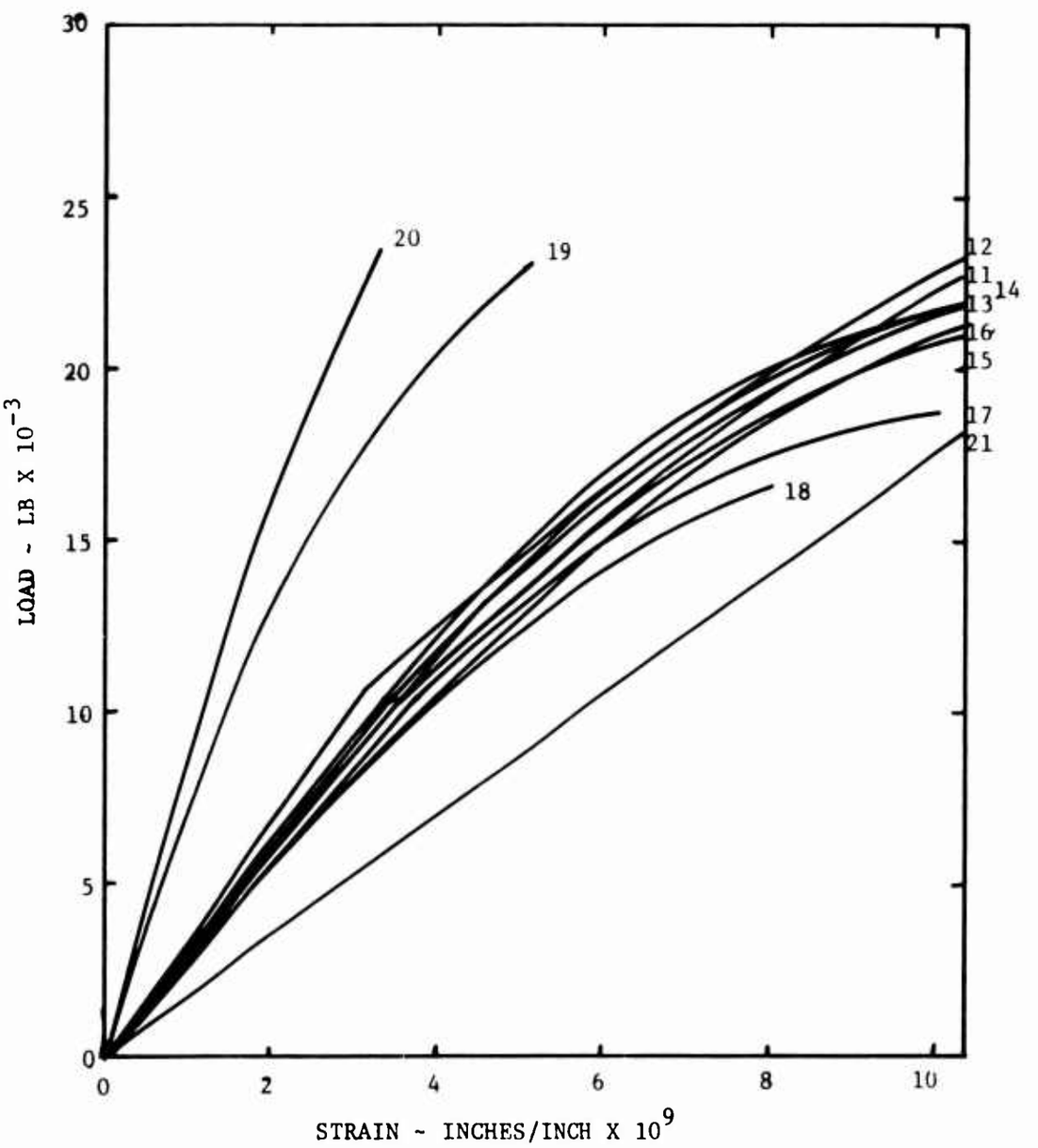

b. Gages 10 through 21

Figure 7. Continued.

validity of the tests in this regard was that the fracture went through at least a part of the test section in 36 of the 54 final data-gathering specimens. (This compares very favorably with the zero percent failures in the main section in the tests reported by Grimes et al in Reference 63).

In view of the good strain distribution achieved in the 1:1 biaxial-load specimens, a much more limited strain-field survey was conducted for the 1:2 biaxial-load specimens (see Figure 8).

The final specimen designs are shown in Figure 9. The strain gages used were metallic-foil type (Budd C6-141B), mounted as shown for the main data-gathering tests.

b. Torsion-Tube Shear Specimens

There has been considerable controversy regarding the best way to obtain pure shear data for composite materials. The in-plane panel shear or picture-frame method has been used most extensively in the past (References 52 and 65). However, this method has been subject to criticism because the stress field deviates substantially from pure shear (Reference 66).

The off-axis tensile test has been used in conjunction with orthotropic elasticity relationships to determine the shear modulus (Reference 54). However, this method has been questioned recently, since off-axis loading of anisotropic materials induces in-plane bending (Reference 67) and since, due to the cut-fiber effect, the test is thought to be more of an in-plane shear test of the resin only (Reference 9). The so-called bow-tie specimen was devised to eliminate both of these objections; however, it also has not been entirely satisfactory due to the stress concentration in the fillet at the minimum cross section (Reference 68).

Some of the tests used to determine shear properties of composites result in out-of-plane shear loading, i.e., out-of-plane twisting, and thus are not valid for determining the in-plane shear modulus. One widely used test of this type is the so-called plate twist test in which a square plate is loaded downward at two diagonal corners and upward at the other two diagonal corners (Reference 69). Another is the split-ring out-of-plane shear test (Reference 70).

Many other types of shear specimens, such as double-notched and S-shaped tension specimens (Reference 71), deep, short-span beams (Reference 72), and solid circular torsion bars (Reference 73), have been investigated to a limited extent. However, the most popular shear test at present is the torsion of a thin-walled cylinder. Whitney (Reference 74) has shown that such a test is insufficient to obtain the shear modulus for unsymmetrically laminated composites. However, in the present research, only symmetrical lamination arrangements are used; thus, the test is sufficient to determine the laminate shear modulus directly. The torsion-tube

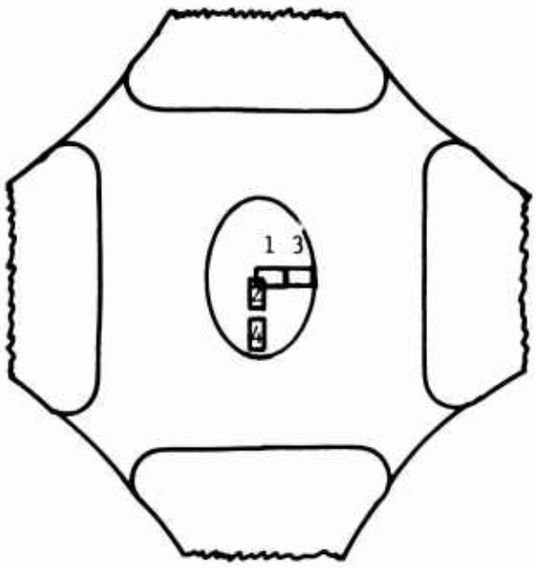

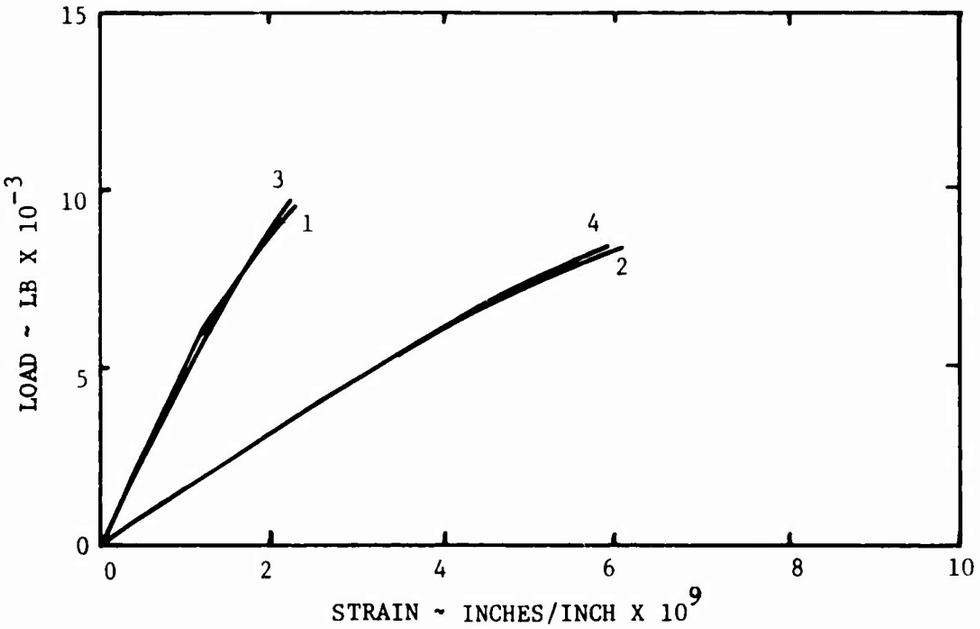

Figure 8. Load-Strain Data from Preliminary Strain Field Evaluation of 1:2 Biaxial-Load Specimen.

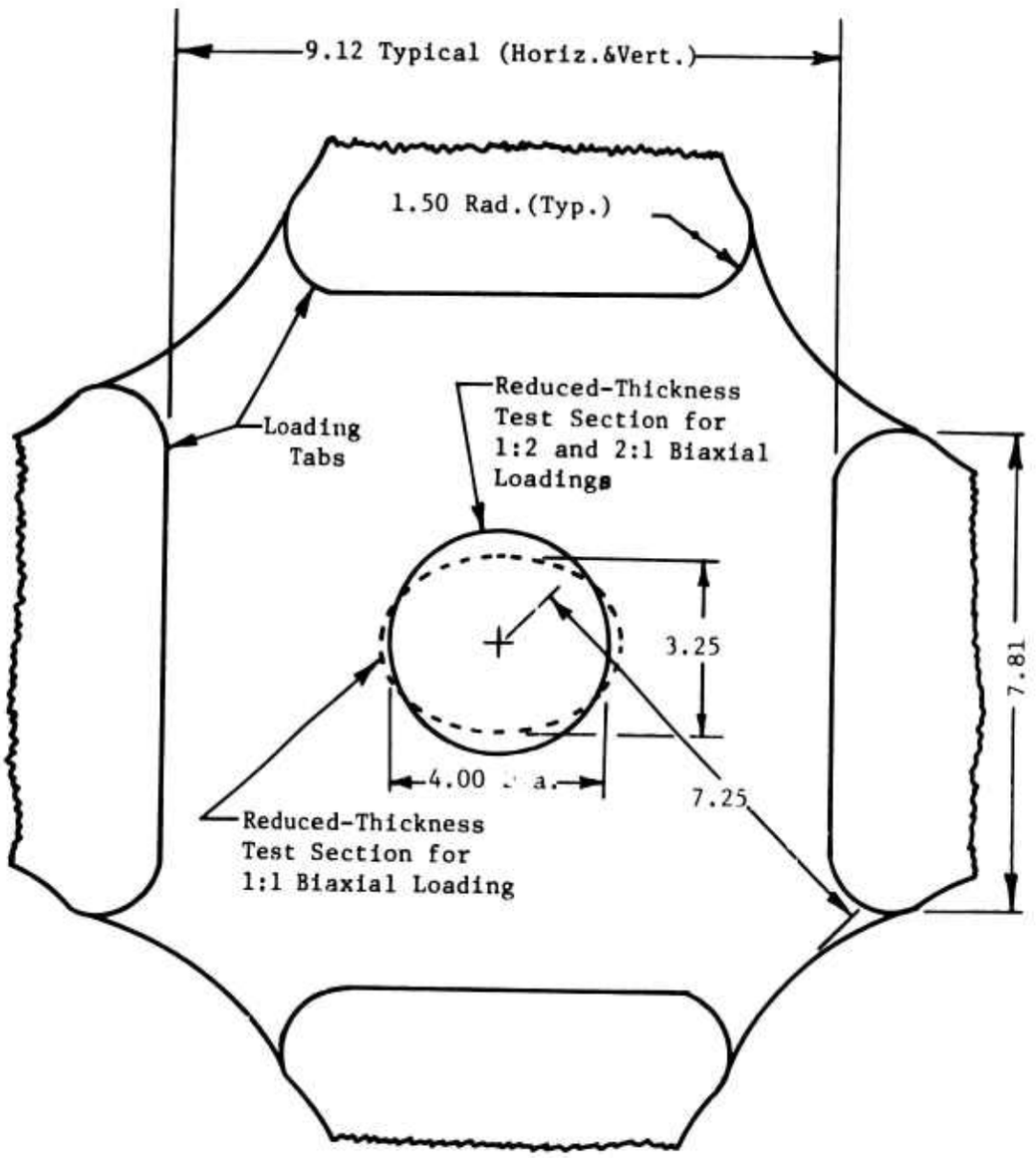

All dimensions Are in Inches

Figure 9. Biaxial-Loading Specimen Designs.

shear test is believed to be the only method which meets all of the following requirements for a good shear test method:

(1) Development of a uniform state of pure shear stress over a significant portion of the specimen.

(2) Capability of determining both shear modulus and shear strength in one test of a single specimen with a minimum of data reduction.

(3) Ease of specimen fabrication from a minimum amount of preimpregnated laminate.

(4) Simplicity of test apparatus.

(5) Simplicity and repeatability of test procedure.

Preliminary torsion tests were conducted on tubes laminated of two plies oriented longitudinally, to check out the torsion test equipment (see Section 5b). The dimensional and failure data for the specimens are listed in Table III.

TABLE III. RESULTS OF PRELIMINARY TORSION-TUBE TESTS

Nominal Diameter, in.	Operating Length, in.	Shear Stress at Failure, psi	Type of Failure	Calculated $(\sigma_{xy})_{cr}$, psi
1.590	1.907	18,100	Torsional buckling	18,600
1.590	1.250	28,000	Torsional buckling	23,000

Since these two specimens failed due to torsional buckling, calculations were made using the following approximate equation, derived from the work of Simitses (Reference 75), for the critical shear stress $(\sigma_{xy})_{cr}$ for torsional buckling of orthotropic tubes with clamped edges:

$$(\sigma_{xy})_{cr} = (1.03\ \pi^2/12)\ E_{22}^{5/8}\ E_{11}^{3/8}\ t^{5/4}\ L^{-1/2}\ R^{3/4} \qquad (56)$$

where t = wall thickness, L = operating length, and R = mean radius. As can be seen in Table III, the agreements between the buckling stresses and the theoretical predictions were fairly good.

To ensure that the undesirable buckling would not occur in the final specimens, on the basis of the above equation, it was decided to use an operating length of only 5/8 inch and an inside diameter of 1.50 inches.

The use of such a short operating length raised several questions. One was the possibility of end effects on the shear-stress distribution. This was investigated theoretically, and it was found that a thin-walled tube clamped at the ends, but free to move axially and subject to torsion loading, can experience only axial and circumferential displacement (no normal displacement) so long as the buckling load is not reached. Another question was the possibility of an effect of length on the shear strength of the composite, since increasing the length of single glass fibers decreases their tensile strength (Reference 76). This question was investigated by testing three tubes, each having parallel plies oriented longitudinally.

One specimen had an operating length of 3 inches and six plies, the second had a length of 5/8 inch and six plies, and the third had a length of 5/8 inch and two plies. All of the specimens had very nearly the same shear stress-strain results, and thus it was decided to standardize on the operating length of 5/8 inch for all of the torsion tubes. The final specimen dimensions and strain-gage locations are shown in Figure 10.

c. Uniaxial Tension Specimens

In previous research on FRP laminate properties (Reference 1), the tensile-test specimen design selected was a straight-sided specimen with very shallow circular notches (0.007 inch deep) on each side and having a net-section width of 0.75 inch. The purposes of the notch were to minimize failures in the testing-machine grips and to cause failure to occur within the gage length of the extensometer, without significantly reducing the strength values due to geometric stress concentration. Since the notch was very mild and the extensometer gage length was appreciable, the notch had a negligible effect on the extensometer data. However, the notch undoubtedly had some effect on reducing the ultimate strength.

In the present research, in addition to strength and axial strain data (to calculate the longitudinal Young's modulus E_{11}), transverse strain data were required (to calculate Poisson's ratio ν_{12}). Since it was concluded by Trantina (Reference 77) that strain gages can be used to obtain reliable elastic-coefficient data for fiber-reinforced composites, preliminary tensile tests were conducted on parallel-ply specimens identical to those described in Reference 1, except that a longitudinal and a transverse strain gage were mounted at the center of the specimen. The results were unsatisfactory because the notches increased the longitudinal strain proportionally more than they did the transverse strain. In fact, the data were not in agreement with Equation (10), which is a fundamental relation based on basic thermodynamic considerations (see Section 2a).

To alleviate the difficulty described above, plain, straight-sided specimens (see Figure 10), instrumented with two strain gages, were

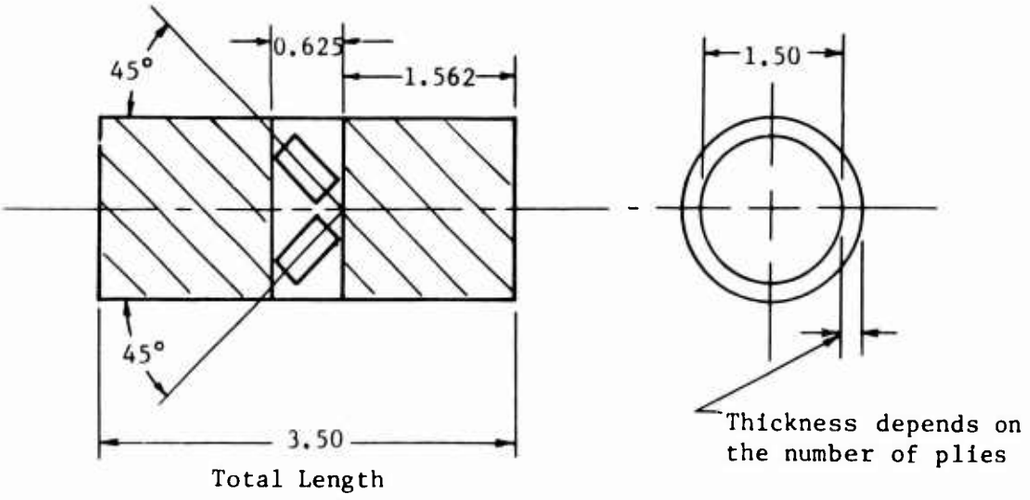

a. Torsion-Tube Specimen for Shear Tests

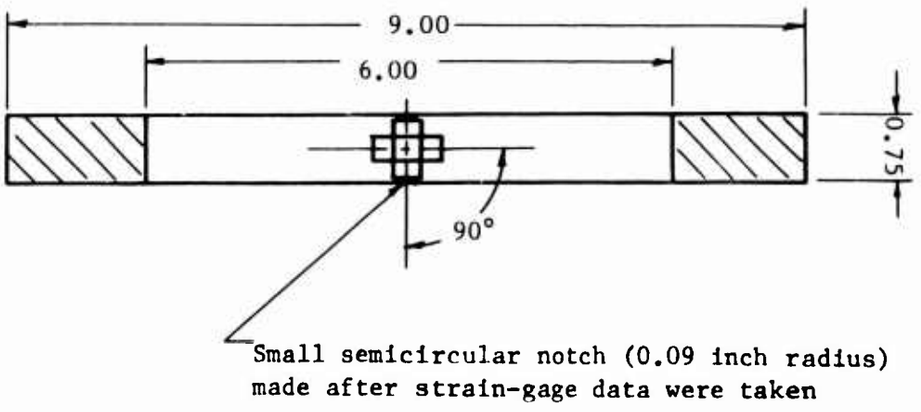

b. Uniaxial Tension Specimens

Figure 10. Shear and Uniaxial Tension Specimens. (All Dimensions Are in Inches.)

used to obtain the strain data. Then the specimens were notched with shallow circular notches (0.01 inch deep) and tested to failure.

The question arose as to whether the biaxial strength values differed from the uniaxial ones due to the differences in specimen thickness, length, and width between the two types of specimens. To help provide an answer to this question, two additional series of specimens were made and tested. One series of specimens was designed to investigate the effects of number of plies and the length between grips, with specimen width held constant at the same value as the specimens shown in Figure 10. The test results for the parallel-laminated specimens loaded at 0 deg are shown in Figure 11, while Figure 12 gives limited test results for the parallel-ply 90-deg specimens, cross-ply specimens, and quasi-isotropic specimens. The decrease in strength with increasing test-section length follows the trend reported by Metcalfe and Schmitz (Reference 41) for glass fibers alone, and the increase in strength with increasing number of plies is in agreement with FRP test results reported by many laboratories, and recently explained on a quantitative statistical basis by Scop and Argon (Reference 78).

The second series of additional specimens was to study effects of specimen width and stepped thickness. Some specimens were simple rectangular but with a length equal to the distance between the loading tabs on the biaxial specimens. As was expected on the basis of width-effect tests reported by Kaman Aircraft Corporation (Reference 79), the strength decreased with increasing width (see the circle data points in Figure 13). The remainder of the specimens were cut from some 1:1 biaxial specimens to various widths and loaded uniaxially with 9.25 inches between grips. Thus, these specimens had a reduced thickness with a step change in thickness. The results of these tests are shown in Figure 13 as square data points. Surprisingly these specimens exhibited an increase in strength with increasing width. This opposite effect is obviously due to the different restraint in the stepped-thickness specimens.

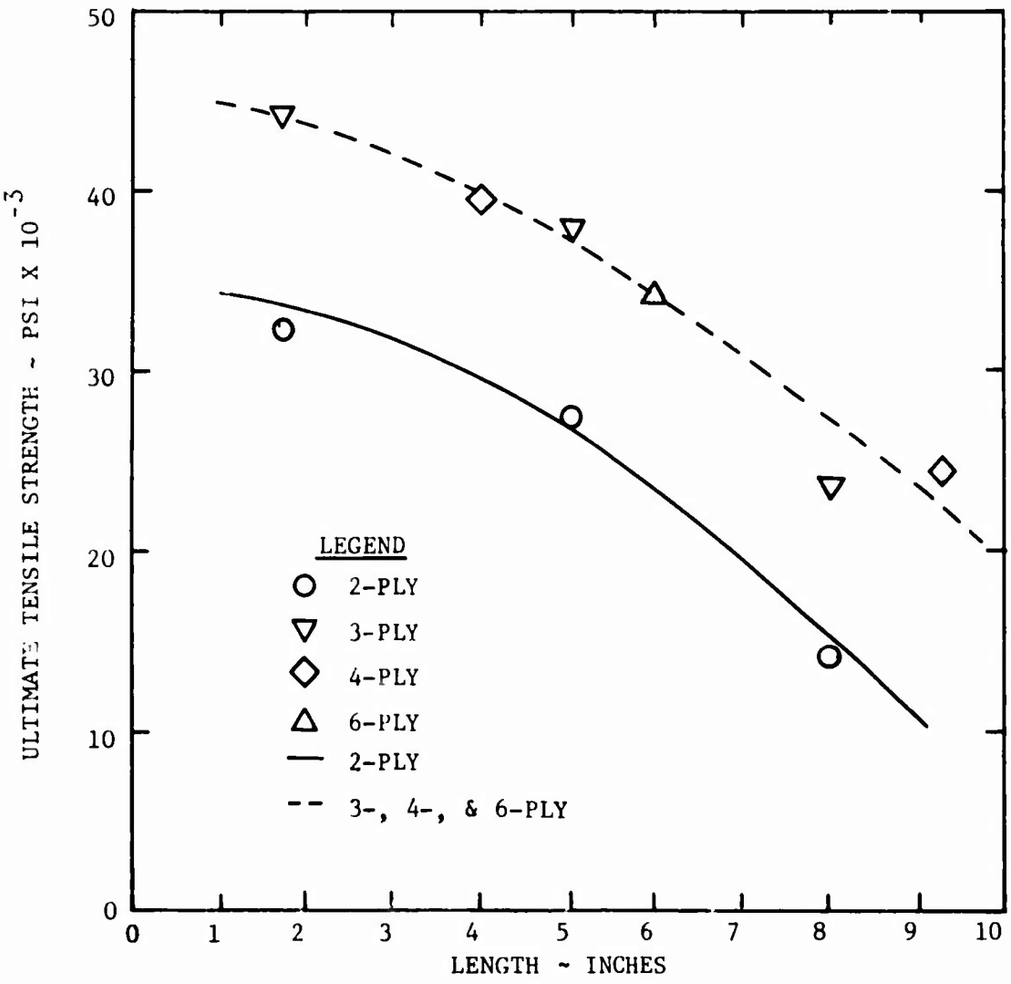

Figure 11. Effect of Number of Plies and Length Between Grips on the Strength of Rectangular, Uniform-Thickness Specimens, 0.0750 Inch Wide, Parallel Laminated, Loaded at 0 Degrees to the Warp.

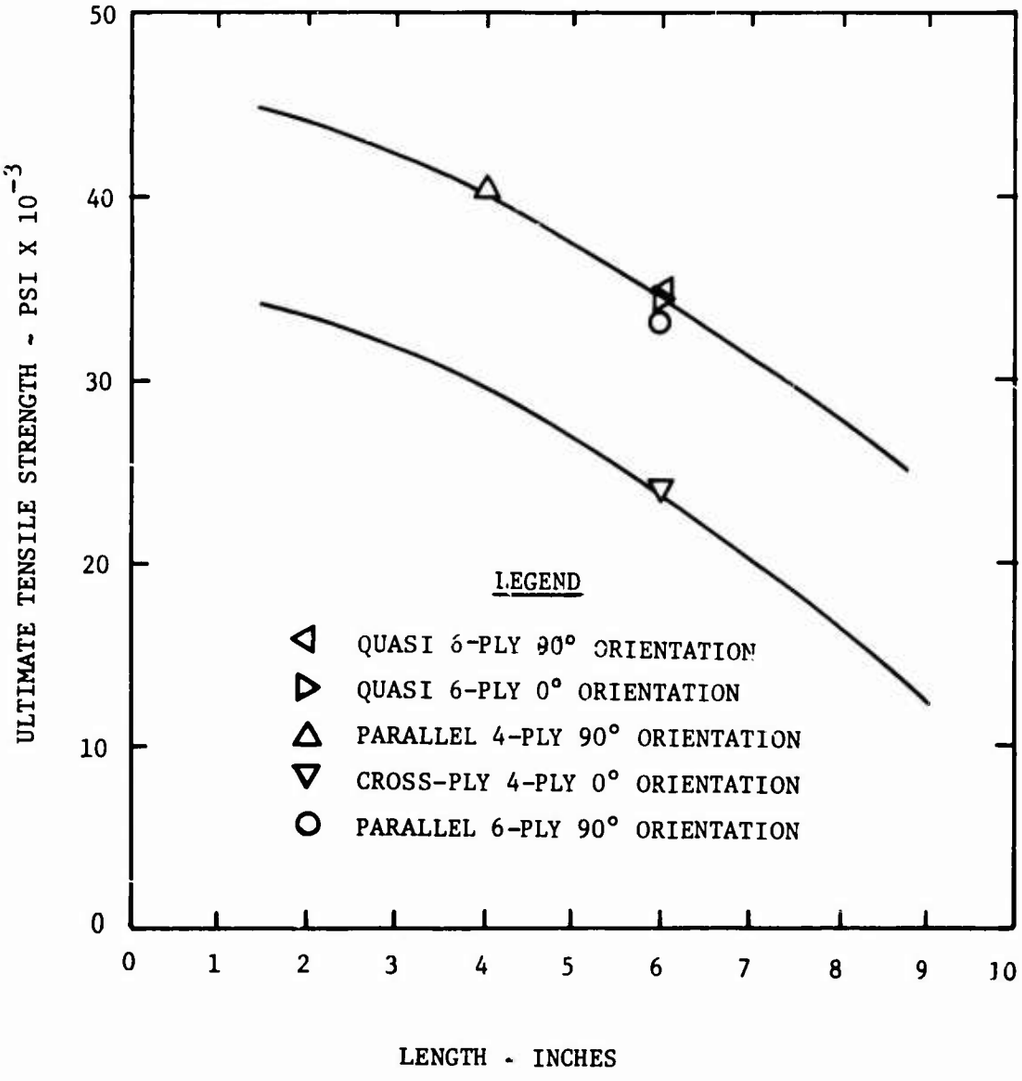

Figure 12. Effect of Number of Plies and Length Between Grips on the Strength of Rectangular, Uniform-Thickness Specimens, 0.750 Inch Wide, With Various Lamination Arrangements and Loading Directions.

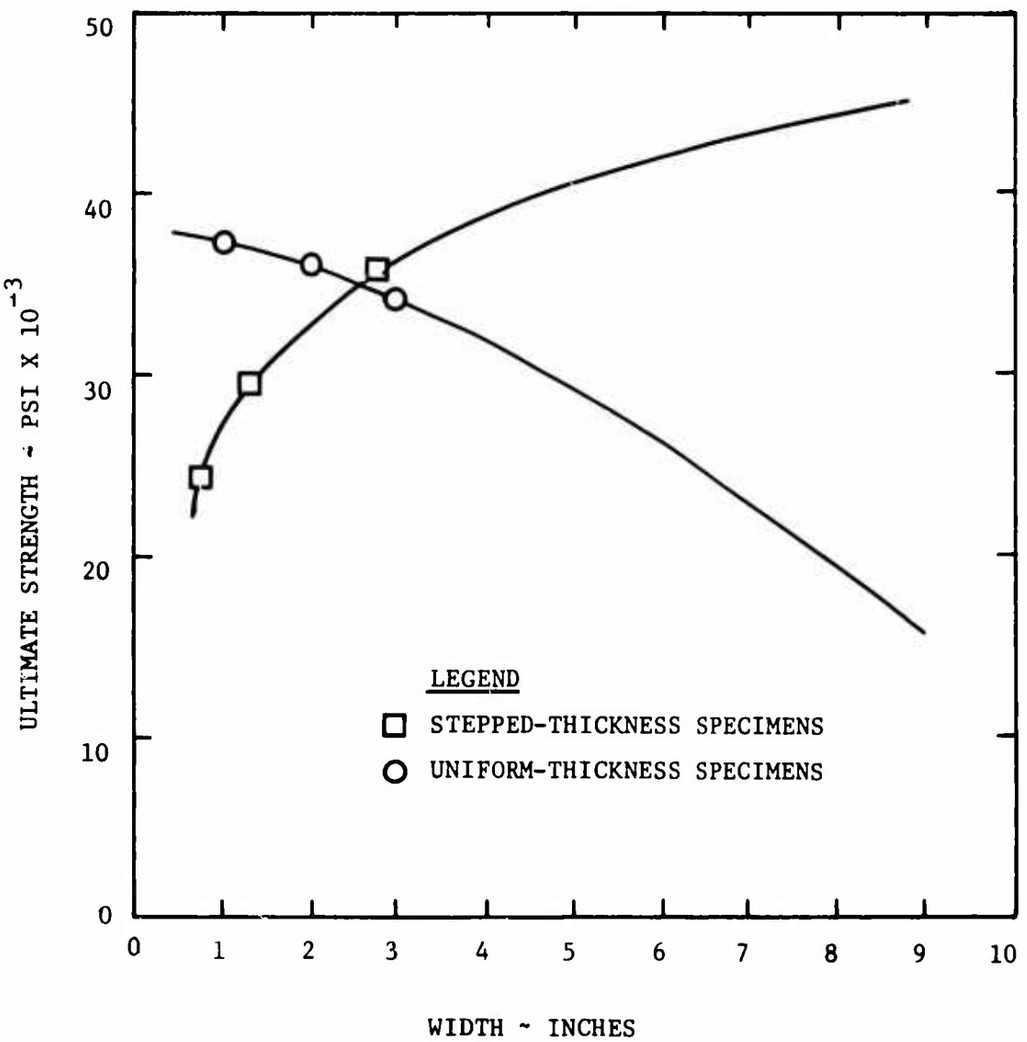

Figure 13. Effect of Specimen Width on Strength of Uniform-Thickness and Stepped-Thickness Specimens, With Four Parallel-Laminated Plies and 9.250 Inches Between Grips.

5. SPECIAL TEST EQUIPMENT

The design and operational features of the special test equipment developed in this research program are described in this section.

a. Biaxial-Loading Fixture

In previous in-plane biaxial-loading fixtures, two or more hydraulic rams were used to load the specimen (References 61 and 62). However, it is a difficult problem in hydraulic control to maintain the same biaxial-load ratio throughout the test of an anisotropic composite. To eliminate this control problem, in the present program, an original cable-and-pulley system reacted by a rigid steel frame was used to load the specimen biaxially. Simplicity is the major feature of this loading device.

After the present device was developed, the authors learned of the development of another simple biaxial-loading device by Grimes et al (Reference 63). Although their device is probably simpler, it developed only one biaxial-load ratio and their test results were somewhat questionable, as discussed later.

Figure 14 is a schematic diagram of the basic concept of the cable-and-pulley biaxial-loading fixture. It is noted that the fixture can be converted from a 1:1 biaxial-load ratio to a 1:2 ratio by merely changing the cable path and pulleys used. Figure 15 shows the fixture in place between the platens of the 60,000-pound-capacity Riehle hydraulically operated universal testing machine.

Although the pulley system used in the biaxial-loading fixture appears at first glance to be unduly complicated, it was gradually evolved by means of a wooden mockup and found to be most advantageous in meeting these design objectives: (1) development of maximum load in the specimen equal to twice that applied by the testing machine in the case of both 1:1 and 1:2 loading, (2) minimization of the maximum load applied to any bearing in the fixture, (3) sufficiently compact overall dimensions to fit between the platens of the universal testing machine, (4) ability to change biaxial-load ratio, and (5) allowance for adequate space for the specimen and loading tabs.

The cable type and size were chosen to meet these two objectives: (1) maximum flexibility to enable easy bending over the pulleys during operation, and (2) adequate static load capacity. Since the motion involved during loading was very small, the cable was sized on the basis of a strictly static load (no motion over the pulleys). The cable finally selected was 5/8-inch 6 x 36.

The standard cable-socket method was used to attach to the cable for maximum load capacity. This method entailed putting the cable end into a tapered steel socket and flaring the cable end until each strand was separated. Next the individual strand ends were bent back approximately

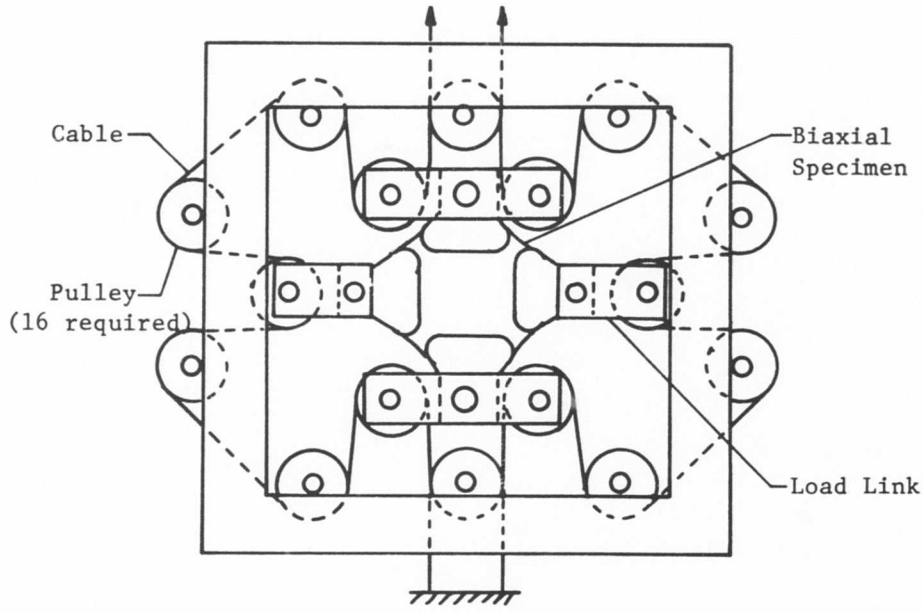

Figure 14. Schematic of Basic Concept of Biaxial-Loading Device.

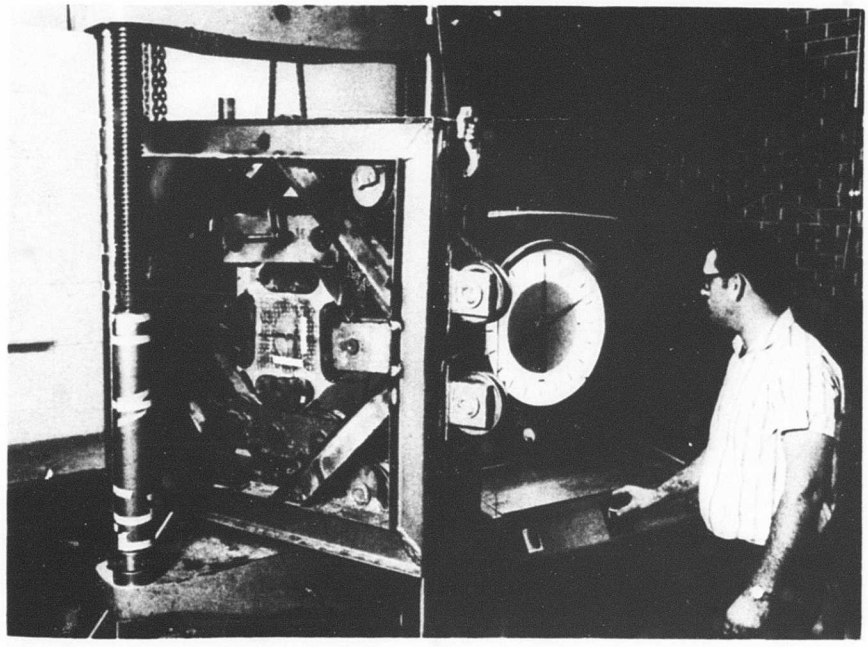

Figure 15. Biaxial Device Installed in Universal Test Machine.

90 to 180 deg. Then a high-zinc No. 1 Babbitt was poured into the socket, forming a solid mass which resulted in a high load-carrying capability as verified by preliminary tensile tests before cable was installed in the loading fixture.

The pulley size was standardized at a diameter of 6 inches for all of the pulleys. This size was much smaller than that recommended by the cable manufacturer; however, it proved to be adequate in this negligible-movement application. Each pulley contained a cylindrical-roller bearing, which operated on a 1.5-in.-diameter hardened steel shaft, which, in turn, was pressed into the loading fixture.

To permit the specimen to be self-aligning, a load link was provided between each loading tab on the specimen and the biaxial-loading fixture.

The loading tabs by which the biaxial loads were transferred from the load link in the biaxial-loading fixture to the specimen were made of hardened SAE 4140 steel. Eight tabs were used for each specimen: one on each side of the specimen (to minimize out-of-plane bending in the specimen) at each of the four loading ears. To provide the necessary shear area, the tabs were wider (7.81 inches wide) where they were bonded to the specimen. To promote a more uniform transfer of load from the steel loading tabs to the FRP specimen, the thickness of the tabs was tapered to a minimum of 0.0625 inch.

Prior to testing FRP specimens in a given configuration, the cables of the loading fixture were "set" by applying load to an aluminum plate.

b. Torsion-Tube Shear Test Apparatus

To permit proper testing of the tubular specimens (see Section 4b), rather massive end fittings were designed (see Figure 16). One of these was bonded to each end of the specimen over a length of 1.5 inches in order to achieve adequate shear load-carrying capacity. The end fittings were mounted on a shaft, and one fitting was free to slide axially on the shaft to prevent the development of axial forces as a consequence of change in specimen length during loading.

Pure torque was applied to the specimen via the end fittings by means of a protrusion on each end fitting. The end fittings were bonded to the specimen in such a way that the protrusions were 180 degrees apart. This minimized the change in moment arm as the specimen twisted during loading. However, the total angular rotation to failure was very small in all cases, since the operating length of the tube was quite short.

The loading protrusions on the end fittings were loaded by another fitting on the end of the hydraulic ram. Figure 17 is a photograph of the shear test apparatus with specimen bonded in place.

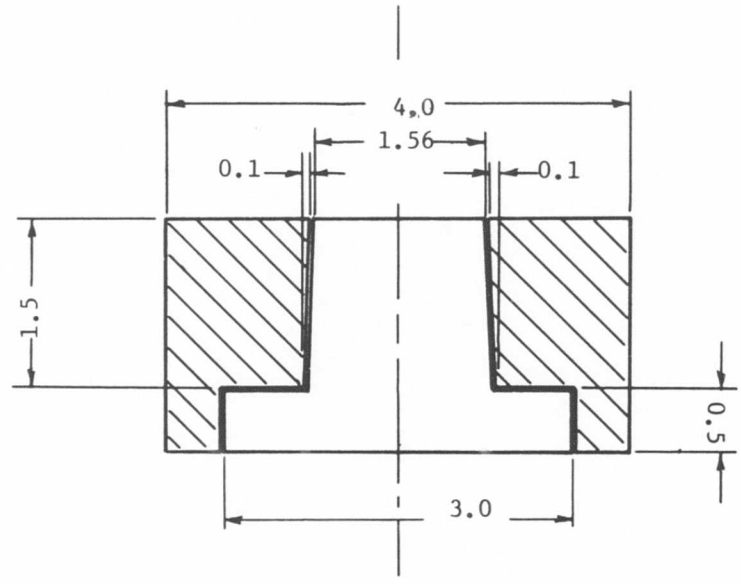

All Dimensions Are in Inches

Figure 16. Detailed Dimensions for End Fittings of Torsion Shear Apparatus.

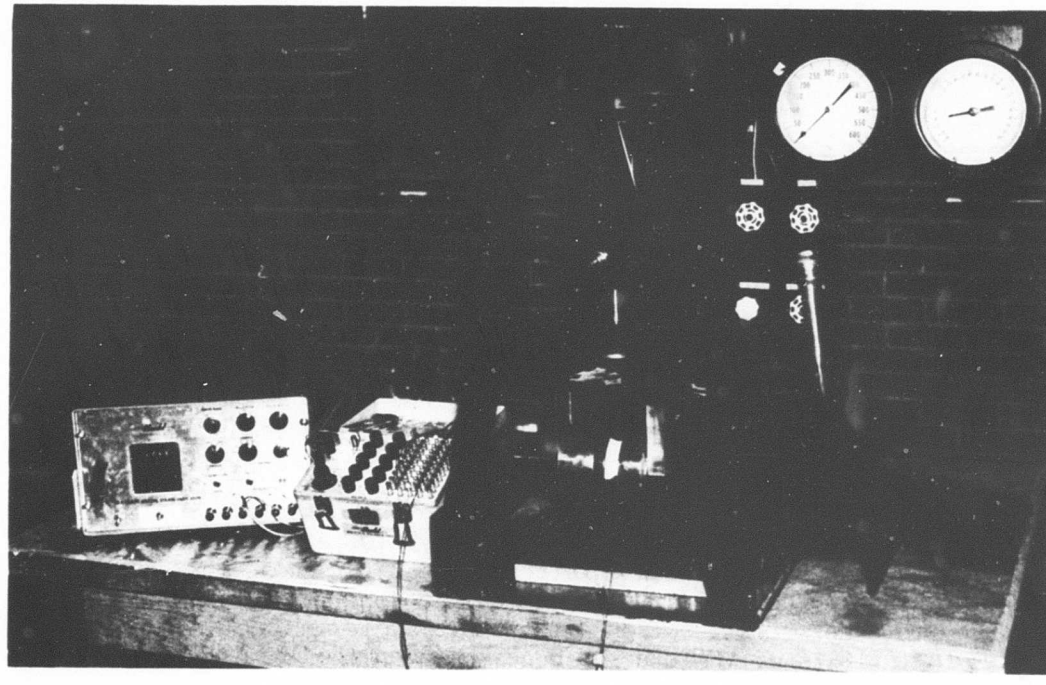

Figure 17. Shear Test Apparatus With Specimen Bonded in Place.

6. EXPERIMENTAL PROCEDURES

a. Specimen Fabrication

All of the specimens were fabricated by OURI from FRP laminates consisting of 181-style-weave, E-glass cloth, with a Volan-A-finish and impregnated with Epon-828 epoxy activated by curing agent Z. First the material was made in the form of a two- or three-layer preimpregnated laminate (called prepreg), using the wide multilayer prepreg machine reported in Reference 9. Prepreg 52 inches wide and in lengths up to 2800 inches was produced in this manner and stored in cold storage until ready to be fabricated into specimens.

The procedure for layup of the specimens began with removing the prepreg from cold storage and cutting it to proper size depending on the type of specimen. In all cases, a dry layer of 181-style fiber glass cloth was used as a bleeder to improve resin-content uniformity and to insure that uniform venting occurred over the entire laminate surface during autoclave vacuum and pressure application. Teflon FEP film, one-half mil thick and perforated with 3/16-inch-diameter holes spaced 1/2 inch apart in a rectangular array, was used as the parting agent between the bleeder and the prepreg.

Regardless of the type of specimen (biaxial, uniaxial, or tube), a B-stage time of approximately 7 hours, from time of removal from cold storage to time of placement in the autoclave for curing, was used. The cure used was the same as that used for the large-shell facings reported in Reference 9; namely, 160° F and a total pressure of 70 psi (10 psi vacuum plus 60 psi autoclave) for 100 minutes, with a zero-pressure precure of 23 minutes. Curing was conducted in the large autoclave described in References 9 and 11. The post cure was 350° F for 2 hours.

To fabricate the biaxial-load specimens, the prepreg was arranged in the proper lamination arrangement and then cut to conform to a sheet-metal template. The template has a small bevel cut at one corner; this served to index the prepreg layers during final layup for curing. For prepreg which was to become the top and bottom reinforcing material (i.e., all of the specimen except the reduced-thickness test section), a circular or elliptical hole was cut out of the center, the shape of the hole depending upon whether or not the specimen was to be for a 1:1 or a 1:2 biaxial-load ratio. For prepreg which was to become the test section and the central layers of the rest of the specimen, no hole was cut out. Special slightly undersize sheet-metal inserts which fitted into the cut-out hole were used to prevent excess resin flow into the reduced-thickness test section. Final curing in the autoclave resulted in a specimen having the desired reduced-thickness test section with naturally formed fillets of resin. Next, the fillets at the exposed edges between the loading tabs were machined; and, finally, eight loading tabs were bonded to each specimen. Bonding was accomplished with 828-epoxy and V140-polyamide curing agent. The bonding cure served as the post cure for the torsion-tube specimens.

The uniaxial tensile specimens were cut to approximate dimensions from a large, completely cured sheet of the proper lamination arrangement. Then they were machined to final dimensions.

b. Test Procedures

During all tests, both wet and dry bulb temperatures were measured. Also, an attempt was made to run all of the tests at approximately the same rate of loading.

To install a biaxial-load specimen in the loading fixture, a portable hoist was used. The weight of the specimen plus the heavy loading tabs was balanced out to prevent loading the top part of the specimen in tension and the bottom part in compression. Then the slack was pulled out of the cable, and the specimen was loaded at an approximately constant rate. Strain readings from the two strain gages were taken on a digital-dial strain indicator at predetermined load intervals.

After testing, the central portion of the specimen was cut out and was saved for future study. Then the specimen material remaining on the loading tabs was removed by sand-blasting so that the loading tabs would be ready to be used again.

Testing of the torsion-tube and uniaxial tension specimens was standard.

7. EXPERIMENTAL RESULTS

This section presents the reduced data from the main data-gathering portion of the experimental program. The experimental stress-strain or load-strain data, from which the reduced data were derived, are presented in Appendix II.

It must be emphasized that the stress values used in specifying the strengths are nominal composite stresses, i.e., total load divided by cross-sectional area. These are the values that an aircraft designer needs directly in design. However, in general, they are not the same as the stresses physically present in each individual ply of the laminate.

a. Uniaxial Tensile Tests

The individual uniaxial tensile specimens used in the main data-gathering series were designated U1 through U20. Their dimensions are shown in Figure 10b. The data reduced for individual specimen were as follows:

$$\text{Initial Young's modulus, } E = \frac{\text{Uniaxial stress}}{\text{Strain in direction of stress}} \tag{57}$$

$$\text{Initial Poisson's ratio, } \nu = -\frac{\text{Transverse strain}}{\text{Strain in direction of stress}} \tag{58}$$

$$\text{Limit strength in tension, } S_L = \text{Stress at 0.01 percent offset strain} \tag{59}$$

$$\text{Ultimate tensile strength, } S_U = \text{Stress at maximum load reached in test} \tag{60}$$

The stress values used are the engineering ones, i.e., load divided by original cross-sectional area. The strain values used are those measured by variable-electric-resistance strain gages.

The initial Young's moduli, E, and initial Poisson's ratios, ν, were both determined in the initial straight-line elastic portion of the stress-strain curves.

In aircraft metallic alloys, the criterion used to define limit strength is the 0.2-percent-offset yield strength. However, many composite materials, including glass fiber-reinforced plastics (FRP), do not reach this high of an offset strain. Therefore, for such materials, a new limit-strength criterion must be used. The limit-strength criterion used here is the 0.01-percent-offset yield strength, which is the strain associated with an offset of 0.01 percent strain.

The ultimate tensile strength is defined in the traditional manner. For many composite materials, including FRP, there is no drop in load with continuing strains; i.e., the fracture strength coincides with the ultimate tensile strength.

The reduced data for the main series of uniaxial tensile tests are presented in Table IV. (Additional exploratory uniaxial data are presented in Section 4c.) It is noted that the cross-ply specimens were not tested at a 90-degrees orientation, since this is no different than 0-degree orientation for such a specimen (symmetrically laminated with an equal number of plies at 0 and 90 degrees).

Mean values of the moduli (E and ν), used in determining biaxial stress values, are presented in Table V.

b. Torsion-Tube Shear Tests

The individual torsion-tube shear specimens used in the main data-gathering series (see Figure 10a) were designated S1 through S24. The data reduced for each specimen were as follows:

Initial shear modulus, G ≡ shear stress/shear strain (61)

Limit shear strength, S_{L6} = shear stress at 0.01 percent offset shear strain (62)

Ultimate shear strength, S_{U6} = shear stress at maximum torque reached in test (63)

Since the lamination arrangements were all symmetric about the middle of the thickness and since the specimens were thin-walled and circular in cross section, the following expression for shear stress is valid throughout the test:

$$\sigma_6 = TR_o/J = 2TR_o/(R_o^4 - R_i^4) \tag{64}$$

where T = torque, J = polar area moment of inertia, R_o = outside radius, and R_i = inside radius.

For a state of pure shear strain, application of the Mohr strain circle shows that the shear strain is equal to twice the reading of an electric-resistance strain gage, which measures normal strain only, at an orientation of 45 degrees with the plane on which the shear strain takes place. To average out any small amount of bending which may have been induced, two gages were used, one at +45 and the other at -45 degrees. Thus, the shear strain plotted in Appendix I is merely the sum of the strain readings from the two gages.

The shear moduli and shear strengths are defined in a fashion analogous to that used for the corresponding uniaxial quantities. Figure 18 shows a typical shear specimen fracture.

The reduced data are presented in Table VI. Mean values of the shear moduli for each laminate at 0-degree orientation are listed in Table V.

TABLE IV. RESULTS OF UNIAXIAL TENSILE TESTS

Specimen No.	E, psi	ν	S_L, psi	S_U, psi
Four-Ply Parallel Laminated, 0-deg Orientation				
U1	3.34×10^6	0.148	13,250	37,400
U2	3.24×10^6	0.144	11,750	41,150
U3	3.36×10^6	0.132	13,500	40,500
Four-Ply Parallel Laminated, 90-deg Orientation				
U4	3.14×10^6	0.193	10,000	41,400
U5	3.19×10^6	0.181	12,000	42,600
U6	3.11×10^6	0.192	12,750	42,200
Four-Ply Cross Laminated, 0-deg Orientation				
U7	4.55×10^6	0.252	11,750	23,200
U8	3.10×10^6	0.152	11,250	25,500
U9	3.16×10^6	0.148	14,750	22,200
U10	3.33×10^6	0.095	10,500	25,600
Six-Ply Quasi-Isotropic Laminated, 0-deg Orientation				
U11	3.59×10^6	0.297	13,250	33,700
U12	3.42×10^6	0.324	12,500	35,000
U13	3.68×10^6	0.320	15,750	31,100
U14	3.79×10^6	0.323	19,000	34,000
U15	3.63×10^6	0.323	12,250	39,600
Six-Ply Quasi-Isotropic Laminated, 90-deg Orientation				
U16	3.63×10^6	0.286	10,500	36,400
U17	3.85×10^6	0.336	13,250	33,800
U18	3.62×10^6	0.312	13,500	33,700
U19	3.57×10^6	0.328	12,000	35,500
U20	3.61×10^6	0.291	11,250	34,500

TABLE V. SUMMARY OF MEAN VALUES OF INITIAL COMPOSITE MODULI

Lamination Arrangement	Parallel-Ply	Cross-Ply	Quasi-Isotropic
Major elastic modulus, $\bar{E}_{11}$	3.304×10^6	3.196×10^6	3.62×10^6**
Minor elastic modulus, $\bar{E}_{22}$	3.15×10^6	3.196×10^6	3.66×10^6**
Major Poisson's ratio, $\bar{\nu}_{12}$	0.1410	0.1316	0.317***
Minor Poisson's ratio, $\bar{\nu}_{21}$	0.188*	0.1316	0.311***
Shear modulus, $\bar{G}$	1.325	1.31×10^6	1.93×10^6

* This value appears to be erroneously high, so a value of 0.1342, calculated from the reciprocal relationship (0.1410 x 3.15/3.304), was used in all subsequent data reduction.

** Since these values are not significantly different, within experimental error, a single value of 3.64×10^6 psi is used in all subsequent data reduction.

*** Since these values are not significantly different, within experimental error, a single value of 0.314 is used in all subsequent data reduction.

TABLE VI. RESULTS OF TORSION-TUBE SHEAR TESTS

Specimen No.	G, psi	S_{L6}, psi	S_{U6}, psi
Four-Ply Parallel Laminated, 0-deg Orientation			
S1	1.47×10^6	7,000	30,100
S2	1.25×10^6	7,200	31,256
S3	1.53×10^6	4,000	79,862
S4	1.05×10^6	8,500	28,040
Four-Ply Parallel Laminated, 45-deg Orientation			
S5	3.68×10^6	6,800	57,400
S6	3.13×10^6	5,500	54,000
S7	7.7×10^6*	7,200	80,800*
S8	3.37×10^6	9,000	66,500
Four-Ply Cross Laminated, 0-deg Orientation			
S9	1.3×10^6	4,800	28,125
S10	1.43×10^6	7,000	21,350
S11	0.96×10^6	10,200	24,766
S12	1.75×10^6	5,000	32,260
S13	1.11×10^6	7,000	25,620
S14	2.3×10^6*	10,500	32,238
Four-Ply Cross Laminated, 45-deg Orientation			
S15	2.5×10^6	10,200	50,000
S16	3.34×10^6	10,500	46,875
S17	2.22×10^6	7,000	46,875

TABLE VI - Continued

Specimen No.	G, psi	S_{L6}, psi	S_{U6}, psi
Six-Ply Quasi-Isotropic Laminated, 0-deg Orientation			
S18	2.0×10^6	9,800	55,510
S19	2.22×10^6	11,000	53,375
S20	1.82×10^6	10,500	55,510
Six-Ply Quasi-Isotropic Laminated, 45-deg Orientation			
S21	1.82×10^6	7,500	26,218
S22	1.62×10^6	14,800	49,105
S23	1.82×10^6	10,000	49,319
S24	2.22×10^6	16,400	50,386

* Values too high; not used in final data reduction.

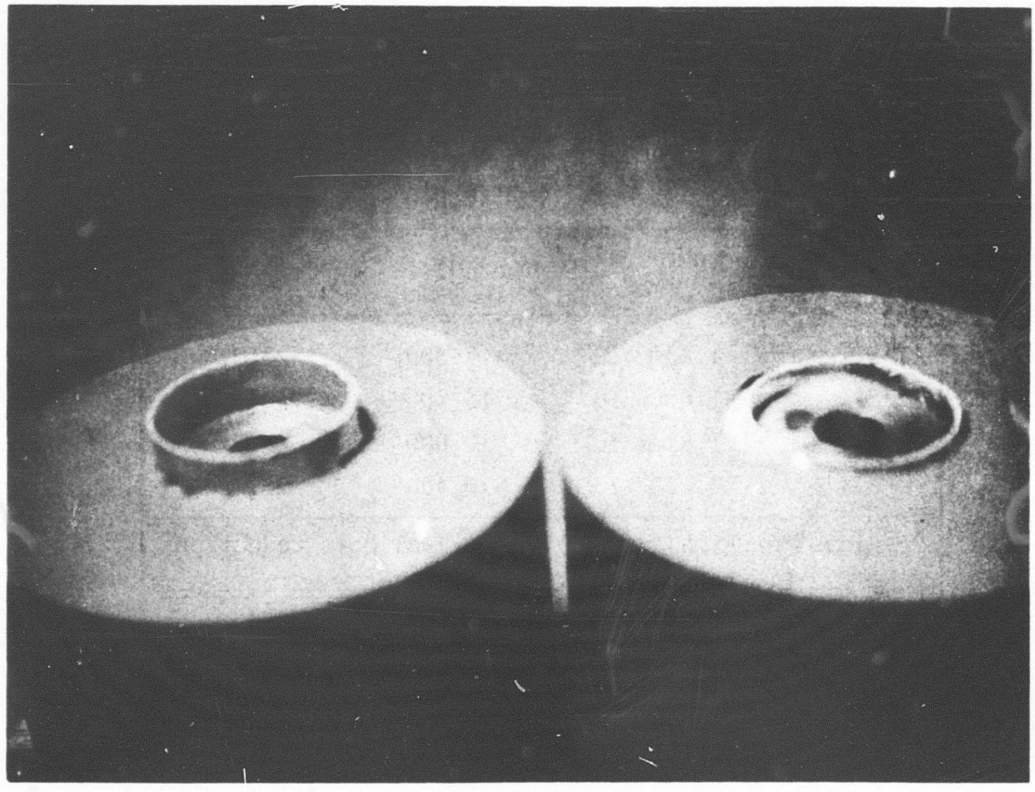

Figure 18. A Typical Shear Specimen Fracture.

The value for the minor Poisson's ratio for the parallel ply presented in Table V appears to be high, so a calculated value was used for all data reduction.* Also, the values for the major and minor elastic moduli were not different, within experimental error, so a mean value was used for each of them. This mean value was taken for the quasi-isotropic and was an average of the values. The minor and major moduli for the parallel and cross ply were close, within experimental error; therefore, the data were not averaged for the data reduction.

c. Biaxial-Loading Tests

The individual biaxial-loading specimens used in the main data-gathering series (see Figure 9) were designated B1 through B54, and the corresponding load-strain curves are presented in Appendix II.

The composite biaxial-stress values were obtained by multiplying the measured load value, P, by the following factors:

$$\sigma_1'/P = (\bar{Q}_{11}')(\varepsilon_1'/P) + (\bar{Q}_{12}')(\varepsilon_2'/P), \tag{65}$$

$$\sigma_2'/P = (\bar{Q}_{12}')(\varepsilon_1'/P) + (\bar{Q}_{22}')(\varepsilon_2'/P), \tag{66}$$

where directions 1 and 2 are the major and minor material-symmetry directions (see Section 2), ε_1'/P and ε_2'/P are taken from the biaxial-load versus strain data presented in Appendix II, and $\bar{\nu}_{12}$ and $\bar{\nu}_{21}$ are composite Poisson's ratios taken from Table V. For $\theta = 0$ degrees, the primes can be removed and

$$\bar{Q}_{11}' = \bar{Q}_{11} = \bar{E}_{11}/\bar{\lambda},\ \bar{Q}_{12}' = \bar{Q}_{12} = \bar{\nu}_{21}\bar{E}_{11}/\bar{\lambda},\ \bar{Q}_{22}' = \bar{Q}_{22} = \bar{E}_{22}/\bar{\lambda} \tag{67}$$

where $\bar{\lambda} = 1 - \bar{\nu}_{12}\bar{\nu}_{21}$

For $\theta = 45$ degrees.

$$\begin{aligned}\bar{Q}_{11}' = \bar{Q}_{22}' &= (1/4\bar{\lambda})(\bar{E}_{11} + 2\bar{\nu}_{21}\bar{E}_{11} + \bar{E}_{22} + 4\bar{\lambda}\bar{G}) \\ \bar{Q}_{12}' &= (1/4\bar{\lambda})(\bar{E}_{11} + 2\bar{\nu}_{21}\bar{E}_{11} + \bar{E}_{22} - 4\bar{\lambda}\bar{G})\end{aligned} \tag{68}$$

Table VII presents the results obtained by applying Equations (65) and (66) to the load-strain data of Appendix II.

The limit and ultimate strength criteria are the same as those used for the uniaxial tensile specimens. There appears to be some theoretical

*The calculated value was obtained from the reciprocal relationship:

$$0.1410 \times 3.15/3.304.$$

TABLE VII. RESULTS OF BIAXIAL-LOADING TESTS

Specimen No.	S'_{L1}, psi	S'_{U1}, psi	S'_{L2}, psi	S'_{U2}, psi
Four-Ply Parallel Laminated, 0-deg Orientation, 1:2 Nominal Loading				
B12	18,900	33,000	9,700	14,900
B13	19,650	26,500	9,150	12,420
B14	15,800	29,000	6,370	12,150
B15	17,900	35,100	7,560	15,550
B16	14,980	28,500	6,840	13,750
Four-Ply Parallel Laminated, 0-deg Orientation, 1:1 Nominal Loading				
B1	13,200	29,500	13,280	28,400
B2*	18,000	28,000	17,200	30,800
B3*	16,820	30,850	14,650	29,650
B4	16,700	28,450	15,500	29,250
B5	20,500	28,200	15,850	29,000
B6	15,750	36,000	12,850	37,000
B17	12,950	33,700	15,200	35,900
Four-Ply Parallel Laminated, 0-deg Orientation, 2:1 Nominal Loading				
B18	6,800	11,700	12,300	27,000
B19	7,650	13,000	25,700	36,300
B20	10,350	13,800	18,000	28,400
B21	8,320	14,650	19,300	35,100
B22	11,300	14,250	20,900	29,750
Four-Ply Parallel Laminated, 45-deg Orientation, 1:1 Nominal Loading				
B7	25,200	38,800	23,200	38,800
B8	15,100	24,200	13,600	28,400
B9*	10,950	26,500	14,350	28,000
B10*	14,100	23,800	11,040	25,100
B11	10,250	20,850	16,100	29,300

TABLE VII - Continued

Specimen No.	S'_{L1}, psi	S'_{U1}, psi	S'_{L2}, psi	S'_{U2}, psi
Four-Ply Cross Laminated, 0-deg Orientation, 1:1 Nominal Loading				
B23*	14,200	23,000	14,350	26,960
B24	15,200	31,700	16,700	31,700
B25	19,100	26,500	19,100	26,500
B26	19,100	27,200	20,950	27,200
B27	18,400	26,400	15,400	26,400
B28	17,650	28,400	17,650	28,400
Four-Ply Cross Laminated, 0-deg Orientation, 1:2 Nominal Loading				
B29*	6,800	13,250	16,700	30,400
B30	9,520	16,350	21,000	38,200
B31	11,400	18,900	13,300	23,000
B32*	6,750	10,200	14,100	19,400
B33*	4,000	4,000	9,000	10,200
B34	9,370	13,350	16,000	25,300
B35*	6,790	11,430	15,250	26,700
Six-Ply Quasi-Isotropic Laminated, 0-deg Orientation, 1:1 Nominal Loading				
B36	12,600	26,850	13,580	28,000
B37*	13,500	39,100	9,450	32,500
B38	10,650	34,100	11,700	34,100
B39	13,000	38,600	16,200	41,600
B40	5,930	24,800	6,000	26,900
Six-Ply Quasi-Isotropic Laminated, 45-deg Orientation, 1:1 Nominal Loading				
B41*	14,200	27,700	14,950	27,700
B42	7,300	14,000	11,850	19,500
B43	15,600	28,300	17,350	24,700

TABLE VII - Continued

Specimen No.	S'_{L1}, psi	S'_{U1}, psi	S'_{L2}, psi	S'_{U2}, psi
B44	12,350	20,800	14,300	22,200
B45	15,750	18,950	13,200	20,900
Six-Ply Quasi-Isotropic Laminated, 0-deg Orientation, 2:1 Nominal Loading				
B50*	20,700	33,900	10,600	13,350
B51	25,300	36,800	13,050	13,900
B52*	22,000	41,200	12,200	16,600
B53*	21,100	34,600	11,350	12,400
B54*	22,700	41,000	14,600	15,300
Six-Ply Quasi-Isotropic Laminated, 0-deg Orientation, 1:2 Nominal Loading				
B46*	7,150	12,600	21,950	36,000
B47	7,360	9,700	18,600	23,600
B48*	6,600	11,350	14,500	33,000
B49*	9,600	13,420	20,600	36,000

* In each specimen marked with an asterisk, the fracture did not pass through the reduced-thickness test section.

basis for using an "equivalent" offset strain for biaxial loading. However, practical design usage appears to favor using the same offset for all types of loading, as discussed by Bert et al (Reference 36).

It should be mentioned that the method used here to determine the stress from measured strains is quite accurate in the linear elastic range. When the load-strain curve becomes nonlinear, the accuracy of the stress values is not known. There are two factors, both of which would tend to reduce the actual stress to a lower value than predicted by the calculation. If the material in the reduced test section is yielding (i.e., undergoing higher strains than it would if it were elastic), its effective moduli would be lower than the corresponding elastic moduli and thus would lower the actual stress. However, if material not in the reduced-thickness test section yields first, additional load may be dumped into the test section, causing the strain gages to read erroneously high for a given value of load applied to the edge of the specimen. Thus, the calculated ultimate strength values presented represent upper bounds.

Figure 19 shows photographs of typical fracture patterns for both specimen types (1:1 and 1:2 or 2:1). The fact that a number of the fractures of the 1:1 type specimens were multiple is additional testimony to the very good attainment of a uniform balanced-biaxial stress field in the test section. Of the 54 biaxial-loading specimens tested in the data-gathering series, only 18 (marked with an asterisk in Table VII) did not fracture through the test section. However, a study of the apparent ultimate strength data in Table VII shows that these specimens failed at values very close to those of the other specimens, i.e., neither abnormally high nor abnormally low. This indicates that, in most cases, test-section failure was probably imminent.

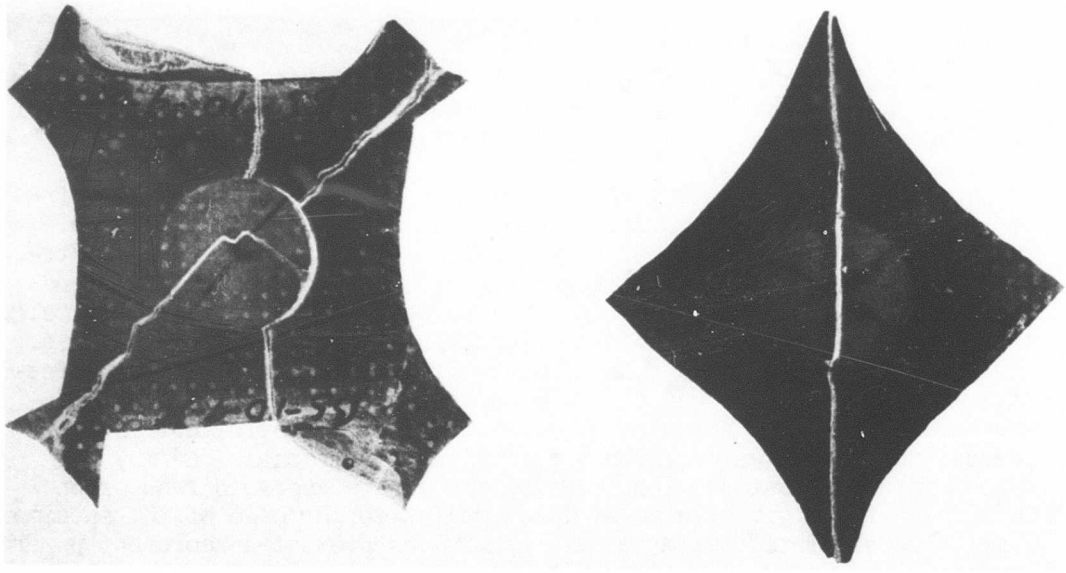

a. Nominal 1:1 Biaxial-Loading Specimens

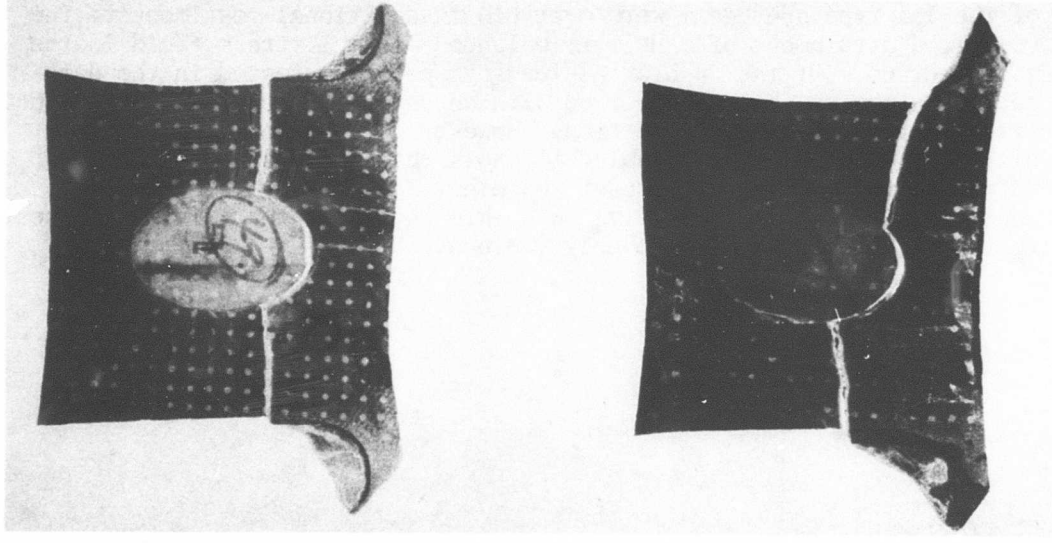

b. Nominal 1:2 Biaxial-Loading Specimens

Figure 19. Photographs of Typical Fracture Patterns for Biaxial-Loading Specimens.

8. EVALUATION OF EXPERIMENTAL RESULTS

In this section, the experimental results presented in Section 7 are evaluated in the light of the theoretical stiffness and strength considerations presented in Sections 2 and 3.

a. Parallel-Ply Laminates

Since there is presently no composite micromechanics analysis known to the authors to be applicable to fabric-reinforced composites, no quantitative prediction of the individual stiffnesses of parallel-ply laminates can be made on the basis of the properties of the constituent materials (glass and epoxy, in this case.) However, since the reciprocal relationship is based on very fundamental thermodynamics principles, as discussed in Section 2a, it should hold. The two parallel-ply moduli values presented in Table V appear to be reasonable for the resin content (34-36 percent by weight), and so does the value of $\bar{\nu}_{12}$. However, the $\bar{\nu}_{21}$ value appears to be erroneous, and since the reciprocal relation was violated, a value of 0.1342 given by the reciprocal relation appears to be more valid. The $\bar{\nu}_{12}$ and the corrected $\bar{\nu}_{12}$, as well as the E_{11} and E_{22} values, are quite close to those reported by Youngs (Reference 80) and Military Handbook 17 (Reference 81).

The value of G presented in Table V, 1,386,000 psi, is approximately 71 percent higher than the 810,000-psi value given in Military Handbook 17. Part of the difference may be due to the type of specimen, since the Military Handbook 17 values were obtained by in-plane panel-shear tests. Sidorin (Reference 82) obtained 11 percent higher shear-modulus values by torsion-tube tests than by panel-shear tests for the same fabric orientation under discussion here.

The value of $\bar{G}'$ corresponding to an orientation, θ, of 45 degrees can be predicted from the values of $\bar{G}$, $\bar{E}_{11}$, $\bar{E}_{22}$, and $\bar{\nu}_{12}$, by adapting the last of Equations (17) as follows:

$$1/\bar{G}' = (1/\bar{G}) + [(1 + 2\bar{\nu}_{12})\,\bar{E}_{11}^{-1} + (1/\bar{E}_{22}) - (1/\bar{G})]\,\sin^2 2\theta \qquad (69)$$

Equation (69) gives a value of 1,370,000 psi, which is considerably lower than the 3,390,000-psi value of $\bar{G}'$ determined experimentally for $\theta = 45$ degrees.*

Figure 20 presents the limit and apparent ultimate strength results from Table VII in the form of strength envelopes. It is noted that there

*It appears that the incompatibility of the torsion-tube properties and the properties of the flat specimens (uniaxial and biaxial) was due to a difference in resin content. The torsion-tube specimens did not bleed adequately, resulting in a resin content of approximately 40 percent, compared with 34 percent for the flat specimens.

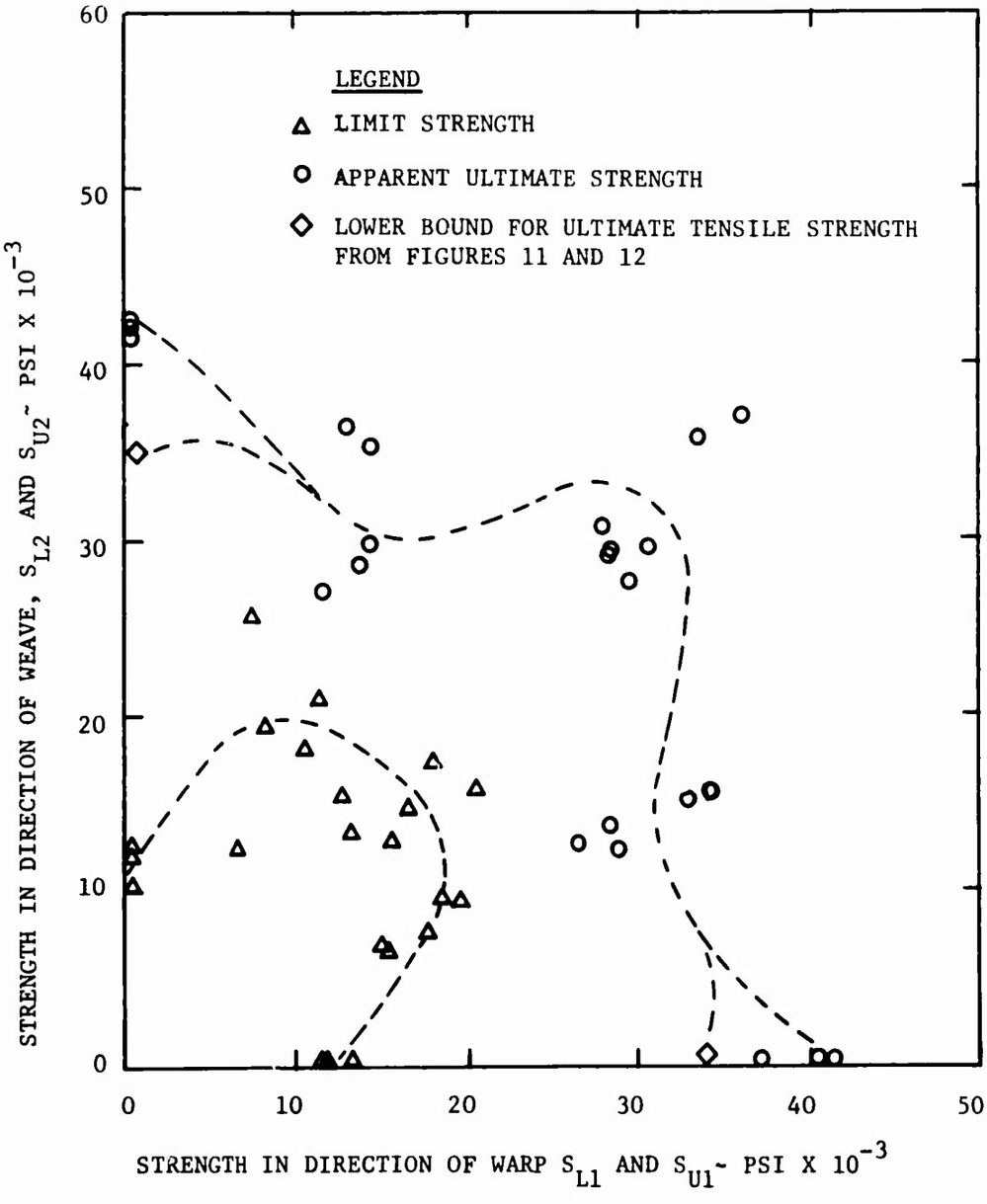

Figure 20. Biaxial-Tension Strength Envelope for 4-Parallel-Ply Laminate.

appears to be considerable symmetry about the 1:1 biaxial data; i.e., the 2:1 data and 1:0 data are symmetric with the 1:2 and 0:1 data, respectively. No attempt was made to fit a strength theory to the data presented.

b. Cross-Ply Laminates

In Section 2d, it was shown that laminate stiffness theory predicts that the stiffness properties of a symmetrically laminated cross-ply laminate are simply the mean values of the properties of the individual plies. Thus, the predicted values would be as follows:

$$\bar{E}_{11} = \bar{E}_{22} = 3.23 \times 10^6 \text{ psi}, \quad \bar{\nu}_{12} = \bar{\nu}_{21} = 0.1376$$

Both of these values are slightly higher than the corresponding values listed in Table V for the cross-ply laminate.

Figure 21 shows the limit and apparent ultimate strength envelopes for the cross-ply laminate, drawn from data in Table VII.

c. Quasi-Isotropic Laminates

The predicted quasi-isotropic stiffness values obtained by using parallel-ply stiffness properties in Equations (37), Section 2, are as follows:

$$\bar{E}_{11} = \bar{E}_{22} = 3.04 \times 10^6 \text{ psi},$$
$$\bar{\nu}_{12} = \bar{\nu}_{21} = 0.160,$$
$$\bar{G} = 1.31 \times 10^6 \text{ psi}.$$

These values compare very poorly with the mean quasi-isotropic values listed in the last column of Table V.

Figure 22 shows the limit and apparent ultimate strength envelopes for the quasi-isotropic laminate, using values from Table VII. The obviously higher yield strength at a biaxial-load ratio of 2:1 as compared to 1:1 is not explained.

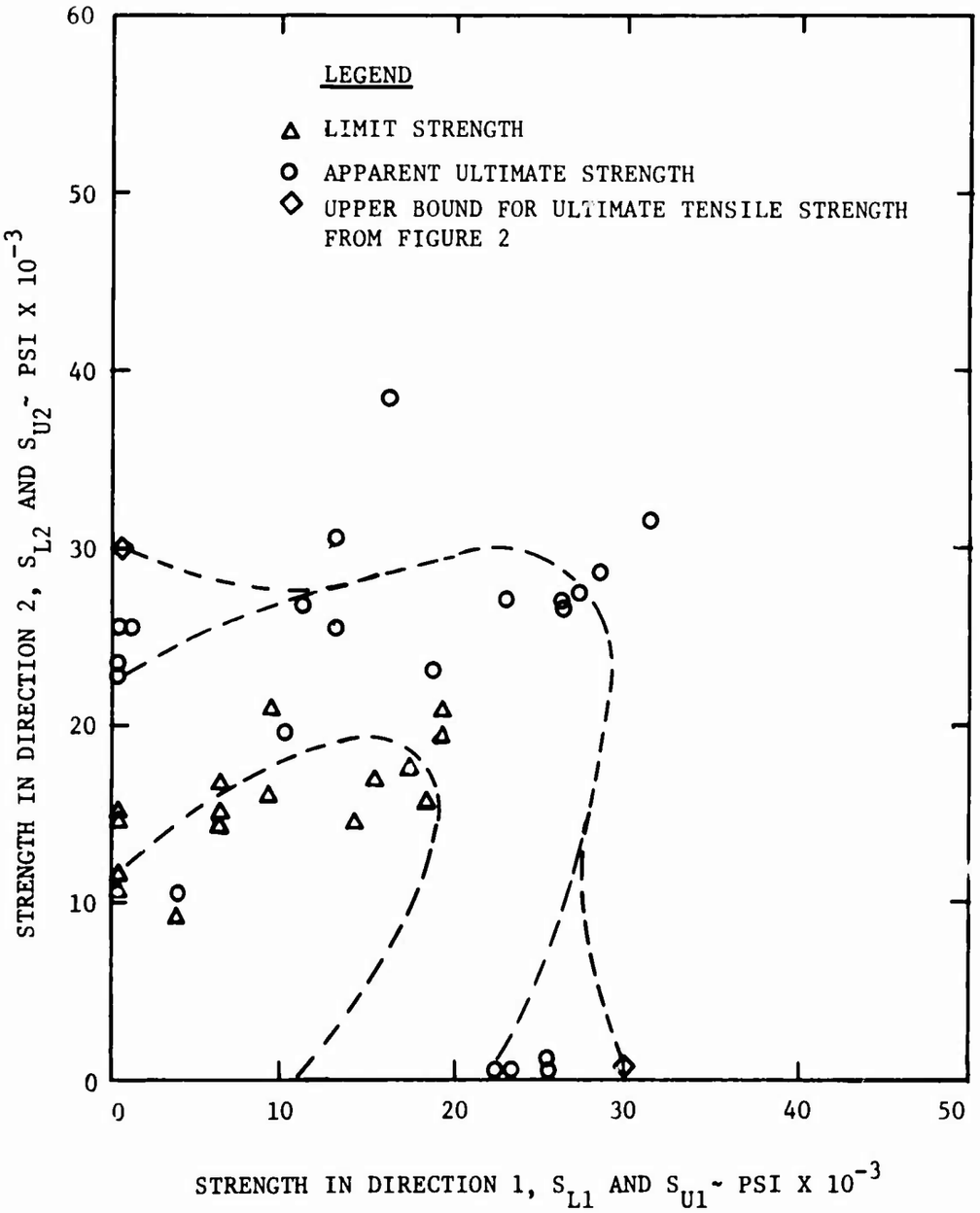

Figure 21. Biaxial-Tension Strength Envelope for 4-Ply, Symmetrically Cross Laminated Material.

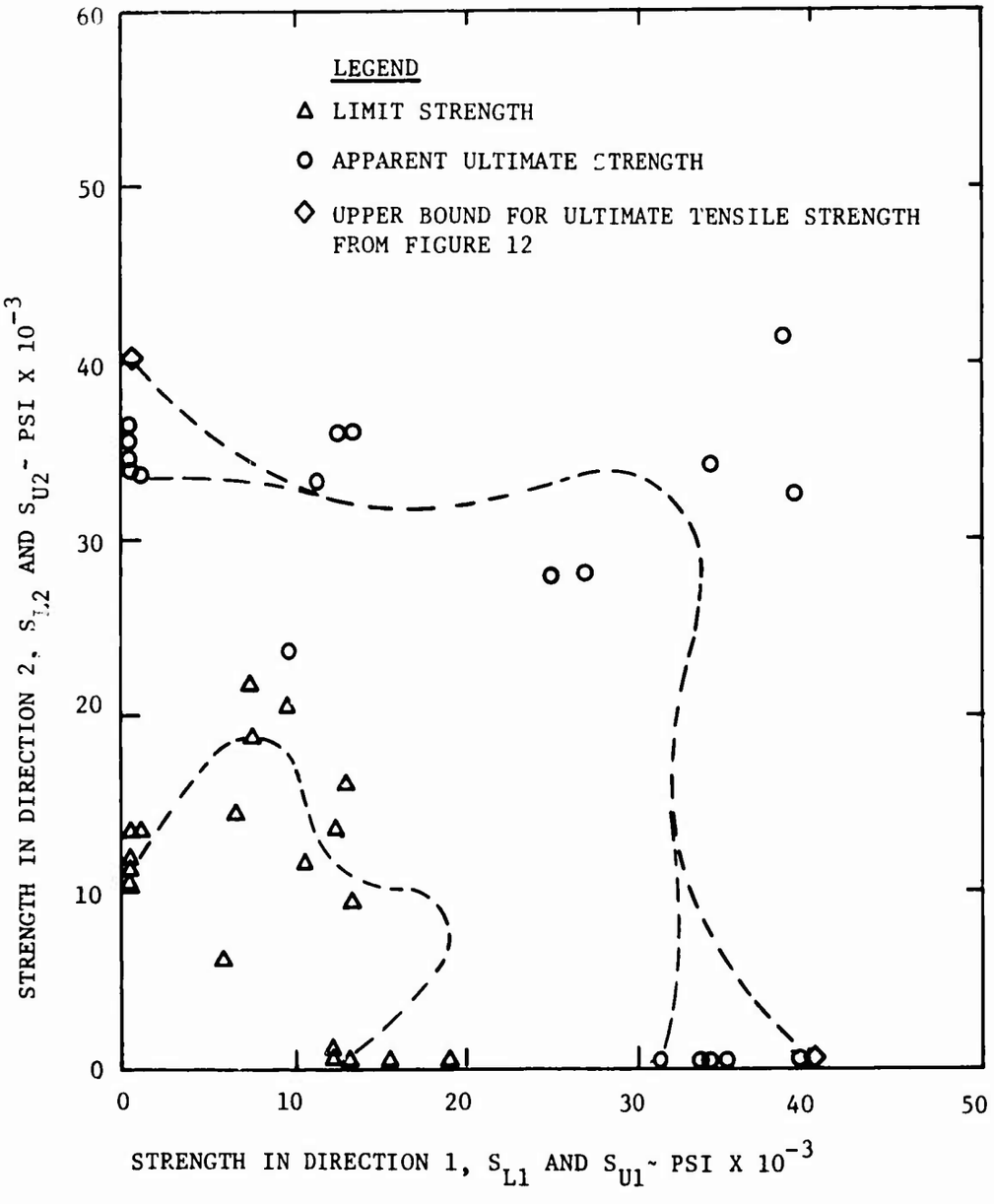

Figure 22. Biaxial-Tension Strength Envelope for 6-Ply Quasi-Isotropic Laminate.

9. CONCLUSIONS AND RECOMMENDATIONS

a. Conclusions

(1) Use of the biaxial-loading specimens and associated biaxial-loading fixture developed in this program is believed to be the most accurate, reliable, and simple-to-fabricate method for obtaining strength data on flat-sheet composite materials subjected to biaxial-tension loading.

(2) The Volan-A-finish, E-glass, 181-style fabric/828-Z eopxy laminates tested in this program generally exhibited considerably higher limit strengths (and slightly lower apparent ultimate strengths) under 1:1, 1:2, and 2:1 biaxial-load ratios than in uniaxial tension.

(3) Of the three lamination arrangements evaluated (parallel-ply, cross-ply, and quasi-isotropic), the parallel-ply laminate was slightly superior under biaxial loading, although the differences were small. This suggests that for this particular weave, combination of materials, and type of loading (uniaxial or biaxial tension), parallel-ply lamination is advantageous structurally as well as being easier to fabricate. (This same conclusion would not be expected to hold true for a more highly unidirectional composite such as a tape or a filament-wound composite.)

(4) The thin-walled torsion-tube specimen used in this program is believed to be an accurate and reliable method for obtaining shear modulus and shear strength data on composite materials. However, it does suffer from the requirement that the composite must be fabricated into the form of a tube.

b. Recommendations

(1) Additional composite materials of importance for Army aircraft primary structures should be evaluated in biaxial-tension loading using the types of specimens and loading device developed in the program. In view of Conclusion (3), it would be especially important to evaluate a more highly unidirectional material such as a tape. The fiber material may be commercial S-glass, boron, silicon carbide, graphite, etc.

(2) In conjunction with Recommendation (1), it is recommended that the optimal lamination arrangement be determined for each combination of composite material and biaxial-loading ratio.

(3) In view of the strong dependence of uniaxial tensile strength values on specimen width, length, number of plies, and presence of stress-concentration-producing discontinuities, such as changes in thickness, it is recommended that more research be devoted to this problem. A more extensive experimental program, coupled with an

appropriate analytical investigation, appears to be advisable in order to arrive at sufficiently definitive information for more reliable design of uniaxially loaded structures of composite materials.

LITERATURE CITED

1. Nordby, G.M., and W.C. Crisman, RESEARCH IN THE FIELD OF FIBER-GLASS-REINFORCED SANDWICH STRUCTURE FOR AIRFRAME USE, University of Oklahoma Research Institute; TRECOM Technical Report 64-37, U.S. Army Transportation Research Command, Fort Eustis, Virginia, July 1964, AD 607339.

2. Nordby, G.M., W.C. Crisman, and C.W. Bert, THE EFFECT OF RESIN CONTENT AND VOIDS ON THE STRENGTH OF FIBERGLASS-REINFORCED PLASTICS FOR AIRFRAME USE, University of Oklahoma Research Institute; USAAVLABS Technical Report 65-66, U.S. Army Aviation Materiel Laboratories, Fort Eustis, Virginia, November 1965, AD 627362.

3. Nordby, G.M., and W.C. Crisman, FABRICATING LAMINATES FOR SPECIFIC PROPERTIES, Modern Plastics, Vol. 44, No. 2, October 1966, pp. 135-136.

4. Harris, B.J., and W.C. Crisman, FACE-WRINKLING MODE OF BUCKLING OF SANDWICH PANELS, Journal of the Engineering Mechanics Division, Proceedings of the American Society of Civil Engineers, Vol. 91, No. EM3, June 1965, pp. 93-111.

5. Nordby, G.M., and W.C. Crisman, STRENGTH PROPERTIES AND RELATIONSHIPS ASSOCIATED WITH VARIOUS TYPES OF FIBERGLASS-REINFORCED FACING SANDWICH STRUCTURE, University of Oklahoma Research Institute; USAAVLABS Technical Report 65-15, U.S. Army Aviation Materiel Laboratories, Fort Eustis, Virginia, August 1965, AD 621522.

6. Nordby, G.M., W.C. Crisman, and C.W. Bert, DYNAMIC ELASTIC, DAMPING, AND FATIGUE CHARACTERISTICS OF FIBERGLASS-REINFORCED SANDWICH STRUCTURE, University of Oklahoma Research Institute; USAAVLABS Technical Report 65-60, U.S. Army Aviation Materiel Laboratories, Fort Eustis, Virginia, October 1965, AD 623128.

7. Nordby, G.M., and W.C. Crisman, FATIGUE CHARACTERISTICS OF AN RP SANDWICH STRUCTURE, Modern Plastics, Vol. 43, No. 10, June 1966, pp. 120 ff.

8. Bert, C.W., D.J. Wilkins, Jr., and W.C. Crisman, DAMPING IN SANDWICH BEAMS WITH SHEAR FLEXIBLE CORES, Journal of Engineering for Industry, Transactions of the American Society of Mechanical Engineers, Vol. 89B, No. 4, November 1967, pp. 662-670.

9. Nordby, G.M., W.C. Crisman, and C.W. Bert, FABRICATION AND FULL-SCALE STRUCTURAL EVALUATION OF SANDWICH SHELLS OF REVOLUTION COMPOSED OF FIBER GLASS-REINFORCED PLASTIC FACINGS AND HONEYCOMB CORES, University of Oklahoma Research Institute; USAAVLABS Technical Report 67-65, U.S. Army Aviation Materiel Laboratories, Fort Eustis, Virginia, November 1967, AD 666480.

10. Bert, C.W., W.C. Crisman, and G.M. Nordby, FABRICATION AND FULL-SCALE STRUCTURAL EVALUATION OF GLASS-FABRIC REINFORCED-PLASTIC SHELLS, Journal of Aircraft, Vol. 5, No. 1, January-February 1968, pp. 27-34.

11. Nordby, G.M., and W.C. Crisman, ANATOMY OF AN AUTOCLAVE, Reinforced Plastics and Composites World, Vol. 7, No. 2, March-April 1968, pp. 20-21.

12. Bert, C.W., W.C. Crisman, and G.M. Nordby, BUCKLING OF CYLINDRICAL AND CONICAL SANDWICH SHELLS WITH ORTHOTROPIC FACINGS, American Institute of Aeronautics and Astronautics (AIAA)/American Society of Mechanical Engineers Ninth Structures, Structural Dynamics and Materials Conference, AIAA Paper No. 68-294, Palm Springs, California, April 1968; to appear in American Institute of Aeronautics and Astronautics Journal.

13. Bert, C.W., B.L. Mayberry, and J.D. Ray, VIBRATION EVALUATION OF SANDWICH CONICAL SHELLS WITH FIBER-REINFORCED COMPOSITE FACINGS, University of Oklahoma Research Institute; USAAVLABS Technical Report 68-85, U.S. Army Aviation Materiel Laboratories, Fort Eustis, Virginia.

14. Ray, J.D., C.W. Bert, and D.M. Egle, THE APPLICATION OF THE KENNEDY-PANCU METHOD TO EXPERIMENTAL VIBRATION STUDIES OF COMPLEX SHELL STRUCTURES, presented at the 39th Shock and Vibration Symposium, Monterey, Calif., Oct. 22-24, 1968; to appear in Shock and Vibration Bulletin No. 39.

15. TESTING TECHNIQUES FOR FILAMENT-REINFORCED PLASTICS, AFML Technical Report 66-274, Air Force Materials Laboratory, Wright-Patterson Air Force Base, Ohio, September 1966, AD 801547.

16. Chamis, C.C., MICRO AND STRUCTURAL MECHANICS AND STRUCTURAL SYNTHESIS OF MULTILAYERED FILAMENTARY COMPOSITE PANELS, Case Western Reserve University, Division of Solid Mechanics, Structures and Mechanical Design, Report No. 9, September 1967.

17. Tsai, S.W., STRUCTURAL BEHAVIOR OF COMPOSITE MATERIALS, Aeronutronic Division, Philco Corporation; Contractor's Report CR-71, National Aeronautics and Space Administration, Washington, D.C., July 1964.

18. Tsai, S.W., STRENGTH CHARACTERISTICS OF COMPOSITE MATERIALS, Aeronutronic Division, Philco Corporation; Contractor's Report CR-224, National Aeronautics and Space Administration, Washington, D.C., April 1965.

19. Huber, M.T., FOUNDATIONS FOR RATIONAL CALCULATION OF CROSS-REINFORCED CONCRETE PLATES (in German), Zeitschrift Osterreiche Ingenieure-und-Architekten Vereines, No. 30, 1914, p. 557.

20. Love, A.E.H., A TREATISE ON THE MATHEMATICAL THEORY OF ELASTICITY, 4th edition, New York, Dover Publications, Inc., 1927, pp. 151-155.

21. Mindlin, R.D., MICROSTRUCTURE IN LINEAR ELASTICITY, Archive for Rational Mechanics and Analysis, Vol. 16, No. 1, 1964, pp. 51-78.

22. Fung, Y.C., FOUNDATIONS OF SOLID MECHANICS, Englewood Cliffs, New Jersey, Prentice-Hall, Inc., 1965, pp. 347-349.

23. Fung, Y.C., FOUNDATIONS OF SOLID MECHANICS, Englewood Cliffs, New Jersey, Prentice-Hall, Inc., 1965, p. 454.

24. Huntington, H.B., THE ELASTIC CONSTANTS OF CRYSTALS, New York, Academic Press, Inc., 1957.

25. Lekhnitskii, S.G., THEORY OF ELASTICITY OF AN ANISOTROPIC ELASTIC BODY, English translation, San Francisco, Holden-Day, Inc., 1963, p. 66.

26. Piehler, H.R., THE INTERIOR ELASTIC STRESS FIELD IN A CONTINUOUS CLOSE-PACKED FILAMENTARY COMPOSITE MATERIAL UNDER UNIAXIAL TENSION, ASRL Technical Report 132-1, Massachusetts Institute of Technology, Aero-elastic and Structures Research Laboratory, Cambridge, Massachusetts, June 1965, AD 624572.

27. Lekhnitskii, S.G., THEORY OF ELASTICITY OF AN ANISOTROPIC ELASTIC BODY, English translation, San Francisco, Holden-Day, Inc., 1963, p. 25.

28. Greszczuk, L.B., EFFECT OF MATERIAL ORTHOTROPY ON THE DIRECTIONS OF PRINCIPAL STRESSES AND STRAINS, Orientation Effects in the Mechanical Behavior of Anisotropic Structural Materials, Special Technical Publication No. 405, Philadelphia, Pennsylvania, American Society for Testing and Materials, 1965, pp. 1-13.

29. Tsai, S.W., and N.J. Pagano, INVARIANT PROPERTIES OF COMPOSITE MATERIALS, Composite Materials Workshop, edited by S.W. Tsai, J.C. Halpin, and N.J. Pagano , Stamford, Connecticut, Technomic Publishing Company, Inc. 1968, pp. 233-253.

30. Stavsky, Y., BENDING AND STRETCHING OF LAMINATED AEOLOTROPIC PLATES, Journal of the Engineering Mechanics Division, Proceedings of the American Society of Civil Engineers, Vol. 87, No. EM6, December 1961, pp. 31-56.

31. Clark, S.K., INTERNAL CHARACTERISTICS OF ORTHOTROPIC LAMINATES, Textile Research Journal, Vol. 3, No. 11, November 1963, pp. 935-953.

32. Greszczuk, L.B., THERMOELASTIC PROPERTIES OF FILAMENTARY COMPOSITES, AIAA Sixth Structures and Materials Conference, Palm Springs, California, April 5-7, 1965, pp. 285-290.

33. Werren, F., and C.B. Norris, MECHANICAL PROPERTIES OF A LAMINATE DESIGNED TO BE ISOTROPIC, Report No. 1841, Forest Products Laboratory, Madison, Wisconsin, May 1953.

34. Hill, R., A THEORY OF THE YIELDING AND PLASTIC FLOW OF ANISOTROPIC METALS, Proceedings of the Royal Society, (London), Vol. 193A, 1948, pp. 281-297.

35. Marin, J., MECHANICAL BEHAVIOR OF ENGINEERING MATERIALS, Englewood Cliffs, New Jersey, Prentice-Hall, Inc., 1962, Chapter 3.

36. Bert, C.W., E.J. Mills, and W.S. Hyler, MECHANICAL PROPERTIES OF AEROSPACE STRUCTURAL ALLOYS UNDER BIAXIAL-STRESS CONDITIONS, Battelle Memorial Institute; AFML Technical Report 66-229, Air Force Materials Laboratory, Wright-Patterson Air Force Base, Ohio, August 1966, AD48304.

37. Norris, C.B., STRENGTH OF ORTHOTROPIC MATERIALS SUBJECTED TO COMBINED STRESSES, Report No. 1816, Forest Products Laboratory, Madison, Wisconsin, July 1950.

38. Ashkenazi, E.K., THE CONSTRUCTION OF LIMITING SURFACES FOR A BIAXIAL-STRESSED CONDITION OF ANISOTROPIC MATERIALS, Industrial Laboratory, Vol. 30, No. 2, 1964, pp. 285-287.

39. Ashkenazi, E.K., PROBLEMS OF THE ANISOTROPY OF STRENGTH, Polymer Mechanics, Vol. 1, No. 2, March-April 1965, pp. 60-70.

40. Norris, C.B., and P.F. McKinnon, COMPRESSION, TENSION, AND SHEAR TESTS ON YELLOW-POPLAR PLYWOOD PANELS OF SIZES THAT DO NOT BUCKLE WITH TESTS MADE AT VARIOUS ANGLES TO THE FACE GRAIN, Report No. 1328, Forest Products Laboratory, Madison, Wisconsin, 1946.

41. Ashkenazi, E.K., ON THE PROBLEM OF STRENGTH ANISOTROPY OF CONSTRUCTION MATERIALS, Soviet Physics-Technical Physics, Vol. 4, No. 3, September 1959, pp. 333-338.

42. Marin, J., THEORIES OF STRENGTH FOR COMBINED STRESSES AND NONISOTROPIC MATERIALS, Journal of the Aeronautical Sciences, Vol. 24, No. 4, April 1957, pp. 265-268, 274.

43. Hu, L.W., and K.D. Pae, INCLUSION OF THE HYDROSTATIC STRESS COMPONENT IN FORMULATION OF THE YIELD CONDITION, Journal of the Franklin Institute, Vol. 275, No. 6, June 1963, pp. 491-502.

44. Rogers, C.W., H.R. Thornton, R.H. Cornish, and A.H. Lasday, APPLICATION OF ADVANCED FIBROUS REINFORCED COMPOSITE MATERIALS TO AIRFRAME STRUCTURES, General Dynamics Corp., Fort Worth Division; AFML Technical Report 66-313, Vol. II, Air Force Materials Laboratory, Wright-Patterson Air Force Base, 1966, AD 803128L.

45. Mc Gill, D.J., A NOTE ON THE SAINT-VENANT THEORY OF FAILURE, Journal of Basic Engineering, Transactions of the American Society of Mechanical Engineers, Vol. 90D, No. 1, March 1968, pp. 138-139.

46. Stassi-D'Alia, F., LIMITING CONDITIONS OF YIELDING OF THICK-WALLED-CYLINDERS AND SPHERICAL SHELLS, University of Palermo, Italy; Final Status Report, Contract No. DA-91-591-EUC-1351, U.S. Army European Research Office, Frankfurt, Germany, November 24, 1959, AD 252029.

47. Hoffman, O., THE BRITTLE STRENGTH OF ORTHOTROPIC MATERIALS, Journal of Composite Materials, Vol. 1, No. 2, April 1967, pp. 200-206.

48. Gol'denblat, I.I., and V.A. Kopnov, STRENGTH OF GLASS-REINFORCED PLASTICS IN THE COMPLEX STRESS STATE, Polymer Mechanics, Vol. 1, No. 2, March-April 1965, pp. 54-59.

49. Capurso, M., YIELD CONDITIONS FOR INCOMPRESSIBLE ISOTROPIC AND ORTHOTROPIC MATERIALS WITH DIFFERENT YIELD STRESS IN TENSION AND COMPRESSION, Meccanica (Milan, Italy), Vol. 2, No. 2, June 1967, pp. 118-125.

50. Stowell, E.Z., and T.S. Liu, ON THE MECHANICAL BEHAVIOR OF FIBER-REINFORCED CRYSTALLINE MATERIAL, Journal of the Mechanics and Physics of Solids, Vol. 9, 1961, pp. 242-260.

51. Griffith, J.E., and W.M. Baldwin, FAILURE THEORIES FOR GENERALLY ORTHOTROPIC MATERIALS, Developments in Theoretical and Applied Mechanics, Vol. 1 (Proceedings of the First Southeastern Conference on Theoretical and Applied Mechanics, 1962), New York, Plenum Press, 1963, pp. 410-420.

52. Werren, F., and C.B. Norris, DIRECTIONAL PROPERTIES OF GLASS-FABRIC-BASE PLASTIC LAMINATE PANELS OF SIZES THAT DO NOT BUCKLE, Report No. 1803, Forest Products Laboratory, Madison, Wisconsin, April 1949.

53. Werren, F., SUPPLEMENT TO DIRECTIONAL PROPERTIES OF GLASS-FABRIC-BASE PLASTIC LAMINATE PANELS OF SIZES THAT DO NOT BUCKLE, Report No. 1803-A, Forest Products Laboratory, Madison, Wisconsin, April 1950.

54. Werren, F., and M.Gish, SUPPLEMENT TO DIRECTIONAL PROPERTIES OF GLASS-FABRIC-BASE PLASTIC LAMINATE PANELS OF SIZES THAT DO NOT BUCKLE, Report No. 1803-C, Forest Products Laboratory, Madison, Wisconsin, May 1957.

55. Tsai, S.W., D.F. Adams, and D.R. Doner, ANALYSES OF COMPOSITE STRUCTURES, Aeronutronic Division, Philco Corporation; Contractor's Report CR-620, National Aeronautics and Space Corporation, Washington, D.C., November 1966.

56. Ely, R.E., BIAXIAL FRACTURE STRESSES FOR GRAPHITE, CERAMIC, AND FILLED AND REINFORCED EPOXY TUBE SPECIMENS, Report RR-TR-65-10, U.S. Army Missile Command, Redstone Arsenal, Alabama, June 1965, AD 469036.

57. Weng. T.L., BIAXIAL FRACTURE STRENGTH AND MECHANICAL PROPERTIES OF GRAPHITE BASE REFRACTORY COMPOSITES, American Institute of Aeronautics and Astronautics (AIAA)/American Society of Mechanical Engineers Ninth Structures, Structural Dynamics and Materials Conference, AIAA Paper No. 68-337, Palm Springs, California, April 1968.

58. Harrington, R.A., C.Chamis, E.H. Rowe, and E.M. Tatarzycki, DESIGN INFORMATION FROM ANALYTICAL AND EXPERIMENTAL STUDIES OF FILAMENT WOUND STRUCTURES SUBJECTED TO COMBINED LOADING, B.F. Goodrich Aerospace and Defense Products, Final Report on Subcontract No. 89 to Hercules Powder Company, Allegany Ballistics Laboratory, Cumberland, Maryland, February 25, 1964, AD 451216.

59. Abbott, B.W., SOME OBSERVATIONS ON THE BIAXIAL COMPRESSIVE CREEP PERFORMANCE OF FILAMENT WOUND LAMINATES, IIT Research Institute, Chicago, Illinois, Contract No. NObs 90329, Special Technical Report, August 1964, AD 610539.

60. Waddoups, M.E., CHARACTERIZATION AND DESIGN OF COMPOSITE MATERIALS, Composite Materials Workshop, edited by S.W. Tsai, J.C. Halpin, and N.J. Pagano, Stamford, Connecticut, Technomic Publishing Company, Inc., 1968, pp. 254-308.

61. Terry, E.L., and S.W. McClaren, BIAXIAL STRESS AND STRAIN DATA ON HIGH STRENGTH ALLOYS FOR DESIGN OF PRESSURIZED COMPONENTS, Chance Vought Corp.; ASD Technical Documentary Report 62-401, Aeronautical Systems Division, Wright-Patterson Air Froce Base, Ohio, May 1962, AD 283348.

62. CRACK PROPAGATION PREDICTION AND CRACK-STOPPER TECHNIQUES FOR STIFFENED AND UNSTIFFENED FLAT SHEET IN A SUPERSONIC TRANSPORT ENVIRONMENT, Douglas Aircraft Company, Inc., Aircraft Division; ASD Technical Documentary Report 63-773, Aeronautical Systems Division, Wright-Patterson Air Force Base, Ohio, September 1963, AD 423568L.

63. Grimes, G., B.J. Pape, and J.H. Ferguson, INVESTIGATION OF STRUCTURAL DESIGN CONCEPTS FOR FIBROUS AIRCRAFT STRUCTURES. VOLUME III. TECHNOLOGY APPRAISAL-EXPERIMENTAL DATA AND METHODOLOGY, Southwest Research Institute; AFFDL Technical Report 67-29, Volume III, Air Force Flight Dynamics Laboratory, Wright-Patterson Air Force Base, Ohio, November 1967, AD 824228.

64. Durelli, A.J., E.A. Phillips, and C.H. Tsao, INTRODUCTION TO THE THEORETICAL AND EXPERIMENTAL ANALYSIS OF STRESS AND STRAIN, New York, McGraw-Hill Book Company, Inc., 1958, pp. 369-370.

65. Penton, A.P., A NEW DEVICE FOR DETERMINING SHEAR PROPERTIES OF REINFORCED PLASTICS, Society of Plastics Engineers Journal, Vol. 16, No. 11, November 1960, pp. 1246-1247.

66. Bryan, E.L., PHOTOELASTIC EVALUATION OF THE PANEL SHEAR TEST FOR PLYWOOD, Symposium on Shear and Torsion Testing, Special Technical Publication No. 289, Philadelphia, Pennsylvania, American Society for Testing and Materials, 1961, pp. 90-94.

67. Pagano, N.J., and J.C. Halpin, INFLUENCE OF END CONSTRAINT IN THE TESTING OF ANISOTROPIC BODIES, Journal of Composite Materials, Vol. 2, No. 1, January 1968, pp. 18-31.

68. Grinius, V.G., MICROMECHANICS-FAILURE MECHANISM STUDIES, Whittaker Corp., Narmco Research and Development Division; AFML Technical Report 66-177, Air Force Materials Laboratory, Wright-Patterson Air Force Base, Ohio, August 1966, AD 638921.

69. Tsai, S.W., EXPERIMENTAL DETERMINATION OF THE ELASTIC BEHAVIOR OF ORTHOTROPIC PLATES, Journal of Engineering for Industry, Transactions of the American Society of Mechanical Engineers, Vol. 87B, No. 3, August 1965, pp. 315-317.

70. Greszczuk, L.B., DOUGLAS RING TEST FOR SHEAR MODULUS DETERMINATION OF ISOTROPIC AND COMPOSITE MATERIALS, Proceedings of the 23rd Annual Technical Conference, Reinforced Plastics/Composites Division, Society of the Plastics Industry, Inc., Washington, D.C., February 1968, Section 17-D.

71. Iosipescu, N., PHOTOELASTIC INVESTIGATIONS OF AN ACCURATE PROCEDURE FOR THE PURE SHEAR TESTING OF MATERIALS, Revue roumaine des sciences techniques serie de mechanique appliquee, Vol. 8, No. 1, 1963, pp. 145-164.

72. Romstad, K., METHODS FOR EVALUATING SHEAR STRENGTH OF PLASTIC LAMINATES REINFORCED WITH UNWOVEN GLASS FIBERS, Research Note FPL-033, Forest Products Laboratory, Madison, Wisconsin, May 1964, AD 600860.

73. Adams, D.F., and Thomas, R.L., THE SOLID ROD TORSION TEST FOR THE DETERMINATION OF UNIDIRECTIONAL COMPOSITE SHEAR PROPERTIES, paper presented at the Third Annual Symposium on High Performance Composites, Monsanto/Washington University Association, St. Louis, Missouri, October 1967.

74. Whitney, J.M., EXPERIMENTAL DETERMINATION OF SHEAR MODULUS OF LAMINATED FIBER-REINFORCED COMPOSITES, Experimental Mechanics, Vol. 7, No. 10, October 1967, pp. 447-448.

75. Simitses, G.L., INSTABILITY OF ORTHOTROPIC CYLINDRICAL SHELLS UNDER COMBINED TORSION AND HYDROSTATIC PRESSURE, American Institute of Aeronautics and Astronautics Journal, Vol. 5, No. 8, August 1967, pp. 1463-1469.

76. Metcalfe, A.G., and G.K. Schmitz, EFFECT OF LENGTH ON THE STRENGTH OF GLASS FIBERS, Proceedings of the American Society for Testing and Materials, Vol. 64, 1964, pp. 1075-1093.

77. Trantina, G.G., PRELIMINARY INVESTIGATION OF MEASUREMENT OF ELASTIC MODULI OF COMPOSITES USING STRAIN GAGES, T & AM Report 271, University of Illinois, Department of Theoretical and Applied Mechanics, Contract No. NOw-66-0360, September 1967, AD 664690.

78. Scop, P.M., and A.S. Argon, STATISTICAL THEORY OF STRENGTH OF LAMINATED COMPOSITES, Journal of Composite Materials, Vol. 1, No. 1, January 1967, pp. 92-99.

79. COMPILATION AND ANALYSIS OF TEST DATA ON FIBERGLASS-REINFORCED PLASTICS, Kaman Aircraft Corporation; TRECOM Technical Report 64-9, U.S. Army Transportation Research Command, Fort Eustis, Virginia, March 1964, AD 600514.

80. Youngs, R.L., POISSON'S RATIOS FOR GLASS-FABRIC-BASE PLASTIC LAMINATES, Report No. 1860, Forest Products Laboratory, Madison, Wisconsin, January 1957.

81. PLASTICS FOR FLIGHT VEHICLES, PART 1: REINFORCED PLASTICS, Military Handbook MIL-HDBK-17, Armed Forces Supply Support Center, Washington, D.C., November 1959.

82. Sidorin, Ya.S., EXPERIMENTAL INVESTIGATION OF THE ANISOTROPY OF FIBER-GLASS-REINFORCED PLASTICS DURING SHEAR, Industrial Laboratory, Vol. 32, No. 5, January 1967, pp. 723-726.

SELECTED BIBLIOGRAPHY*

Tensile-Fracture Mechanics of Filamentary Composites

Arridge, R.G.C., A CRITERION FOR TENSILE FAILURE IN A FIBRE-REINFORCED MATERIAL, British Journal of Applied Physics, Vol. 16, August 1965, pp. 1181-1186.

Atkinson, G., THE PROPAGATION OF FRACTURE IN AEOLOTROPIC MATERIALS, International Journal of Fracture Mechanics, Vol. 1, No. 1, March 1965, pp. 47-55.

Atkinson, C., and A.K. Head, THE INFLUENCE OF ELASTIC ANISOTROPY ON THE PROPAGATION OF FRACTURE, International Journal of Fracture Mechanics, Vol. 2, No. 3, September 1966, pp. 489-505.

Baker, B.R., DUCTILE YIELDING AND BRITTLE FRACTURE AT THE ENDS OF PARALLEL CRACKS IN A STRETCHED ORTHOTROPIC SHEET, International Journal of Fracture Mechanics, Vol. 2, No. 4, December 1966, pp. 576-596.

Becker, H., A FAILURE LAW FOR FILAMENTARY COMPOSITES, American Institute of Aeronautics and Astronautics Journal, Vol. 4, No. 12, December 1966, pp. 2218-2219.

Broutman, L.J., FRACTURE MECHANICS OF STRESS CRACKING AND CRAZING, Society of Plastics Engineers Journal, Vol. 21, No. 3, March 1965, pp. 283-287.

Corten, H.T., MICROMECHANICS AND FRACTURE BEHAVIOR OF COMPOSITES, Modern Composite Materials, edited by L.J. Broutman and R.H. Krock, Reading, Massachusetts, Addison-Wesley Publishing Company, Inc., 1967, Chapter 2, pp. 27-105.

Gol'dshtein, R.V., ON SURFACE WAVES IN JOINED ELASTIC MATERIALS AND THEIR RELATION TO CRACK PROPAGATION ALONG THE JUNCTION, Journal of Applied Mathematics and Mechanics, Vol. 31, No. 3, 1967, pp. 496-502.

Irwin, G.R., FORCE CONCEPTS IN RELATION TO FRACTURE BEHAVIORS OF COMPOSITE MATERIALS, Composite Materials Workshop, edited by S.W. Tsai, J.C. Halpin, and N.J. Pagano, Stamford, Connecticut, Technomic Publishing Company, Inc., 1968, pp. 9-19.

Kies, J.A., PREDICTION OF FAILURE DUE TO MECHANICAL DAMAGE IN THE OUTER HOOP WINDINGS IN FIBERGLASS PLASTIC PRESSURE VESSELS, NRL Report 5736, U.S. Naval Research Laboratory, Washington, D.C., January 18, 1962, AD 271693.

---

*This bibliography does not include any references listed in Literature Cited. Also, in the case of publications which first appeared as a thesis or report and later as a paper in a journal, only the latter form is listed, since it is the most readily accessible.

Manshinha, L., TENSILE FRACTURE ALONG A BIMATERIAL INTERFACE, Rice University; Contractor's Report CR-60708, National Aeronautics and Space Administration, Washington, D.C., 1964, N66-17220.

Mossakovskii, V.I., and M.T. Rybka, GENERALIZATION OF THE CRIFFITH-SNEDDON CRITERION FOR THE CASE OF A NONHOMOGENEOUS BODY, Journal of Applied Mathematics and Mechanics, Vol. 28, No. 6, 1964, pp. 1277-1286.

Mostovoy, S., and E.J. Ripling, FACTORS CONTROLLING THE STRENGTH OF COMPOSITES BODIES (INTERPHASE FRACTURING OF COMPOSITE BODIES), Materials Research Laboratory, Inc., Richton Park, Illinois, Contract No. NOw-64-0414-c, Final Report, 1965, AD 470121.

Mostovoy, S., and E.J. Ripling, INTERPHASE FRACTURING OF COMPOSITE BODIES, Materials Research Laboratory, Inc., Richton Park, Illinois, Contract No. NOw-66-0539-c, Final Report, 1966, AD 655138.

Mullin, J., J.M. Berry, and A. Gatti, SOME FUNDAMENTAL FRACTURE MECHANISMS APPLICABLE TO ADVANCED FILAMENT REINFORCED COMPOSITES, Journal of Composite Materials, Vol. 2, No. 1, January 1968, pp. 82-103.

Outwater, J.O., and W.O. Carnes, THE FRACTURE ENERGY OF COMPOSITE MATERIALS, University of Vermont, Burlington, Vermont, Contract No. DAAA 21-67-C-0041, September 30, 1967, AD 659363.

Patrick, R.L., E.J. Ripling, and S. Mostovoy, FRACTURE MECHANICS APPLIED TO HETEROGENEOUS SYSTEMS, Proceedings of the 19th Annual Technical Conference, Reinforced Plastics Division, Society of the Plastics Industry, Inc., February 1964, Section 3-B.

Riley, V.R., and J.L. Reddaway, TENSILE STRENGTH AND FAILURE MECHANICS IN FIBER COMPOSITES, Journal of Materials Science, Vol. 3, No. 1, 1968, pp. 41-46.

Ripling, E.J., S. Mostovoy, and R.L. Patrick, APPLICATION OF FRACTURE MECHANICS TO ADHESIVE JOINTS, Symposium on Recent Developments in Adhesion Science, Special Technical Publication No. 360, Philadelphia, Pennsylvania, American Society for Testing and Materials, 1963.

Ripling, E.J., S. Mostovoy, and R.L. Patrick, MEASURING FRACTURE TOUGHNESS OF ADHESIVE JOINTS, Materials Research and Standards, Vol. 4, No. 3, March 1964, pp. 129-134.

Rosen, B.W., A NOTE ON THE FAILURE MODES OF FILAMENT REINFORCED MATERIALS - INCLUDING THE INFLUENCE OF CONSTITUENT GEOMETRY AND PROPERTIES, Proceedings of the 19th Annual Technical Conference, Reinforced Plastics Division, Society of the Plastics Industry, Inc., February 1964, Section 6-A.

Rosen, B.W., TENSILE FAILURE OF FIBROUS COMPOSITES, American Institute of Aeronautics and Astronautics Journal, Vol. 2, No. 11, November 1964, pp. 1985-1991.

Rosen, B.W., THE STRENGTH AND STIFFNESS OF FIBROUS COMPOSITES, Modern Composite Materials, edited by L.J. Broutman and R.H. Krock, Reading, Massachusetts, Addison-Wesley Publishing Company, Inc., 1967, Chapter 3, pp. 106-119.

Salganik, R.L., THE BRITTLE FRACTURE OF CEMENTED BODIES, Journal of Applied Mathematics and Mechanics, Vol. 27, No. 5, 1963, pp. 1468-1478.

Schuerch, H., A SEMI-ATOMISTIC MODEL FOR FLAW-INDUCED FRACTURE IN NON-DUCTILE MATERIALS, Astro Research Corp.; Contractor's Report CR-471, National Aeronautics and Space Administration, Washington, D.C., May 1966.

Sih, G.C., P.C. Paris, and G.R. Irwin, ON CRACKS IN RECTILINEARLY ANISOTROPIC BODIES, International Journal of Fracture Mechanics, Vol. 1, No. 3, September 1965, pp. 189-202.

Wu, E.M., APPLICATION OF FRACTURE MECHANICS TO ORTHOTROPIC PLATES, T & AM Report No. 248, Department of Theoretical and Applied Mechanics, University of Illinois, Urbana, Illinois, June 1963, AD 407722.

Wu, E.M., and R.C. Reuter, Jr., CRACK EXTENSION IN FIBERGLASS REINFORCED PLASTICS, T & AM Report No. 275, Department of Theoretical and Applied Mechanics, University of Illinois, Urbana, Illinois, February 1965, AD 613576.

Wu, E.M., A FRACTURE CRITERION FOR ORTHOTROPIC PLATES UNDER THE INFLUENCE OF COMPRESSION AND SHEAR, T & AM Report No. 283, Department of Theoretical and Applied Mechanics, University of Illinois, Urbana, Illinois, September 1965, AD 473618.

Wu, E.M., APPLICATION OF FRACTURE MECHANICS TO ANISOTROPIC PLATES, Journal of Applied Mechanics, Vol. 34, Transactions of the American Society of Mechanical Engineers, Vol. 89E, No. 4, December 1967, pp. 967-975.

Wu, E.M., FRACTURE MECHANICS OF ANISOTROPIC PLATES, Composite Materials Workshop, edited by S.W. Tsai, J.C. Halpin, and N.J. Pagano, Stamford, Connecticut, Technomic Publishing Company, Inc., 1968, pp. 20-43.

Zender, G.W., and J.W. Deaton, STRENGTH OF FILAMENTARY SHEETS WITH ONE OR MORE FIBERS BROKEN, Technical Note D-1609, National Aeronautics and Space Administration, Washington, D.C., March 1963.

Mechanics of Anisotropic Plasticity

Baltov, A., and A. Sawczuk, A RULE OF ANISOTROPIC HARDENING, Acta Mechanica, Vol. 1, No. 2, 1965, pp. 81-92.

Berman, I., A GENERAL THEORY OF PIECEWISE LINEAR PLASTICITY FOR INITIALLY ANISOTROPIC MATERIALS WITH APPLICATIONS, unpublished Ph.D. dissertation, Applied Mechanics, Polytechnic Institute of Brooklyn, Brooklyn, New York, 1959.

Bert, C.W., and W.S. Hyler, ANALYSIS OF DUCTILE BURSTING IN PRESSURE VESSELS OF TEXTURE-HARDENING AND FILAMENT-WRAPPED MATERIALS, Journal of Composite Materials, Vol. 2, No. 3, July 1968.

Borsch, K.I., ON THE THEORY OF PLASTICITY OF ORTHOTROPIC BODIES (in French), Bulletin de l'Academie Polonaise des Sciences, Serie des Sciences Techniques, Vol. 14, No. 9, 1966, pp. 541-544.

Bykovtsev, G.I., ON THE CONSEQUENCES OF DRUCKER'S POSTULATE FOR A PLASTIC ANISOTROPIC MEDIUM, Journal of Applied Mathematics and Mechanics, Vol. 28, No. 2, 1964, pp. 434-439.

Bykovtsev, G.I., V.V. Dudukalenkom, and D.D. Ivlev, ON THE LOADING FUNCTIONS OF ANISOTROPICALLY HARDENING PLASTIC MATERIALS, Journal of Applied Mathematics and Mechanics, Vol. 28, No. 4, 1964, pp. 966-969.

Dorn, J.E., STRESS-STRAIN RELATIONS FOR ANISOTROPIC PLASTIC FLOW, Journal of Applied Physics, Vol. 20, No. 1, January 1949, pp. 15-20.

Gol'denblatt, I.I., THEORY OF SMALL ELASTIC PLASTIC DEFORMATIONS OF ANISOTROPIC MEDIA (in Russian), Doklady Akademii Nauk SSSR, Vol. 101, No. 4, 1955, pp. 619-622.

Hillier, M.J., ON THE TENSILE INSTABILITY OF ORTHOTROPIC PLASTIC MATERIAL, International Journal of Mechanical Sciences, Vol. 7, No. 6, June 1965, pp. 441-445.

Hsu, T.C., A THEORY OF THE YIELD LOCUS AND FLOW RULE OF ANISOTROPIC MATERIALS, Journal of Strain Analysis, Vol. 1, No. 3, April 1966, pp. 204-215.

Hu, L.W., and J. Marin, ANISOTROPIC LOADING FUNCTIONS FOR COMBINED STRESSES IN THE PLASTIC RANGE, Journal of Applied Mechanics, Vol. 22, Transactions of the American Society of Mechanical Engineers, Vol. 77, No. 1, March 1955, pp. 77-85.

Hu, L.W., STUDIES ON PLASTIC FLOW OF ANISOTROPIC METALS, Journal of Applied Mechanics, Vol. 23, Transactions of the American Society of Mechanical Engineers, Vol. 78, No. 3, September 1956, pp. 444-450.

Ivlev, D.D., ON THE THEORY OF IDEALLY PLASTIC ANISOTROPY, Journal of Applied Mathematics and Mechanics, Vol. 23, No. 6, 1959, pp. 1582-1592.

Ivlev, D.D., ON THE PROPERTIES OF THE RELATIONS OF THE LAW OF ANISOTROPIC HARDENING OF PLASTIC MATERIAL, Journal of Applied Mathematics and Mechanics, Vol. 24, No. 1, 1960, pp. 191-194.

Jackson, L.R., K.F. Smith, and W.T. Lankford, PLASTIC FLOW OF ANISOTROPIC SHEET METAL, Metals Technology, Vol. 15, August 1948, Technical Paper 2440.

Keeler, S.P., and W.A. Backofen, PLASTIC INSTABILITY AND FRACTURE IN SHEETS STRETCHED OVER RIGID PUNCHES, Transactions of the American Society for Metals, Vol. 56, 1963, pp. 25-48.

Lomakin, V.A., THEORY OF NONLINEAR ELASTICITY AND PLASTICITY OF ANISOTROPIC MEDIA (in Russian), Izvestiia Akademii Nauk SSSR, Otdelenie Tekhn. Nauk, Mekhanika i mashinostroenie, No. 4, 1960, pp. 60-64.

Lomakin, V.A., and M.A. Yumasheva, STRESS-STRAIN RELATIONSHIPS WITH NON-LINEAR DEFORMATION OF ORTHOTROPIC GLASS-REINFORCED PLASTICS, Polymer Mechanics, Vol. 1, No. 4, 1967, pp. 15-18.

Lomakin, V.A., THEORY OF PLASTICITY OF ANISOTROPIC MEDIA, FTD-MT-64-560, Foreign Technology Division, Wright-Patterson Air Force Base, Ohio, April 27, 1967, pp. 63-69, AD 662584.

Marin, J., and M.G. Sharma, DESIGN OF THIN-WALLED CYLINDRICAL PRESSURE VESSEL BASED UPON THE PLASTIC RANGE AND CONSIDERING ANISOTROPY, Bulletin No. 40, Welding Research Council, New York, May 1958.

Mroz, Z., ON THE DESCRIPTION OF ANISOTROPIC WORKHARDENING, Journal of the Mechanics and Physics of Solids, Vol. 15, May 1967, pp. 163-175.

Olszak, W., and W. Urbanowski, THE PLASTIC POTENTIAL AND THE GENERALIZED DISTORTION ENERGY IN THE THEORY OF NON-HOMOGENEOUS ANISOTROPIC BODIES, Archiwum Mechaniki Stosowanej, Vol. 8, 1956, pp. 85-110.

Sawczuk, A., ON THE THEORY OF ANISOTROPIC PLATES AND SHELLS, Archiwum Mechaniki Stosowanej, Vol. 13, 1961, pp. 355-365.

Shaffer, B.W., STRESS-STRAIN RELATIONS OF REINFORCED PLASTICS PARALLEL AND NORMAL TO THEIR INTERNAL FILAMENTS, American Institute of Aeronautics and Astronautics Journal, Vol. 2, No. 2, February 1964, pp. 348-352.

Shah, J.J., PLASTIC TENSILE INSTABILITY IN ORTHOTROPIC SHEETS SUBJECT TO BIAXIAL LOADING AT AN ARBITRARY ORIENTATION, unpublished Master of Engineering (Mechanical) thesis, University of Oklahoma, Norman, Oklahoma, 1968.

Shu, L.S., and B.W. Rosen, STRENGTH OF FIBER-REINFORCED COMPOSITES BY LIMIT ANALYSIS METHODS, Journal of Composite Materials, Vol. 1, No. 4, October 1967, pp. 366-381.

Smith, G.F., ON THE YIELD CONDITION FOR ANISOTROPIC MATERIALS, Quarterly of Applied Mathematics, Vol. 20, 1962, pp. 241-247.

Ziegler, H., A MODIFICATION OF PRAGER'S HARDENING RULE, Quarterly of Applied Mathematics, Vol. 17, 1959, pp. 55-65.

APPENDIX I

DESIGN OF TEST-SECTION CONTOUR TO ACHIEVE A UNIFORM STRESS STATE OF DESIRED BIAXIAL-LOAD RATIO

As pointed out in Section 4 of the body of the report, for material-property evaluation, it is desirable to have a uniform stress state in the test section. In this appendix, the shape of reduced-thickness test section necessary to achieve a uniform-biaxial-stress state is derived by using two-dimensional theory of elasticity.

1. Hypotheses

The following hypotheses are made in the ensuing synthesis:

(H1) Generalized plane stress conditions exist throughout the reduced-thickness test section and the reinforced section; i.e., all stress components in the thickness direction are neglected.

(H2) The only loadings considered are edge loadings; i.e., all body forces such as those due to gravity and inertia are neglected.

2. Synthesis

To assure that the equations of equilibrium of a body under generalized-plane-stress conditions are satisfied identically, it is customary to introduce the Airy stress function, ϕ, defined as follows:

$$N_x = \phi_{,yy} \quad ; \quad N_y = \phi_{,xx} \quad ; \quad N_{xy} = -\phi_{,xy} \tag{70}$$

where N_x, N_y, N_{xy} are the internal forces per unit length of run (normal to the x and y axes, and shear, respectively), and a subscript comma denotes partial derivatives with respect to the variables appearing in the subscript after the comma.

A uniform stress state requires that N_x, N_y, and N_{xy} all be constants. Then integration of Equations (70) yields the following expression for the Airy stress function associated with such a stress state:

$$\phi = (1/2)(N_x\, y^2 + N_y\, x^2) - N_{xy}\, xy + Ax + By + C \tag{71}$$

where x and y are Cartesian position coordinates, and A, B, and C are arbitrary constants of integration.

The required contour shape (position coordinates x_c, y_c) of reduced-thickness test section is the one in which the stress function is invariant with respect to position x_c, y_c. This is satisfied by the following expression:

$$(1/2)(N_x\, y_c^2 + N_y\, x_c^2) - N_{xy}\, x_c y_c + Ax_c + By_c + K = 0 \tag{72}$$

where $K = \phi(x_c, y_c) - C$.

The constants A and B in Equation (72) can be omitted, since they merely determine the origin of the coordinate system.

Furthermore, for any generalized-plane-stress state (N_x, N_y, N_{xy}), by means of the Mohr's stress circle, an orientation can be found such that the shear force N_{xy} vanishes. The loadings associated with this orientation are known as the principal loadings N_p, N_q. If the axes of the Cartesian coordinate system used to define the shape of the reduced-thickness test section are chosen to coincide with the principal loading directions, N_{xy} can be omitted and N_x and N_y are replaced by N_p and N_q. Thus, Equation (72) can be rewritten as follows:

$$(1/2)(N_p\, y_c^2 + N_q\, x_c^2) + K = 0 \tag{73}$$

Equation (73) can be rewritten in the standard form for an ellipse as follows:

$$(x_c/a)^2 + (y_c/b)^2 = 1 \tag{74}$$

where a and b are the major and minor semi-axes, respectively.

Comparing Equations (73) and (74), it is found that the following relationship must hold:

$$b/a = (N_q/N_p)^{1/2} \tag{75}$$

Furthermore, K is a scale factor given by

$$K = -N_p\, N_q/2 \tag{76}$$

Applying Equation (75), it is seen that for a balanced biaxial loading (biaxial-load ratio $N_q/N_p = 1$), $b/a = 1$; i.e., the required contour of the reduced thickness section is a circle. For a biaxial-load ratio of 1/2, $b/a = (1/2)^{1/2} \approx 0.707$.

It is important to note that only equilibrium considerations have been used; thus, the results are completely independent of the nature of the elastic behavior (anisotropic, orthotropic, or isotropic).

APPENDIX II

STRAIN DATA FROM INDIVIDUAL TESTS

1. Stress-Strain Data from Uniaxial Tension Tests

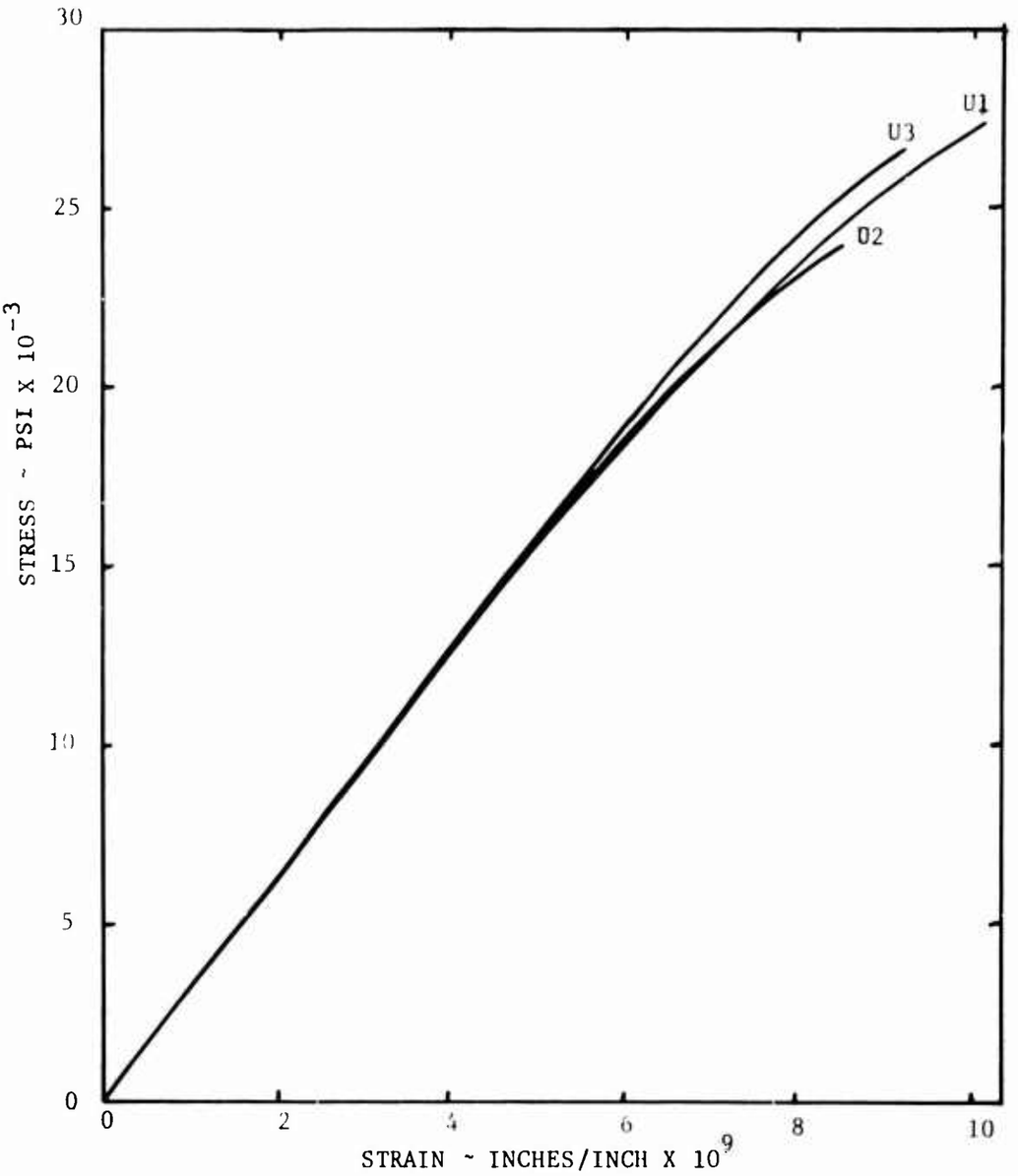

Figure 23. Stress-Strain Plot of Uniaxial, Parallel 4-Ply, 0° Orientation.

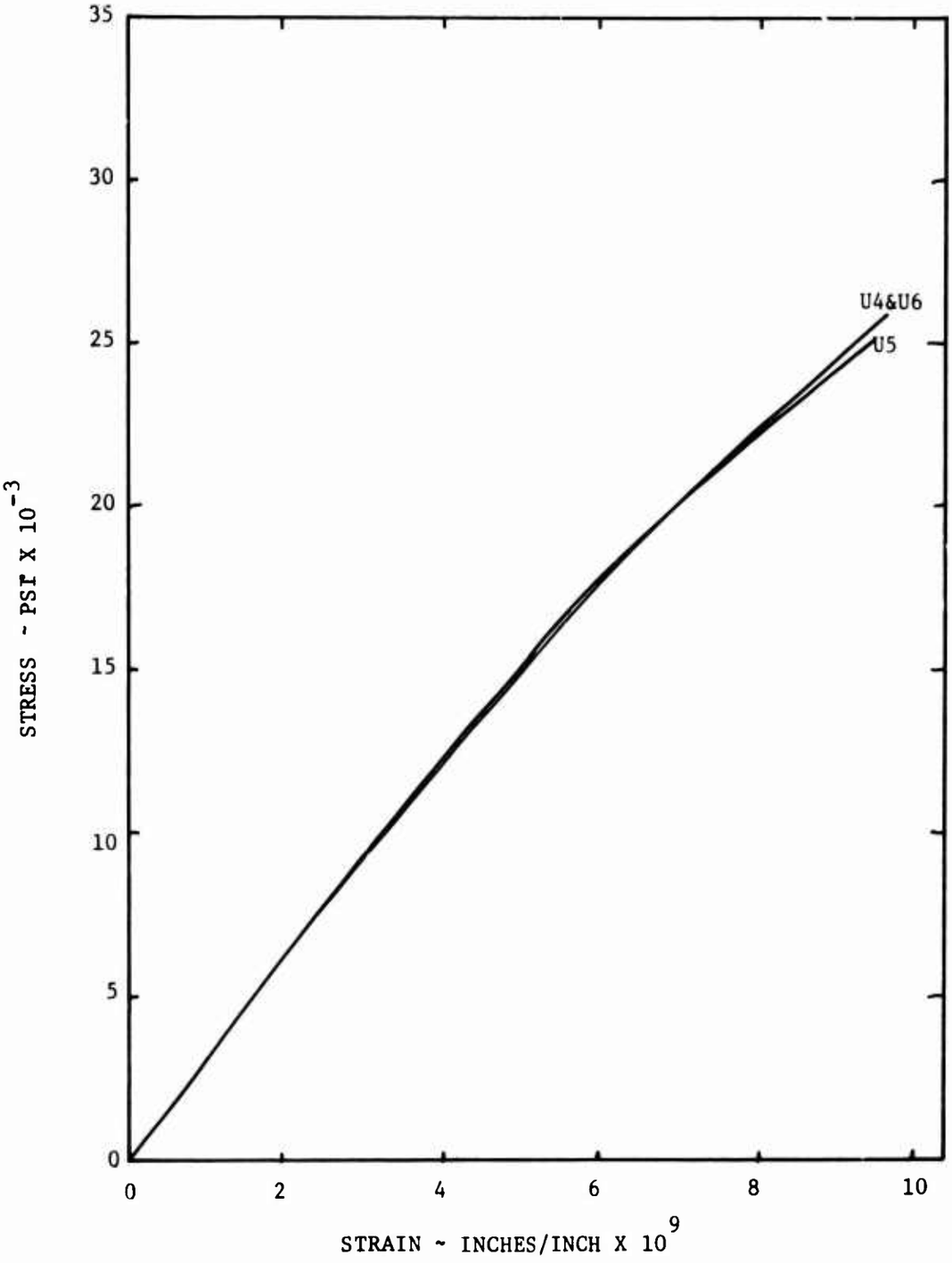

Figure 24. Stress-Strain Plot of Uniaxial, Parallel 4-Ply, 90° Orientation.

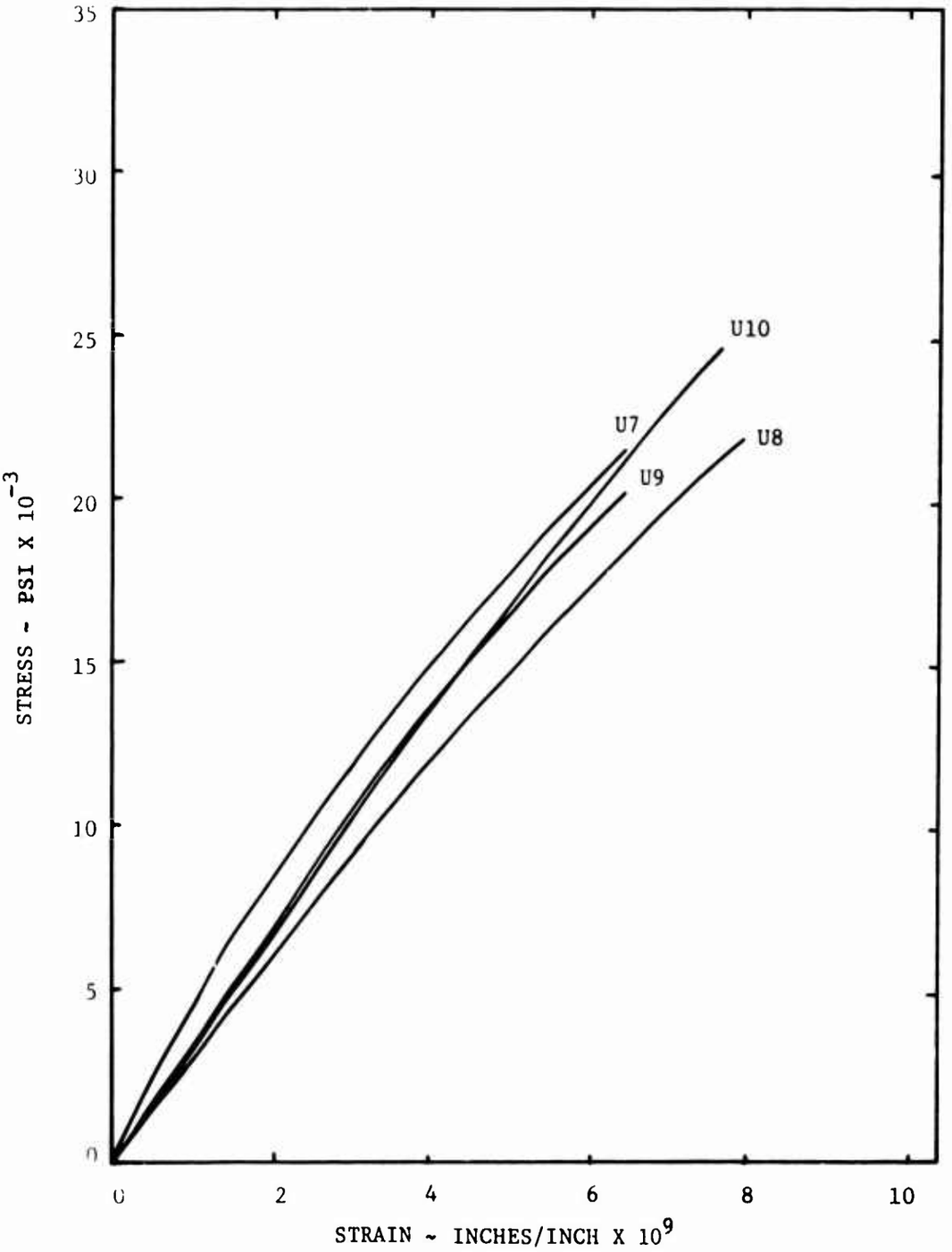

Figure 25. Stress-Strain Plot of Uniaxial, Cross 4-Ply, 0° Orientation.

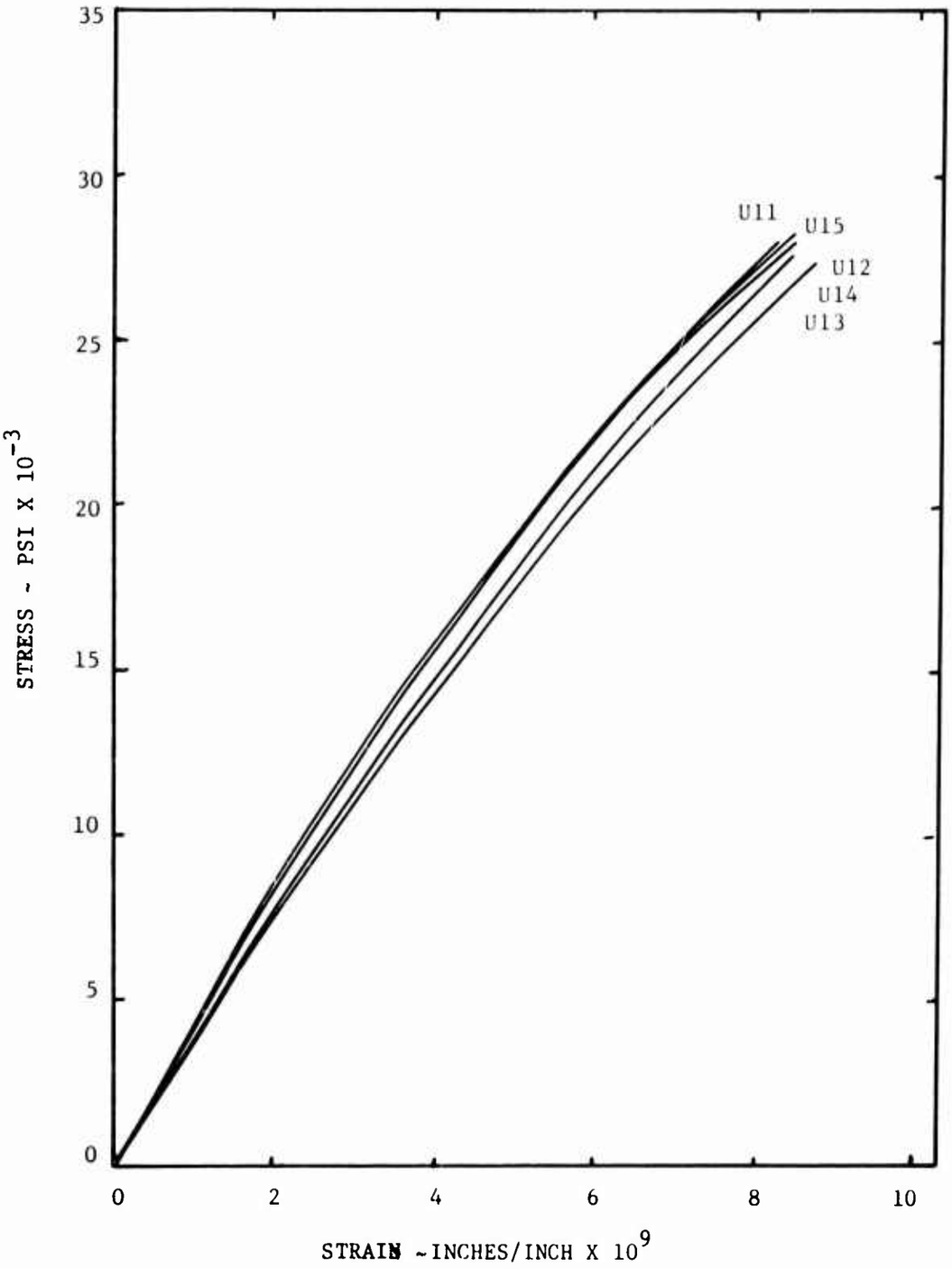

Figure 26. Stress-Strain Plot of Uniaxial, Quasi 6-Ply, 0° Orientation.

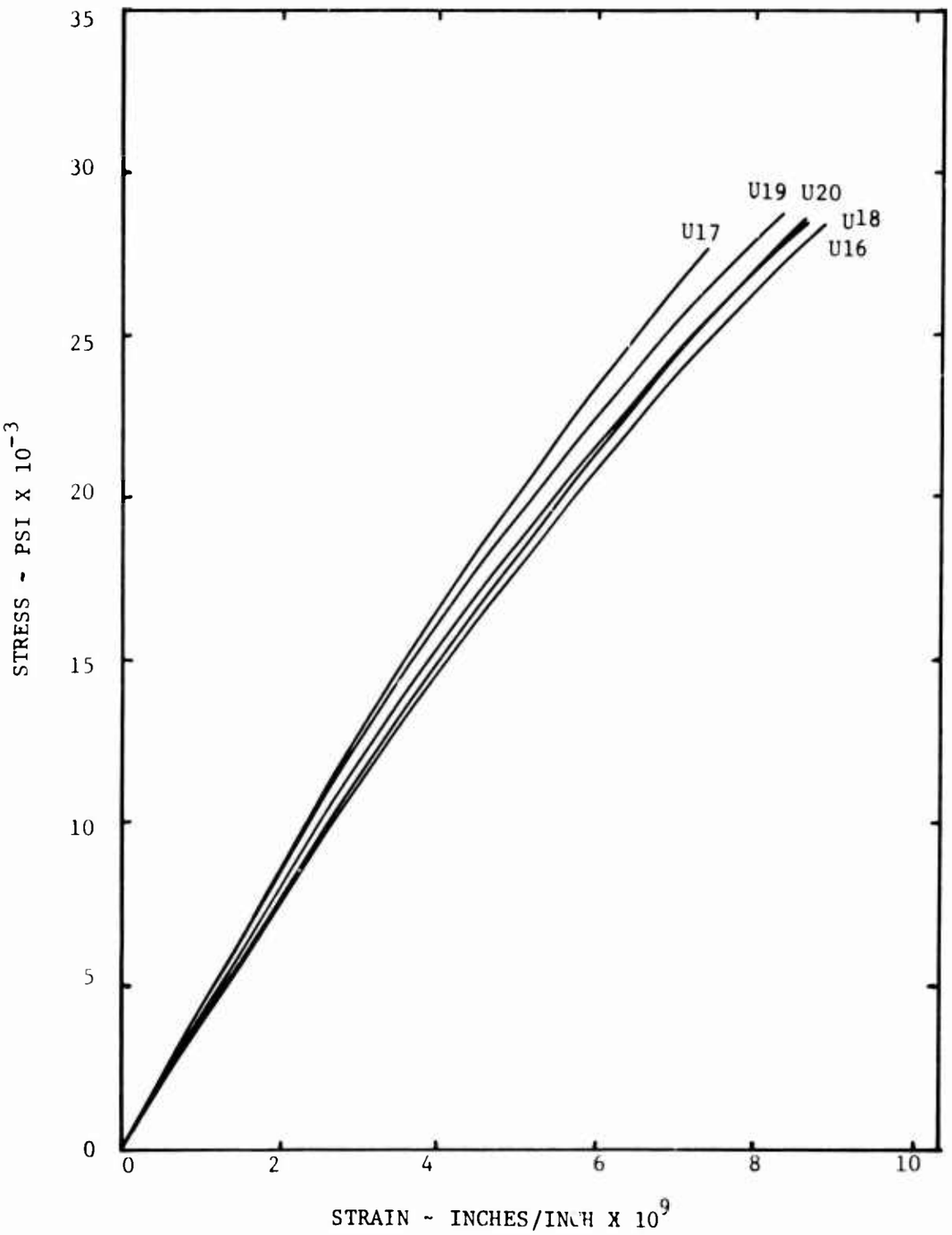

Figure 27. Stress-Strain Plot of Uniaxial, Quasi 6-Ply, 90° Orientation.

2. Shear Stress-Shear Strain Data From Torsion-Tube Tests

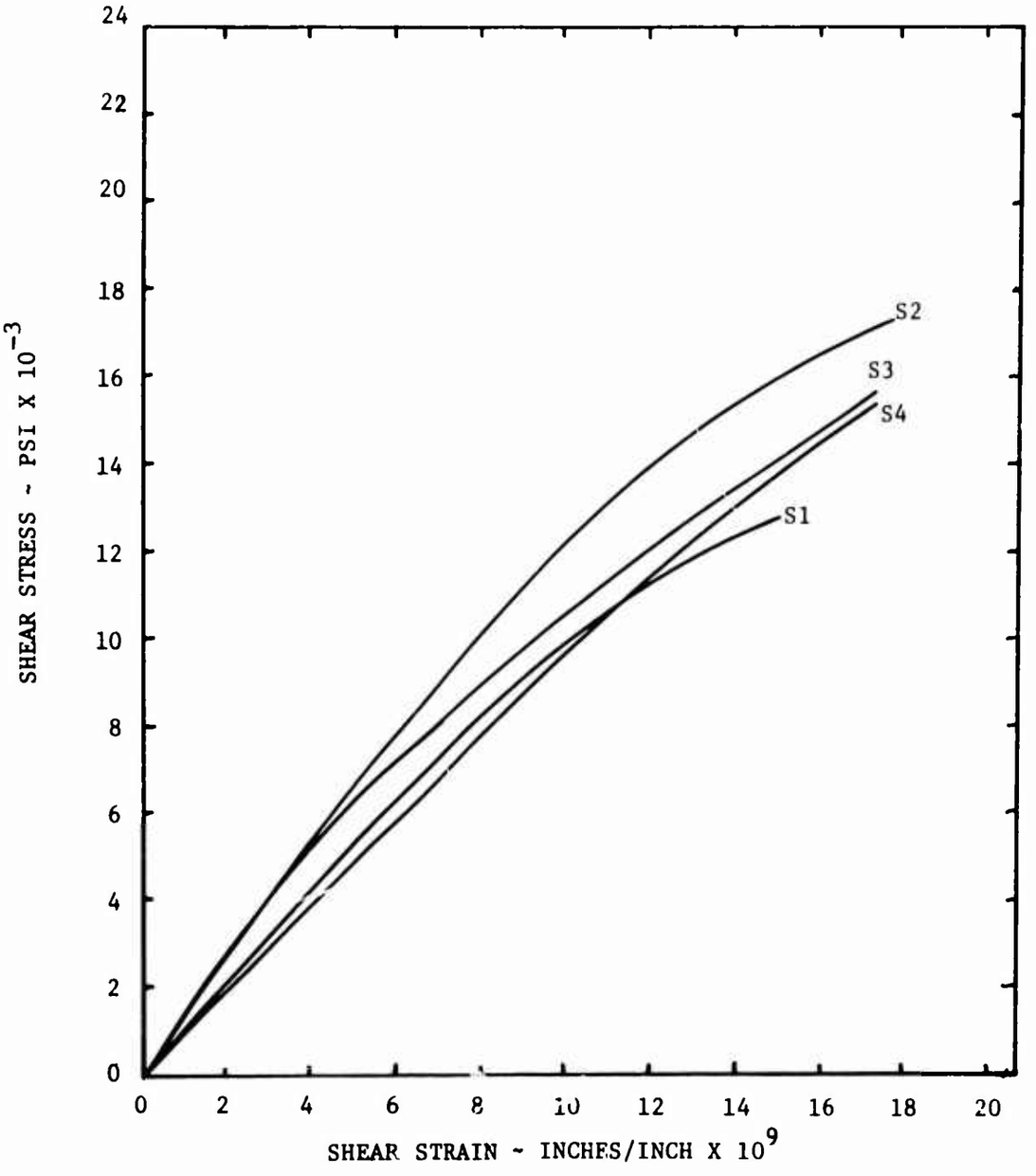

Figure 28. Stress-Strain Plot of Torsion, Parallel 4-Ply, 0° Orientation.

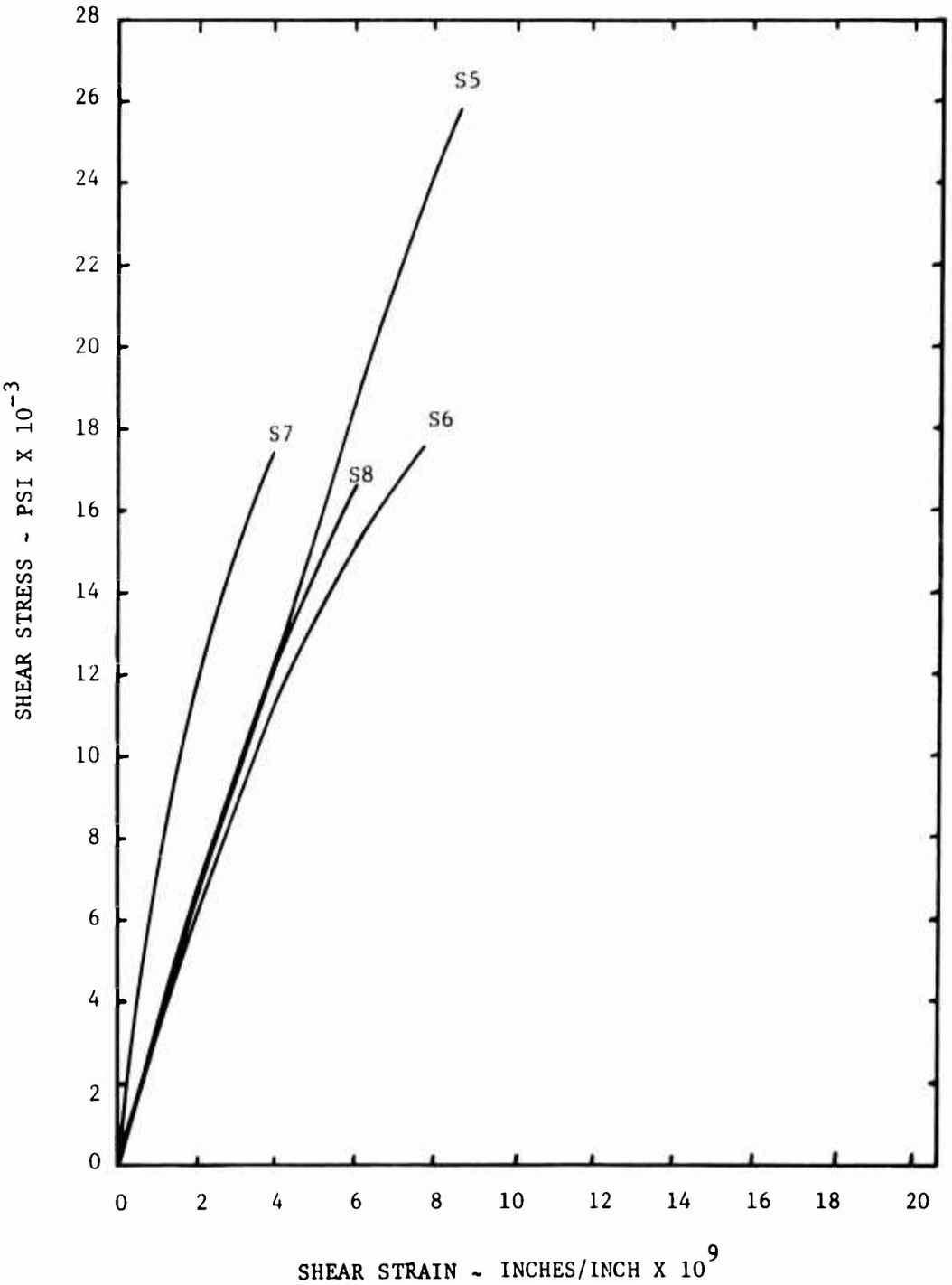

Figure 29. Stress-Strain Plot of Torsion, Parallel 4-Ply, 45° Orientation.

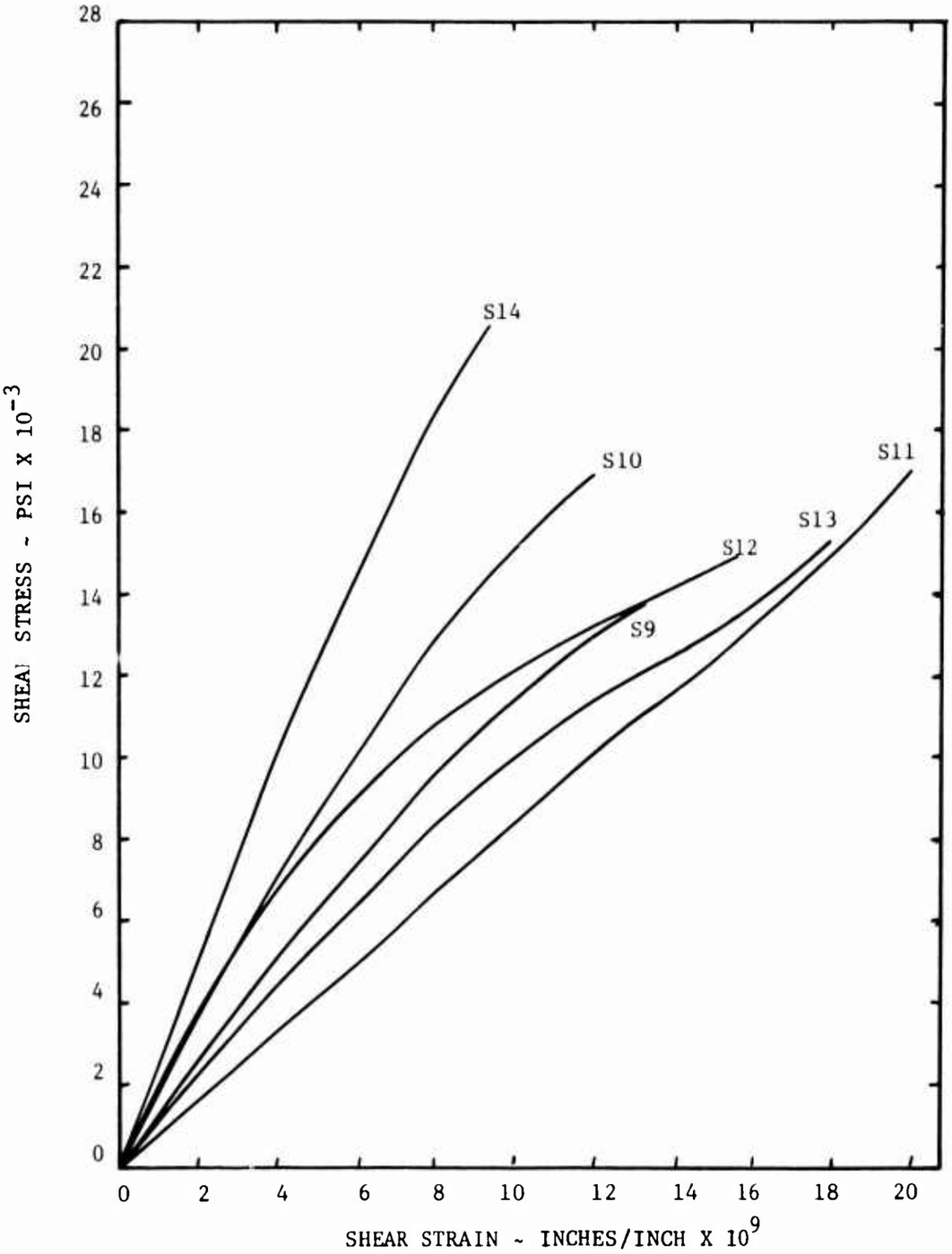

Figure 30. Stress-Strain Plot of Torsion, Cross 4-Ply, 0° Orientation.

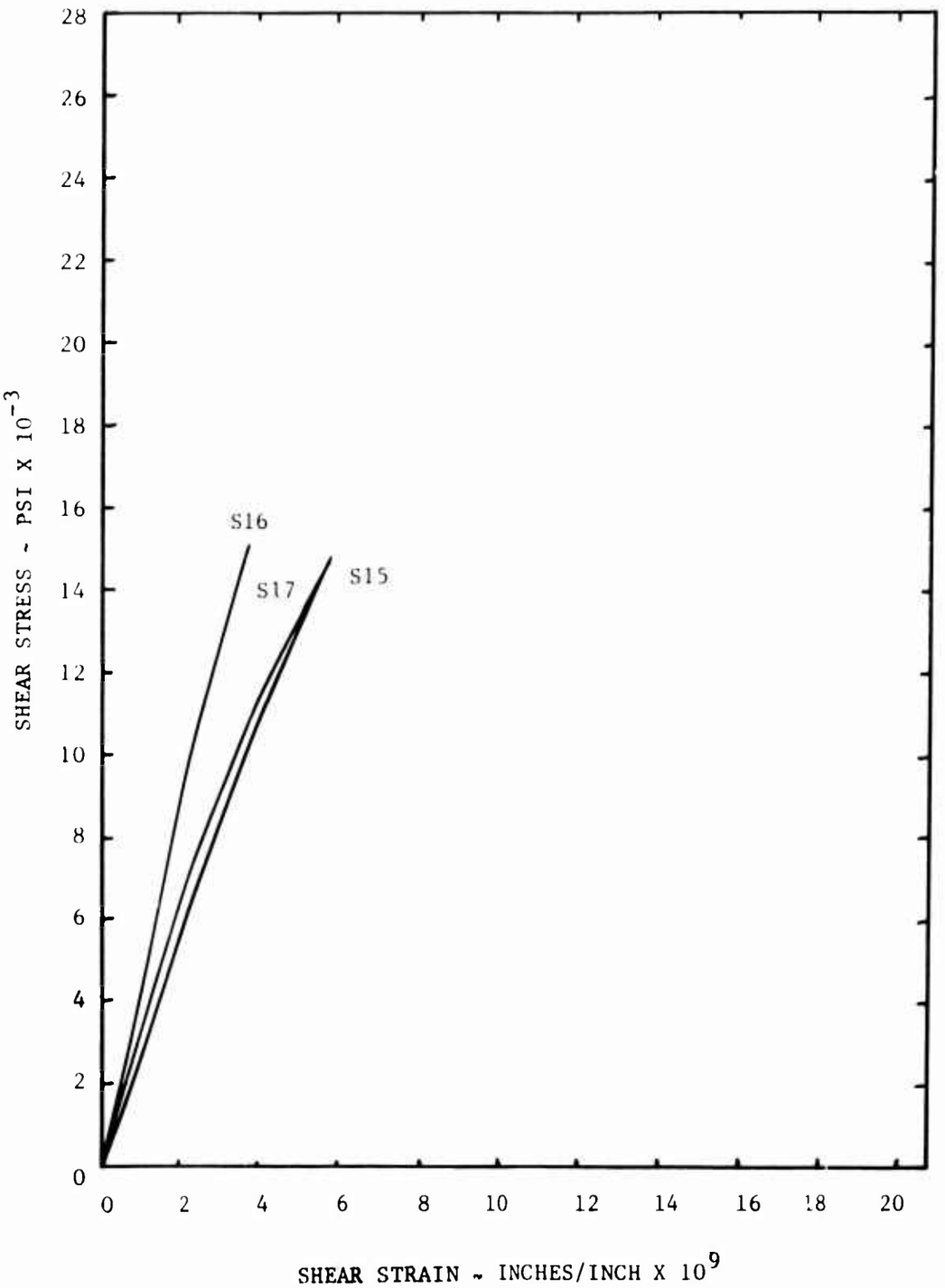

Figure 31. Stress-Strain Plot of Torsion, Cross 4-Ply, 45° Orientation.

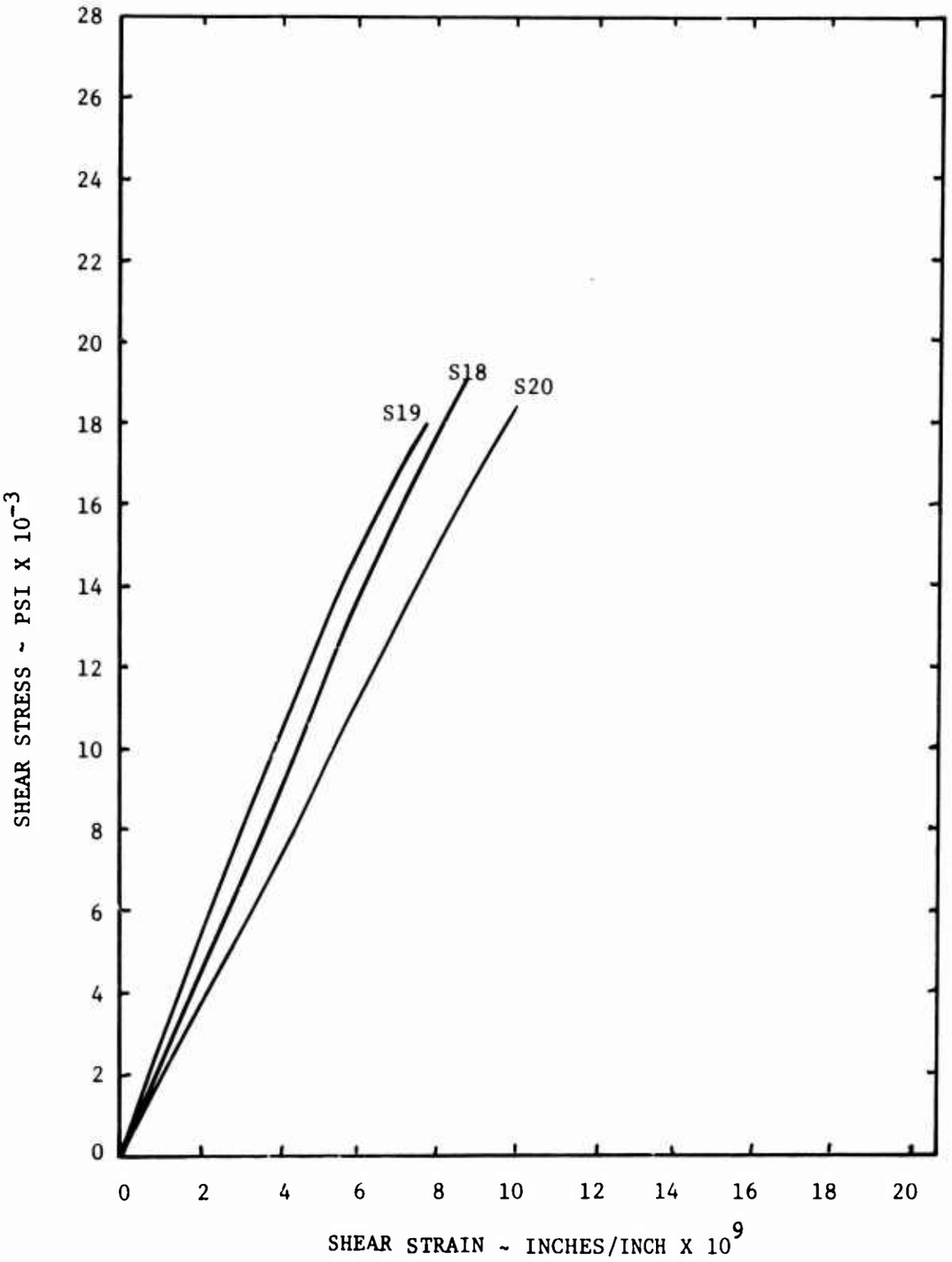

Figure 32. Stress-Strain Plot of Torsion, Quasi 6-Ply, 0° Orientation.

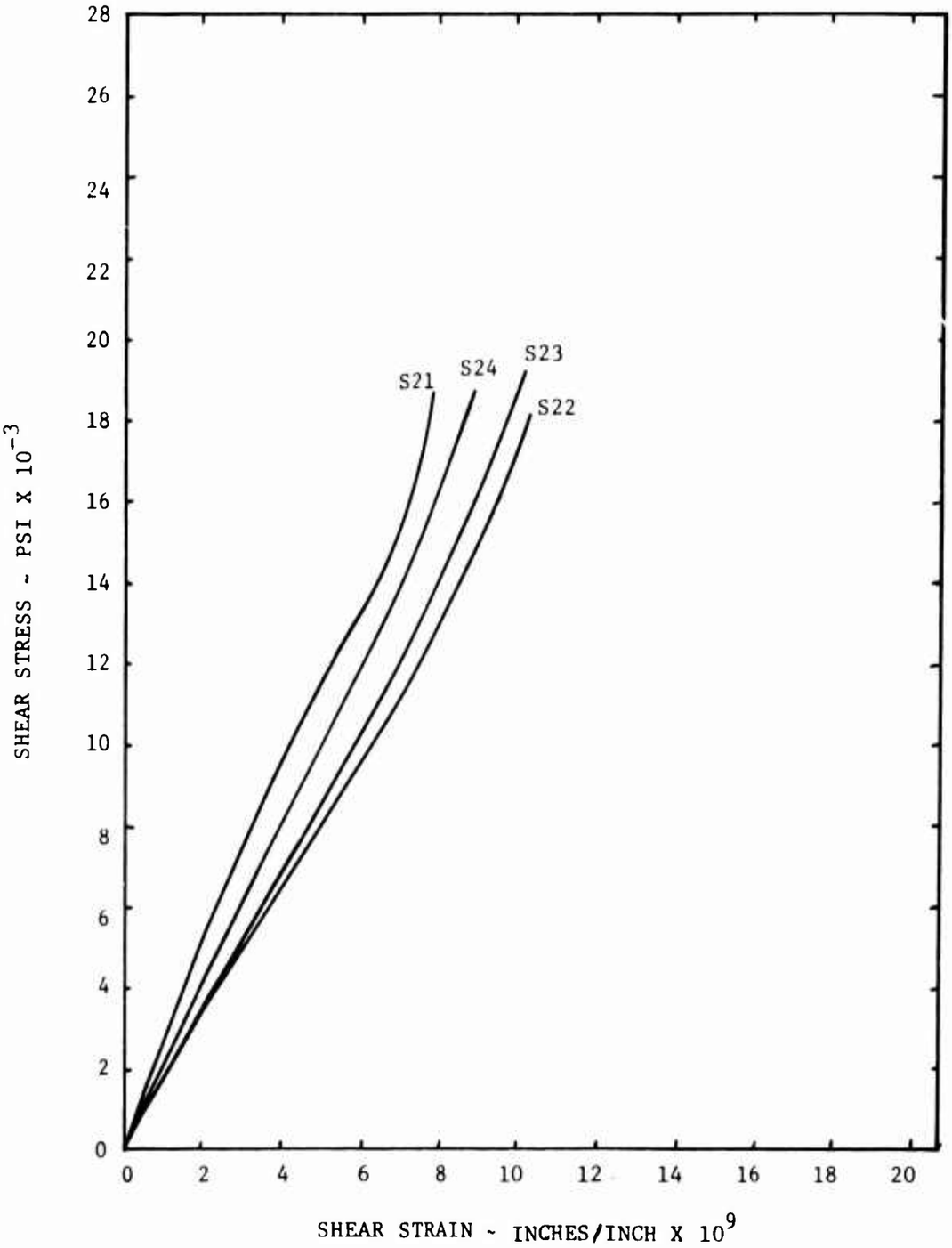

Figure 33. Stress-Strain Plot of Torsion, Quasi Ply, 45° Orientation.

3. Load-Strain Data from Biaxial-Loading Tests

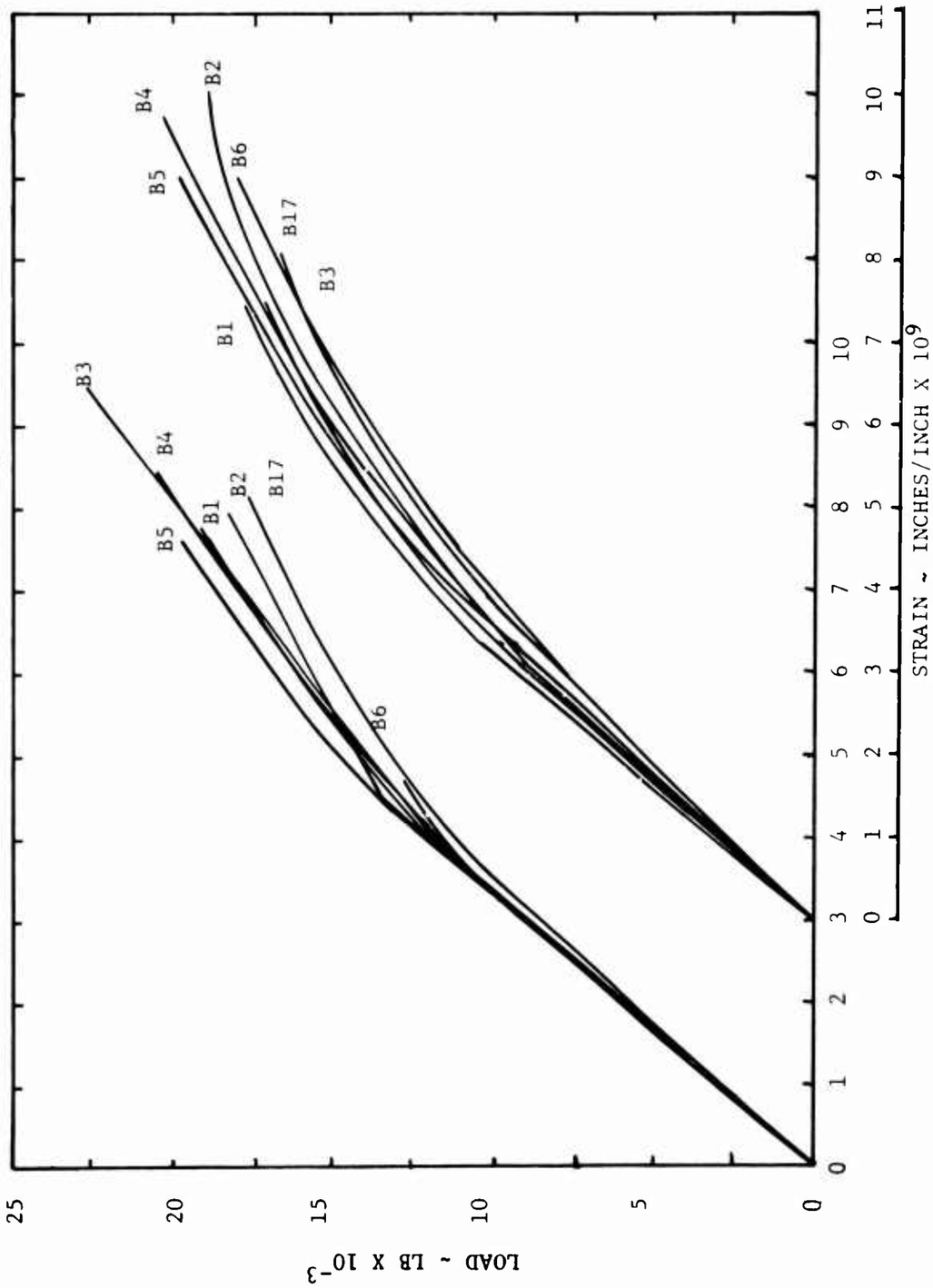

Figure 34. Load-Strain Plot of Biaxial, 1:1, Parallel 4-Ply, 0° Orientation.

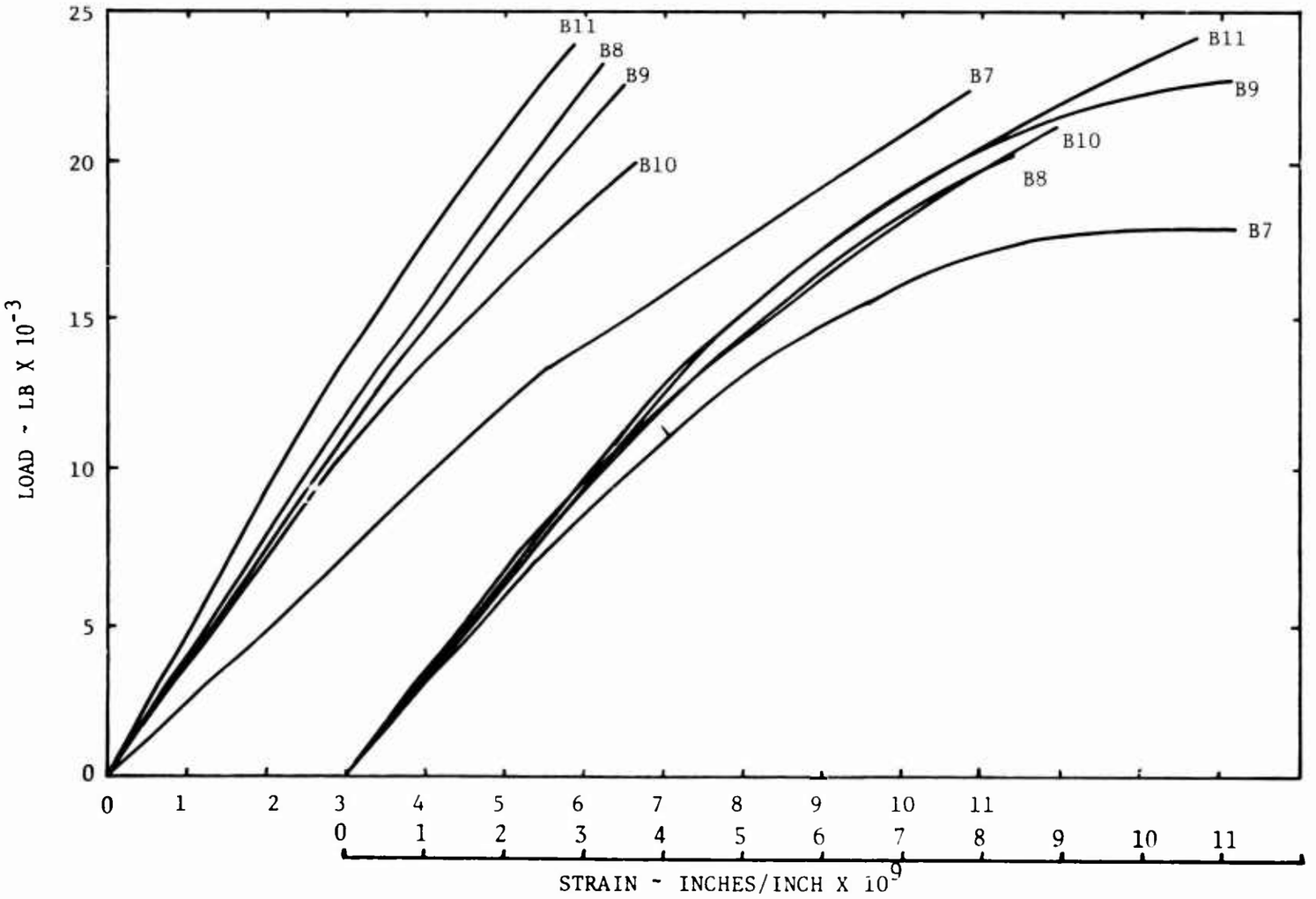

Figure 35. Load-Strain Plot of Biaxial, 1:1, Parallel 4-Ply, 45° Orientation.

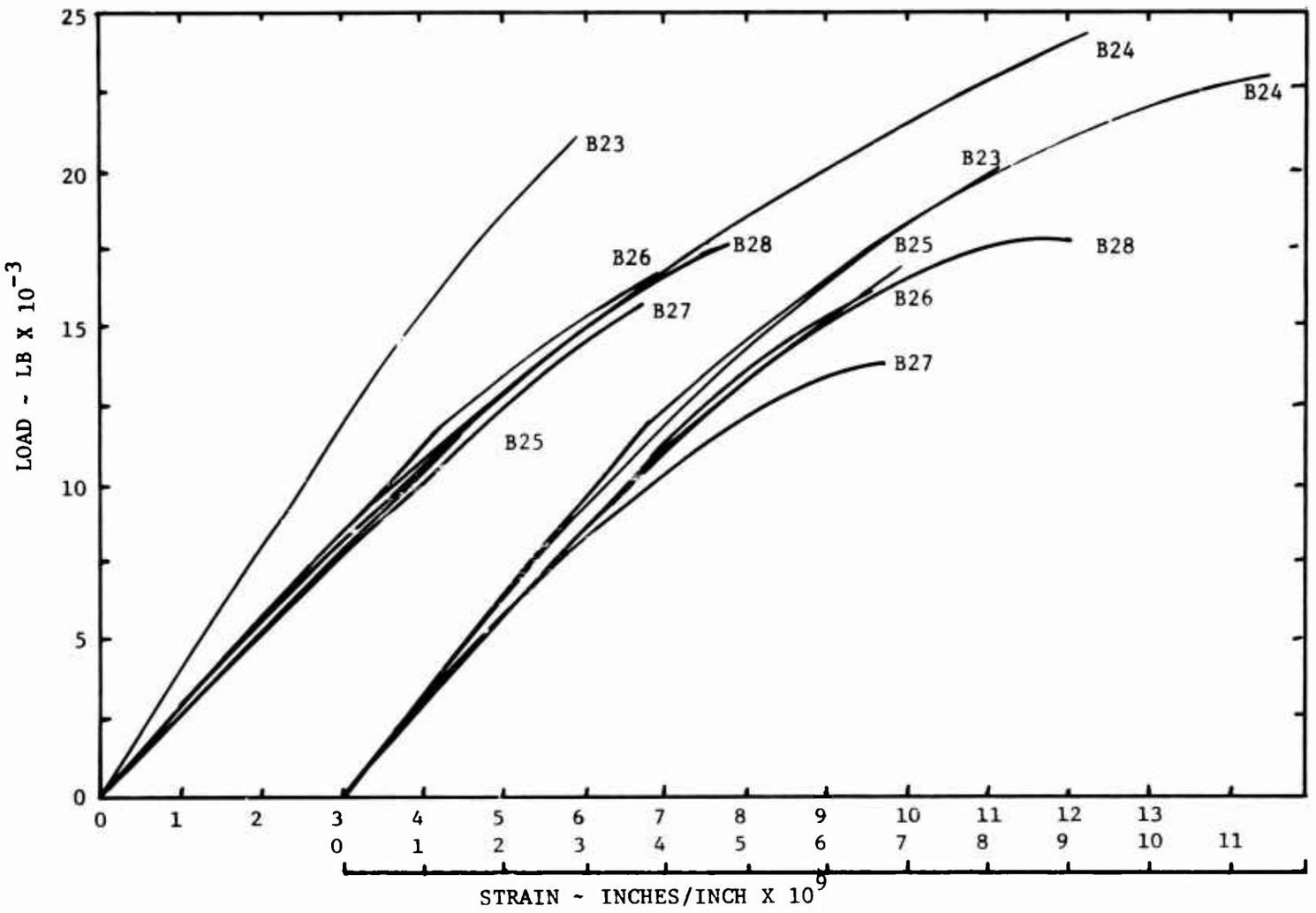

Figure 36. Load-Strain of Biaxial, 1:1 Quasi 4-Ply, 0° Orientation.

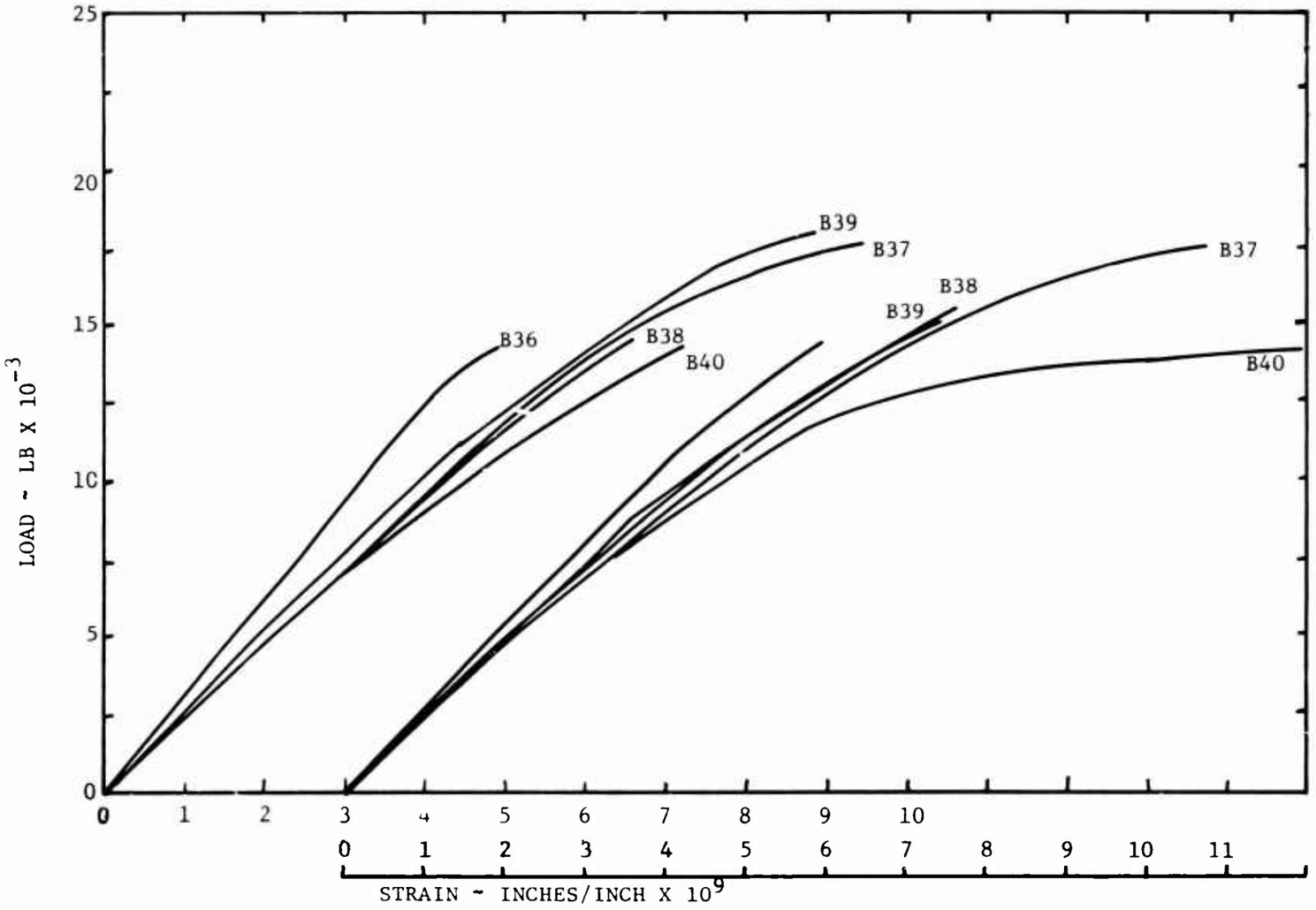

Figure 37. Load-Strain Plot of Biaxial, 1:1, Quasi 6-Ply, 0° Orientation.

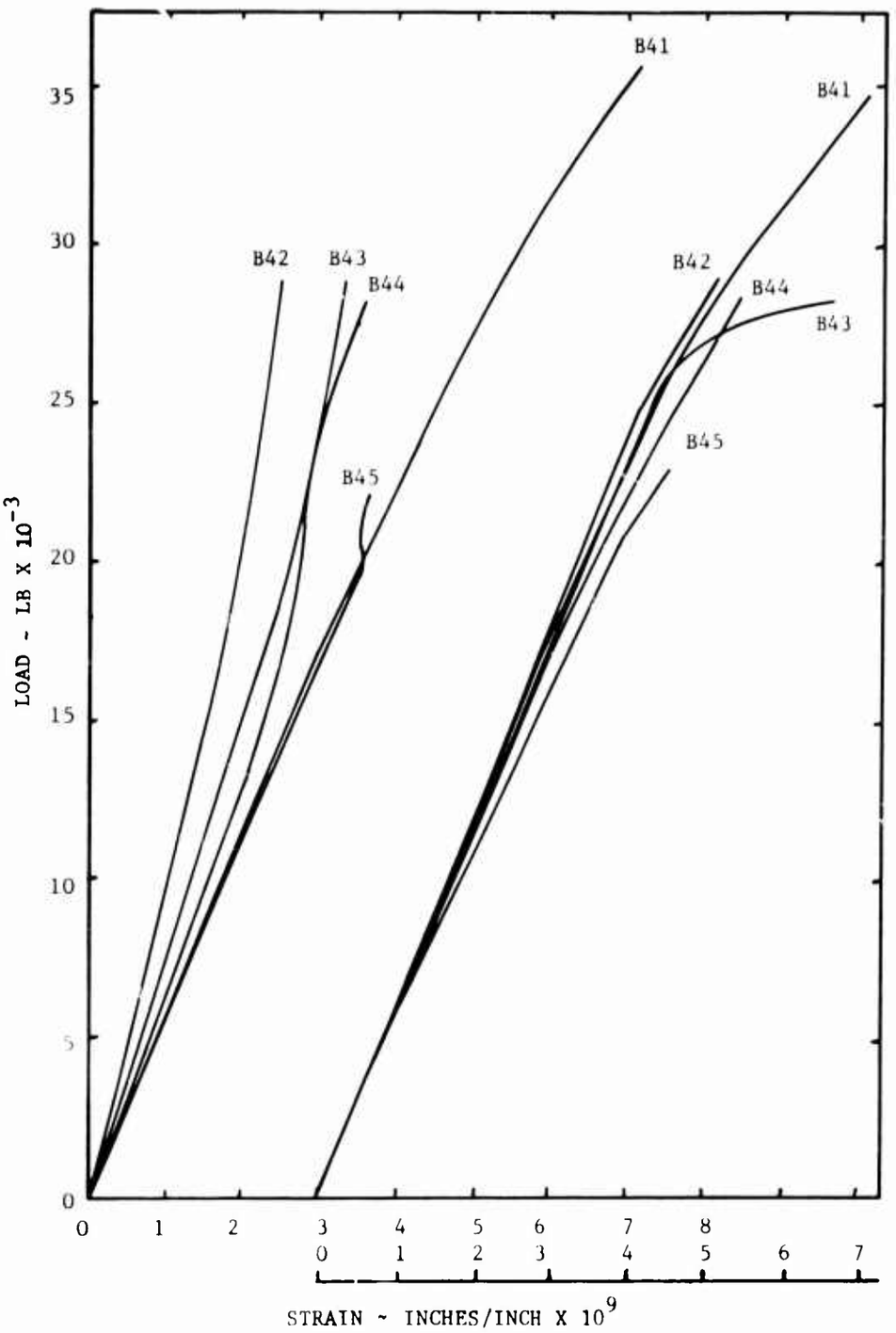

Figure 38. Load-Strain Plot of Biaxial, 1:1, Quasi 6-Ply, 45° Orientation.

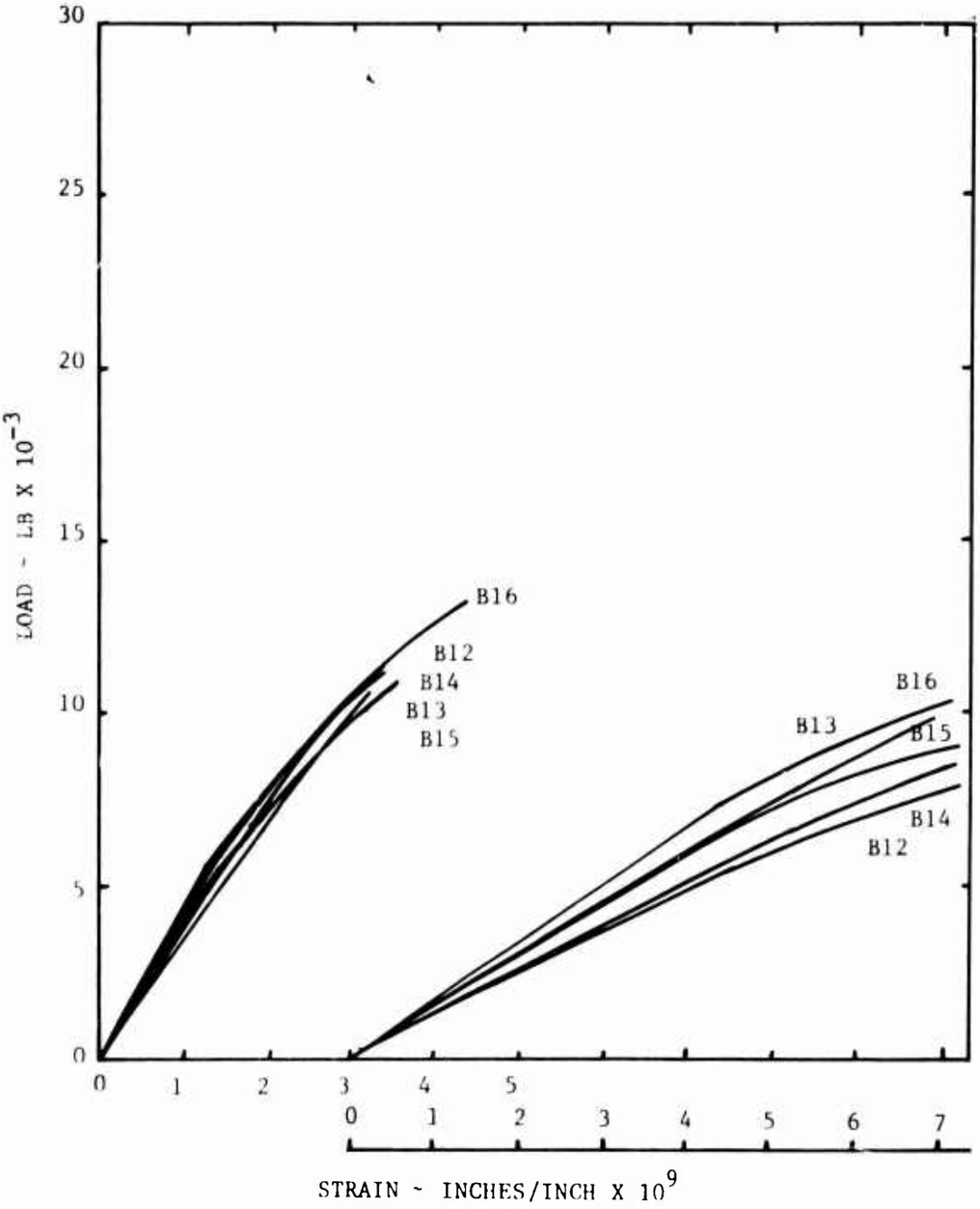

Figure 39. Load-Strain Plot of Biaxial, 1:2, Parallel 4-Ply, 0° Orientation.

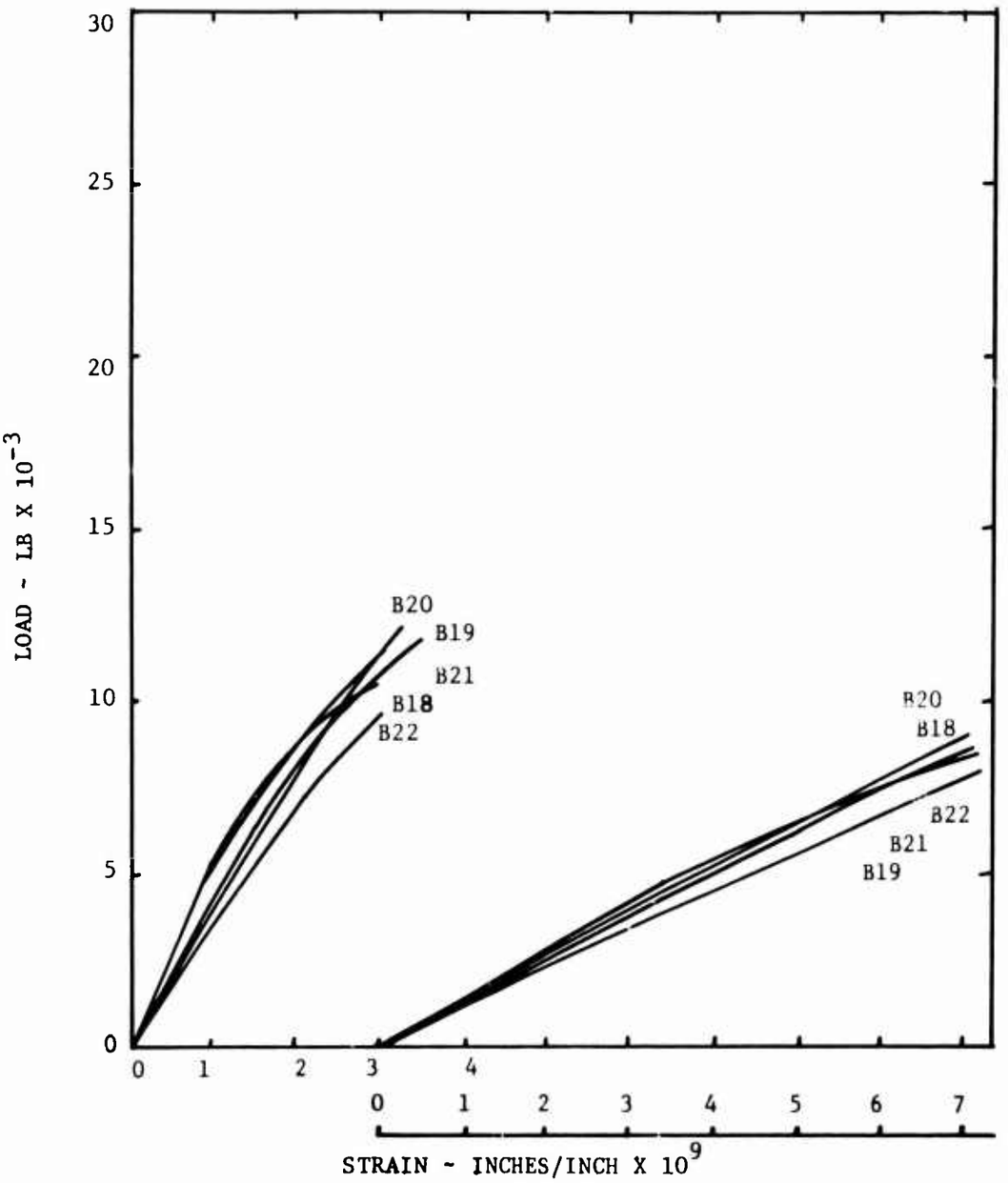

Figure 40. Load-Strain Plot of Biaxial, 2:1, Parallel 4-Ply, 0° Orientation.

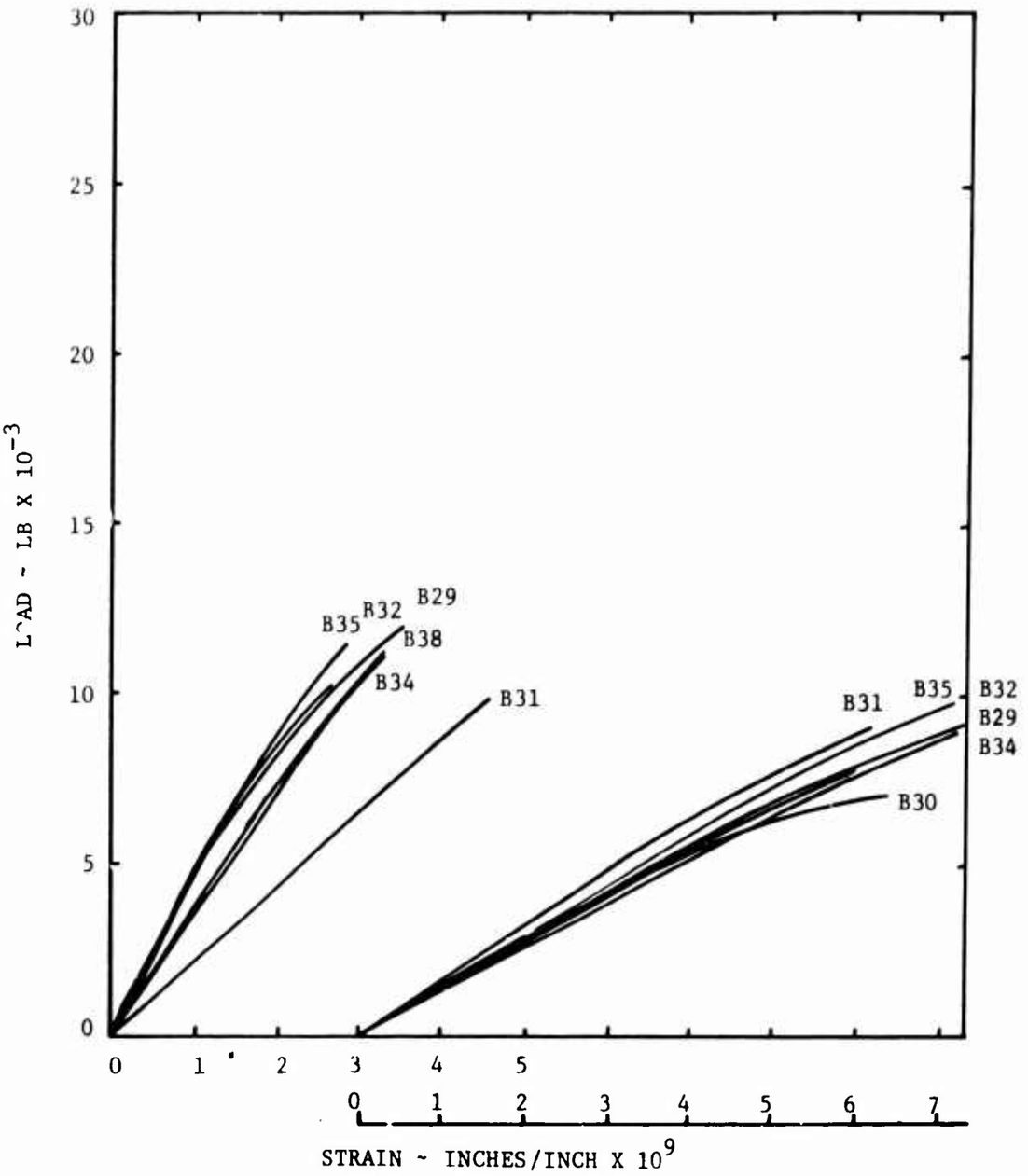

Figure 41. Load-Strain Plot of Biaxial, 2:1, Cross 4-Ply, 0° Orientation.

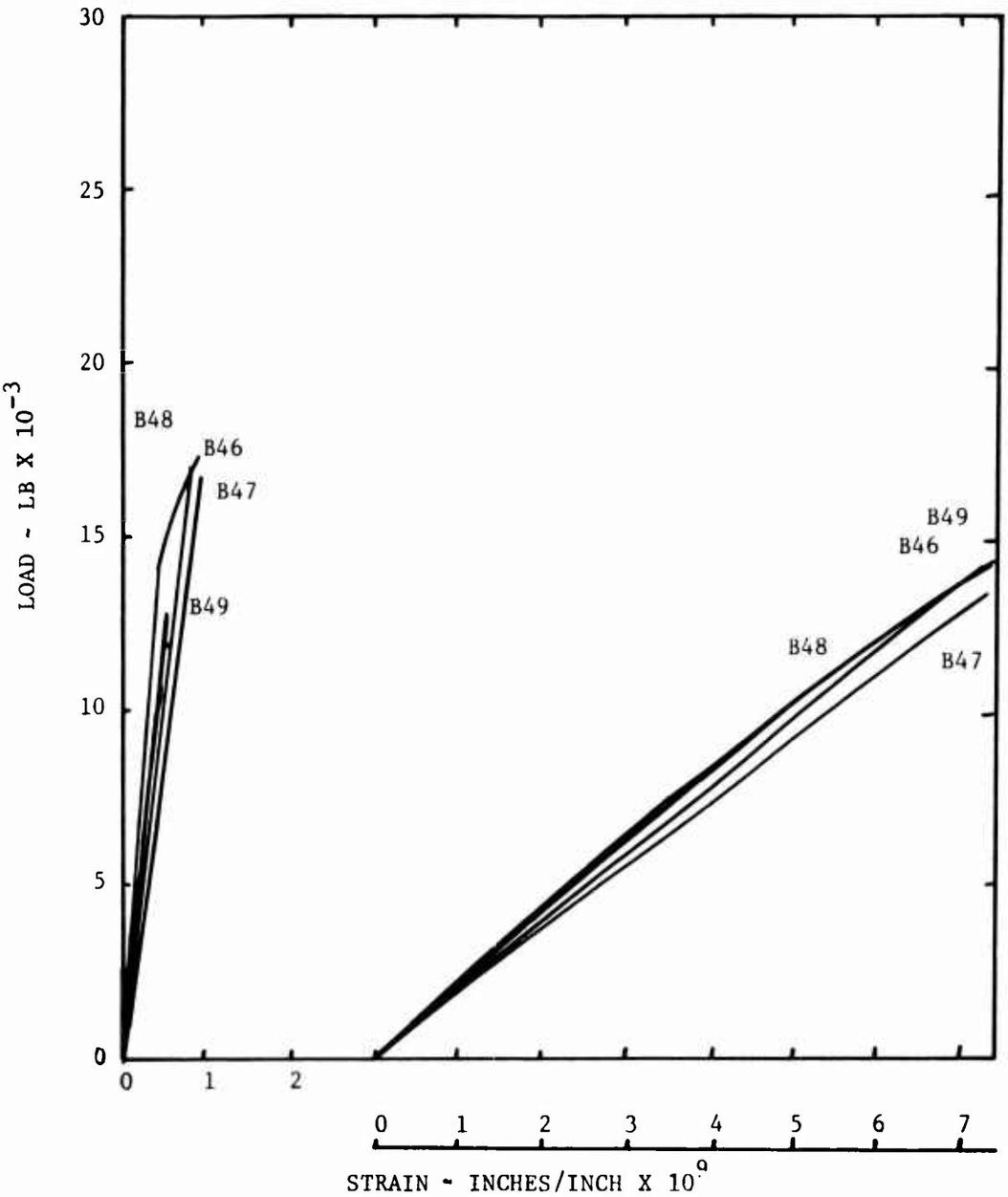

Figure 42. Load-Strain Plot of Biaxial, 2:1, Quasi 6-Ply, 0° Orientation.

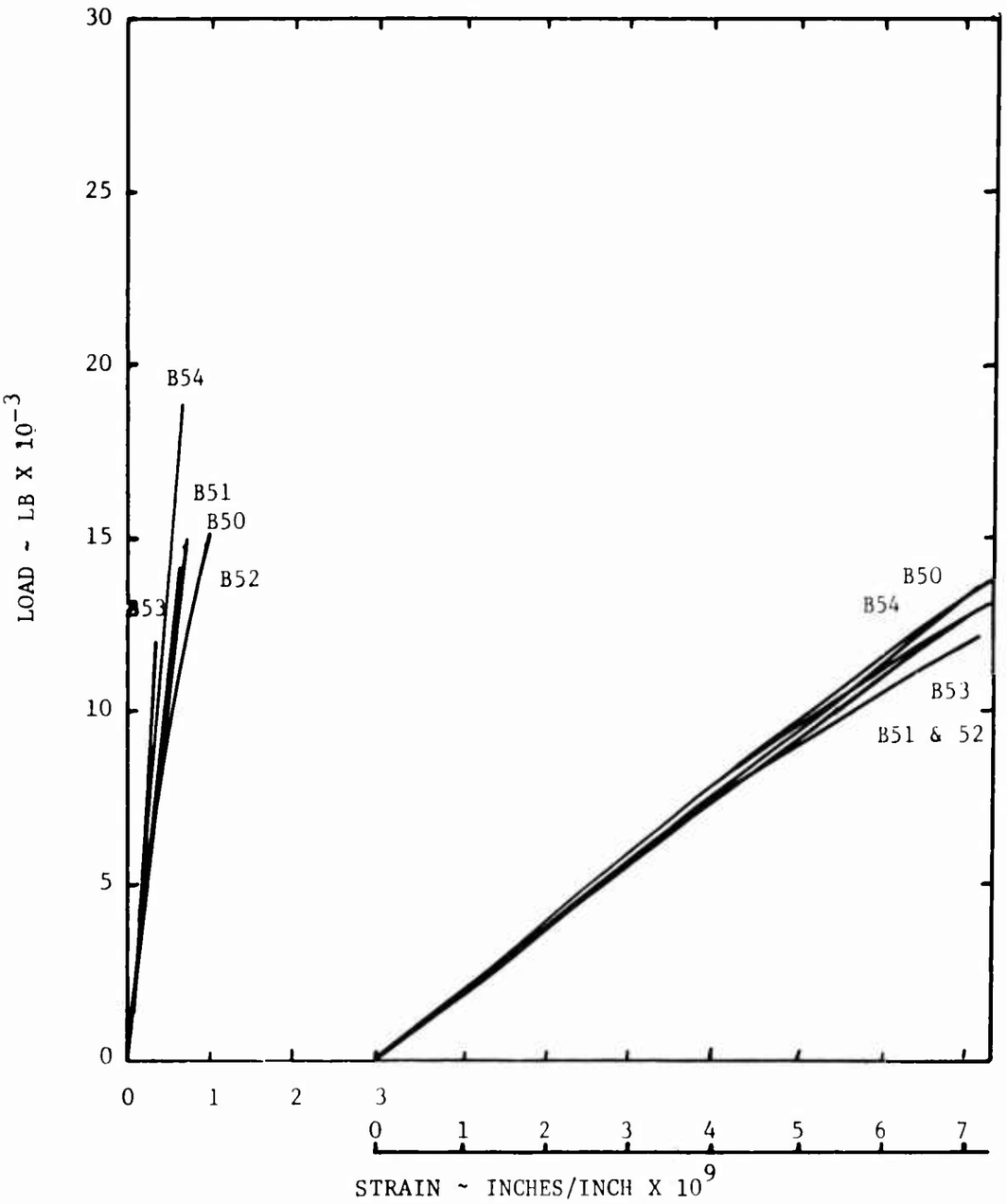

Figure 43. Load-Strain Plot of Biaxial, 2:1, Quasi 6-Ply, 90° Orientation.

Unclassified
Security Classification

DOCUMENT CONTROL DATA - R & D

(Security classification of title, body of abstract and indexing annotation must be entered when the overall report is classified)

1. ORIGINATING ACTIVITY (Corporate author)	2a. REPORT SECURITY CLASSIFICATION
University of Oklahoma Research Institute Norman, Oklahoma	Unclassified
	2b. GROUP

3. REPORT TITLE

BEHAVIOR OF FIBER-REINFORCED PLASTIC LAMINATES UNDER UNIAXIAL, BIAXIAL, AND SHEAR LOADINGS

4. DESCRIPTIVE NOTES (Type of report and inclusive dates)

Final Report 1 July 1967 - 31 July 1968

5. AUTHOR(S) (First name, middle initial, last name)

Charles W. Bert
Byron L. Mayberry
John D. Ray

6. REPORT DATE	7a. TOTAL NO. OF PAGES	7b. NO. OF REFS
January 1969	118	82

8a. CONTRACT OR GRANT NO.	9a. ORIGINATOR'S REPORT NUMBER(S)
DAAJ 02-67-C-0111	USAAVLABS Technical Report 68-86
b. PROJECT NO.	
c. 1F162204A17001	9b. OTHER REPORT NO(S) (Any other numbers that may be assigned this report)
d.	

10. DISTRIBUTION STATEMENT

This document has been approved for public release and sale; its distribution is unlimited.

11. SUPPLEMENTARY NOTES	12. SPONSORING MILITARY ACTIVITY
This report covers Phase II of contract. Phase I is covered in USAAVLABS TR 68-85.	U.S. Army Aviation Materiel Laboratories Fort Eustis, Virginia

13. ABSTRACT

As a part of a larger research program to bring about acceptability of fiber-reinforced plastics for primary load-bearing members of Army aircraft structures, a series of mechanical tests was conducted on fiber glass-epoxy laminates. The loadings used were uniaxial tension; biaxial tension with principal-stress ratios of 1:2, 1:1, and 2:1; and pure shear. The most unique tests were those involving the biaxial loadings. These tests were carried out on a specially designed test fixture using a cable-pulley system in conjunction with a conventional universal testing machine. Data were obtained on the limit strength and apparent ultimate strength of flat laminates subjected to biaxial loading. Under biaxial loading, the parallel-ply lamination arrangement was found to be slightly superior to the cross-ply lamination arrangements. The shear tests were accomplished on thin-walled tubular specimens subjected to pure torsion.

DD FORM 1 NOV 68 1473 REPLACES DD FORM 1473, 1 JAN 64, WHICH IS OBSOLETE FOR ARMY USE.

Unclassified
Security Classification

14 KEY WORDS	LINK A		LINK B		LINK C	
	ROLE	WT	ROLE	WT	ROLE	WT
Biaxial Loading Composite Materials Design Criteria Materials Testing Strength						